Interannual Variability in the Southeastern Tropical Atlantic Ocean: Benguela Niños, Equatorial Atlantic Niños and Interaction with ENSO

Dissertation
zur Erlangung des Doktorgrades
der Mathematisch-Naturwissenschaftlichen Fakultät
der Christian-Albrechts-Universität zu Kiel

vorgelegt von

Joke Friederike Lübbecke

IFM-GEOMAR
Leibniz-Institut für Meereswissenschaften
an der Universität Kiel

Kiel, 2010

Referent: Prof. Dr. Claus Böning

Koreferent: Dr. Noel Keenlyside

Tag der mündlichen Prüfung: 13.07.2010

Zum Druck genehmigt: 13.07.2010

gez. Prof. Dr. Lutz Kipp, Dekan

Zusammenfassung

Zwischenjährliche Schwankungen der Meeresoberflächentemperatur (SST) der tropischen Ozeane sind aufgrund ihres engen Zusammenhanges mit der Niederschlagsvariabilität angrenzender Landregionen von besonderer Bedeutung. Für den östlichen tropischen Atlantik sind zwei wiederkehrende, El Niño-ähnliche Phänomene beschrieben worden, eines zentriert im äquatorialen Bereich als Teil des zonales Modus und eines vor Angola, welches als Benguela Niño bezeichnet wird. Von beiden Ereignissen wird angenommen, dass sie nicht lokal, sondern durch eine Relaxation der Passatwinde im westlichen äquatorialen Atlantik erzeugt werden. Obwohl für beide ein ähnlicher Entstehungsmechanismus vermutet wird, sind Atlantik und Benguela Niños bis vor kurzem als getrennte Ereignisse betrachtet worden.

In dieser Arbeit wird die Verbindung zwischen Benguela und äquatorialen Atlantik Niños sowohl mit Beobachtungsdaten als auch mit Ozeanmodellsimulationen untersucht. Es wird gezeigt, dass sie in einem solchen Ausmaß korreliert sind, dass sie besser gemeinsam als ein Atlantik Niño bezeichnet werden sollten. Verblüffenderweise, kontraintuitiv in Anbetracht des Fernantriebs, treten die SST Anomalien vor Angola ein bis drei Monate vor denen im Bereich der Kaltwasserzunge auf. Es wird gezeigt, dass dieses Verhalten durch Unterschiede in der Tiefe der Temperatursprungschicht sowie in der Saisonabhängigkeit der zwischenjährlichen SST Schwankungen verursacht wird. Während die Kopplung zwischen Oberfläche und darunter liegender Schicht im Bereich der Kaltwasserzunge im Juni/Juli, zur Zeit der flachsten Temperatursprungschicht, am größten ist, erscheinen SST Anomalien vor Angola eher an die Jahreszeit gebunden, in der die Angola Benguela Front ihre südlichste Position erreicht und die zwischenjährliche Variabilität der Stärke der äquatorialen und nachfolgenden Küstenkelvinwelle am höhsten ist. Dies ist zwischen Februar und April der Fall.

Sensitivitätsexperimente mit künstlichen Störungen in der Antriebskonfiguration bestätigen die Wichtigkeit des Fernantriebs vom Äquator für SST Schwankungen vor Angola. Zudem demonstieren sie die führende Rolle der Windschubspannung in der Erzeugung von oberflächennahen Temperaturanomalien im östlichen tropischen Atlantik. Weiterhin wird gezeigt, dass diese mit Schwankungen in der Stärke der subtropischen Antizyklone verbunden sind. Auch die äquatorialen Strömungen reagieren auf Passatwindänderungen und tragen so zu SST Anomalien im Bereich der Kaltwasserzunge bei. Es wird gezeigt, dass Variabilität in der Stärke der südlichen subtropischen Zelle die SST im östlichen tropischen Atlantik auf dekadischer Zeitskala schwach beinflußt.

Schwankungen der Meeresoberflächentemperatur im tropischen Atlantik werden nicht nur von Prozessen innerhalb des Atlantiks bestimmt, sondern sind auch vom tropischen Pazifik beeinflußt. Neuere Studien legen nahe, dass um-

gekehrt auch Variabilität im Atlantik einen Einfluss auf ENSO hat. Wechselwirkungen zwischen SST Schwankungen im tropischen Atlantik und Pazifik werden im letzten Teil der Arbeit unter Einbeziehung von Experimenten mit einem Modell mittlerer Komplexität diskutiert. Die Ergebnisse lassen darauf schließen, dass warme (kalte) Anomalien im östlichen Pazifik die Entwicklung von kalten (warmen) Ereignissen im Atlantik begünstigen, während warme Ereignisse im Atlantik mit darauf folgenden kalten Episoden im Pazifik verbunden zu sein scheinen.

Abstract

Interannual sea surface temperature (SST) variations of the tropical oceans are of particular interest due to their close relation to rainfall variability over adjacent land regions. For the eastern tropical Atlantic two recurring El Niño-like phenomena with high interannual SST anomalies have been described, one centered in the equatorial region as part of the Atlantic zonal mode and one off Angola referred to as Benguela Niño. Both events are supposed to be generated not locally but by a relaxation of the trade winds in the western equatorial Atlantic. Despite their similar assumed forcing mechanisms, until recently Atlantic and Benguela Niños have been viewed as separate events.

In this thesis the connection between Benguela and equatorial Atlantic Niños is investigated with observational data sets as well as ocean model simulations. The study shows that they are correlated to such an extent that they should rather be viewed as one Atlantic Niño. An intriguing feature, counterintuitive in view of the remote forcing mechanism, is that SST anomalies off Angola precede those in the cold tongue region by one to three months. This behaviour is shown to be caused by differences in thermocline depths and in the seasonality of interannual SST variability in the two regions. While the subsurface-surface coupling in the cold tongue region reaches its maximum in June/July when the thermocline is shallowest, SST anomalies off Angola appear rather to be phase-locked to the season in which the Angola Benguela Front is at its southernmost position and the interannual variability in the strength of equatorial and subsequent coastal Kelvin waves is highest in February-March-April.

Sensitivity experiments with artificial perturbations in the forcing configuration confirm the importance of remote forcing from the equator for SST variability off Angola. They also demonstrate the leading role of wind stress, in particular the Southeasterly Trades, in the generation of near surface temperature anomalies in the eastern Tropical Atlantic which are further shown to be linked to variations in the strength of the South Atlantic Anticyclone. The Trade Wind variations also affect the equatorial current system and thus also contribute to SST anomalies in the cold tongue region. Variability in the strength of the southern subtropical cell is shown to have a weak influence on eastern tropical Atlantic SST on decadal time scales.

SST variations in the Tropical Atlantic are not only determined by processes within the Atlantic but appear to be influenced remotely from the Tropical Pacific; recent studies indicate that variability in the Tropical Atlantic might have an impact on ENSO as well. Interactions between SST variations in the Tropical Atlantic and Pacific are discussed in the last part of the thesis taking into account sensitivity experiments with an intermediate complexity model. The results suggest that warm (cold) anomalies in the eastern Tropical Pacific favors the developement of Atlantic cold (warm) events while warm events in the Atlantic appear to be linked to subsequent cold events in the Pacific.

Contents

1 Introduction

Before beginning a hunt, it is wise to ask someone what you are looking for before you begin looking for it.

(Pooh's Little Instruction Book, inspired by A. A. Milne)

1.1 Scientific background

The tropical oceans are of major importance for the climate system. In the Tropics, interactions between ocean and atmosphere are strong and the divergence of the poleward oceanic heat transport is at its maximum causing the tropical regions to play a critical role in the global heat budget (*Chang et al.*, 2006b). Tropical sea surface temperature (SST) anomalies are closely linked to rainfall variability over adjacent land regions. In the Atlantic, interannual rainfall variability over northeast Brazil and the Sahel region is associated with equatorial SST anomalies (e.g. *Moura and Shukla*, 1981; *Giannini et al.*, 2003; *Xie and Carton*, 2004; *Chang et al.*, 2006b). SST variability in the southeastern Tropics off Angola plays an important role in interannual rainfall variations over southern and coastal West Africa (*Rouault et al.*, 2003; *Reason and Rouault*, 2006) and affects the marine ecosystem along the western African coast (e.g. *Binet et al.*, 2001).

The focus of this study is on interannual variations of SST in the eastern equatorial and southeastern Tropical Atlantic ocean, represented respectively by the "Atlantic 3" region (Atl3: 3°S to 3°N, 20°W to 0°W, defined by *Zebiak*, 1993) and the "Angola Benguela area" (ABA: 20°S to 10°S, 8°E to 15°E, defined by *Florenchie et al.*, 2003). Both areas are indicated as lightblue boxes in Fig. 1.1, which provides a schematic representation of the region. While Tropical Pacific variability is clearly dominated by the interannual El Niño–Southern Oscillation (ENSO) phenomenon, the Tropical Atlantic exhibits variability of comparable magnitude on various spatial and temporal scales, both intrinsic

to the basin and remotely forced.

Seasonal cycle

In the eastern equatorial Atlantic SST variability is dominated by the seasonal cycle. As described in *Xie and Carton* (2004) temperatures are highest in boreal spring, when the ITCZ reaches its southernmost position and the equatorial trade winds are weakest. With the onset of the West African Monsoon the southeasterly winds intensify in May and the ITCZ moves northward. This easterly accelaration leads to intensified evaporation, upwelling and, via the associated zonal pressure gradient, a shoaling of the thermocline. The shallow thermocline results in lower temperatures of upwelled subsurface waters. Thus, the eastern equatorial SST reaches its minimum in boreal summer, corresponding to a "cold tongue" that is present from June to September. As

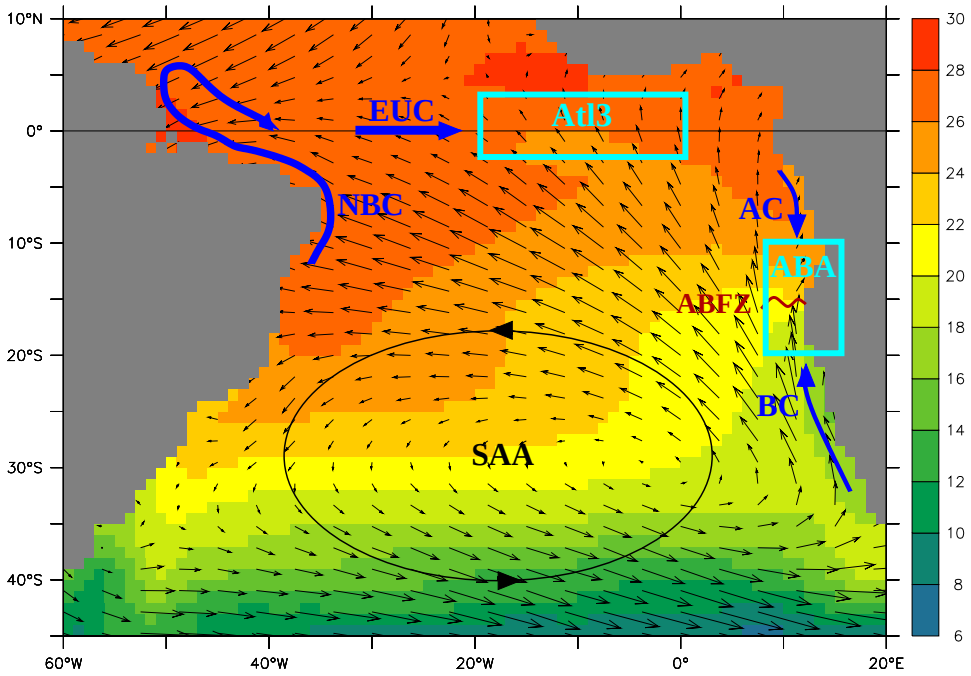

Figure 1.1: Mean SST (from monthly NOAA SST observations, color) and NCEP wind stress (vectors) for 1982 to 2007 combined with a schematic representation of some circulation features and area definitions that are of importance for the present study: the atmospheric South Atlantic Anticyclone (SAA), the North Brazil current (NBC), Equatorial Undercurrent (EUC), Angola current (AC) and Benguela current (BC) as well as the mean position of the Angola Benguela Frontal Zone (ABFZ) and the Atlantic 3 region (Atl3) and Angola Benguela area (ABA).

a result of the cross-equatorial southerlies that induce upwelling south and downwelling north of the equator (first near the coast and subsequently – due to Rossby waves and advection – over the eastern basin, *Philander and Pacanowski*, 1981), the cold tongue is located slightly south of the equator (*Xie*, 1998; *Okumura and Xie*, 2004).

Tropical Atlantic Variability

Regarding interannual to decadal time scales it is common to describe Tropical Atlantic climate variability in terms of two coupled ocean-atmosphere modes (e.g. *Servain*, 1991; *Ruiz-Barradas et al.*, 2000), namely a meridional or gradient mode, and a zonal or equatorial mode, which is also termed Atlantic Niño because of its similarity to the Pacific El Niño phenomenon (*Merle*, 1980). They are shown in Fig. 1.2 as the second and first Empirical Orthogonal Function (EOF) of monthly SST data. The two phenomena together are referred to as Tropical Atlantic variability (TAV) and tightly phase-locked to the seasonal cycle.

The meridional mode represents an interhemispheric, cross-equatorial SST gradient on decadal time scales that is most pronounced in boreal spring when the equatorial Atlantic is uniformly warm (*Ruiz-Barradas et al.*, 2000). It is sometimes referred to as a dipole mode but northern and southern SST anomalies have been shown to vary indepedently of each other (*Mehta*, 1998; *Dommenget and Latif*, 2000, 2002). *Carton et al.* (1996) showed that wind-induced latent heat flux changes play a major role for the off-equatorial SST anomalies. Based on these results, *Chang et al.* (1997) proposed a positive ocean-atmosphere feedback mechanism involving primarily the thermodynamic feedback between surface heat flux and SST. This positive Wind-Evaporation-SST (WES) feedback (introduced originally by *Xie and Philander*, 1994, to explain the northward displacement of the ITCZ in the eastern Pacific) links anomalous trade winds, wind-induced changes in surface evaporation and SST anomalies in the following way: A change in the cross-equatorial SST gradient sets up an anomalous atmospheric pressure gradient through hydrostatic adjustment of the atmospheric boundary layer. The resulting anomalous cross-equatorial flow that (near the equator) is directed down the pressure gradient, i.e. towards the warm SST anomaly, is (away from the equator) deflected by the Coriolis force in such a way that it increases the wind speed in the hemisphere with the negative SST anomaly leading to more evaporation and thus further cooling while it decelerates the trades in the warmer than usual hemisphere which reduces the surface evaporation, thereby increasing the positive SST anomaly (*Xie and Carton*, 2004; *Chang et al.*, 2006b). Through the as-

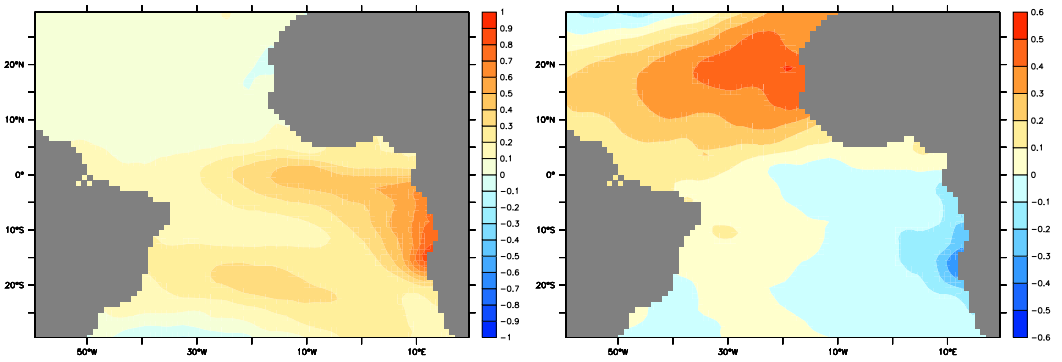

Figure 1.2: First (a) and second (b) EOF of monthly NOAA SST observations for 1982 to 2007 that explain 23% and 16% of the variance, respectively

sociated migration of the ITCZ the cross-equatorial SST gradient is related to rainfall anomalies over Northeast Brazil (e.g. *Moura and Shukla*, 1981; *Chiang et al.*, 2002), whether or not a thermodynamical feedback exists (*Sutton et al.*, 2000).

The zonal mode, that will be the focus of the present study, is most prominent on interannual time scales. While the meridional mode, as described above, is governed by thermodynamic processes at the sea surface, the zonal mode is dominated by ocean dynamics. The dynamical processes are similar to the Bjerknes mechanism (*Bjerknes*, 1969) in the Tropical Pacific in which an eastern equatorial warming causes a relaxation of the trade winds to the west of the SST anomaly leading to reduced upwelling and a deepening of the thermocline in the east which results in further warming. As shown by *Keenlyside and Latif* (2007) all three elements of the positive feedback exist in the Atlantic although weaker than in the Pacific: (1) forcing of surface winds in the west by SST anomalies in the east, (2) forcing of heat content anomalies in the east by winds to the west via variations in thermocline depth and (3) forcing of SST anomalies in the east by heat content anomalies through vertical advection of anomalous subsurface temperatures. Accordingly, the so called Atlantic Niño that occurs mainly in the cold tongue region, is generated by wind anomalies in the western part of the basin and associated with a vertical displacement of the thermocline. It is phase-locked to boreal summer when the trade winds are at their maximum and the thermocline is shallow (*Keenlyside and Latif*, 2007). *Okumura and Xie* (2006) found another period of high interannual SST anomalies in November and December in phase with a second seasonal intensification of easterly winds associated with a SST minimum in the central equatorial Atlantic. During an interannual warm phase, the trade winds in the western equatorial Atlantic are weaker than usual and the thermocline in

the east is anomalously deep (*Zebiak*, 1993; *Carton and Huang*, 1994; *Carton et al.*, 1996).

Benguela Niños

Another El Niño–like phenomenon with high temperature anomalies in the eastern Tropical Atlantic is known as Benguela Niño (*Shannon et al.*, 1986). The strongest Benguela Niños that received a lot of attention because of their impact on local fisheries and rainfall over the region occured in 1934, 1949, 1963, 1984 (*Shannon et al.*, 1986) and 1995 (*Gammelsrød et al.*, 1998). Conversely, extreme cold events as in 1982/83 and 1997 are referred to as Benguela Niñas (*Florenchie et al.*, 2004). Smaller warm and cold events occur frequently, e.g. in 1896 and 1998 (warm) and 1991/92 (cold). Benguela Niños take place in austral fall off Angola in the frontal zone around 15°S where the warm and saline southward flowing Angola Current meets the cooler northwestward flowing Benguela Current (e.g. *Shannon and Nelson*, 1996, schematically shown in Fig. 1.1). The Angola Current is fed by eastward equatorial zonal currents, namely the Equatorial Undercurrent (EUC), the South Equatorial Undercurrent (SEUC) and the South Equatorial Countercurrent (SECC), via the Gabon-Congo Undercurrent (*Peterson and Stramma*, 1991) and it forms the eastern side of the cyclonic Angola Gyre (*Stramma and Schott*, 1999). The Benguela Current, on the other hand, forms the eastern limb of the anticyclonic South Atlantic subtropical gyre (*Peterson and Stramma*, 1991). Starting at the Cape of Good Hope it flows northward until it moves offshore off Lüderitz where the major part of the current bends towards the northwest. Part of it, however, continues along the coast and joins the Angola Current at the ABFZ (*Wedepohl et al.*, 2000). Benguela Niños, too, are supposed to be forced remotely from the equator by a relaxation of the trade winds in the western equatorial Atlantic. Subsurface temperature anomalies associated with the Kelvin waves excited by the wind relaxation progress in the thermocline and then outcrop in the Angola Benguela area as SST anomalies (*Florenchie et al.*, 2003, 2004; *Rouault et al.*, 2007). The contribution of local forcing to the generation of Benguela Niños is under discussion. While previous studies indicate that coastal winds have even been more upwelling favourable during the strongest Benguela Niño events (*Shannon et al.*, 1986; *Florenchie et al.*, 2004; *Rouault et al.*, 2007), recent studies by *Polo et al.* (2008b) and *Richter et al.* (2010) suggest that local wind stress forcing might be important as well. As indicated by Fig. 1.3 that schematically summarizes the forcing mechanisms suggested for equatorial Atlantic as well as Benguela Niños, interannual SST variability in the two regions is likely to be connected. Although there are some studies mentioning that warm events in the two regions might be linked,

little attention has been given to that issue so far.

Subtropical-Tropical Cells

Another potential oceanic remote - forcing mechanism that has been proposed to contribute to the modulation of eastern equatorial SST is the change in the transport of the subtropical - tropical cells (STCs) (*Kleeman et al.*, 1999). STCs are wind-driven shallow meridional overturning cells first described by *McCreary and Lu* (1994) that connect the subtropical subduction regions of both hemispheres to the eastern equatorial upwelling regimes by equatorward thermocline and poleward surface flows (*Schott et al.*, 2004). For the Pacific, it has been shown from both models and observations that wind-driven changes in the STC strength have an impact on equatorial SST via the supply of cold subtropical waters to the equatorial upwelling system (*Nonaka et al.*, 2002; *McPhaden and Zhang*, 2002; *Capotondi et al.*, 2005). For the Atlantic the connection is less clear, most likely due to the pronounced asymmetry of the cells that is caused by the interaction with the northward flowing warm-water branch of the meridional overturning circulation (*Fratantoni et al.*, 2000; *Jochum and Malanotte-Rizzoli*, 2001). There are, however, studies indicating that STC signals might contribute to decadal equatorial SST variations in the Atlantic as well (*Kröger et al.*, 2005).

Equatorial Undercurrent

Along the equator, water subducted in the subtropics is transported in the Equatorial Undercurrent (EUC) as the equatorial branch of the STCs. The

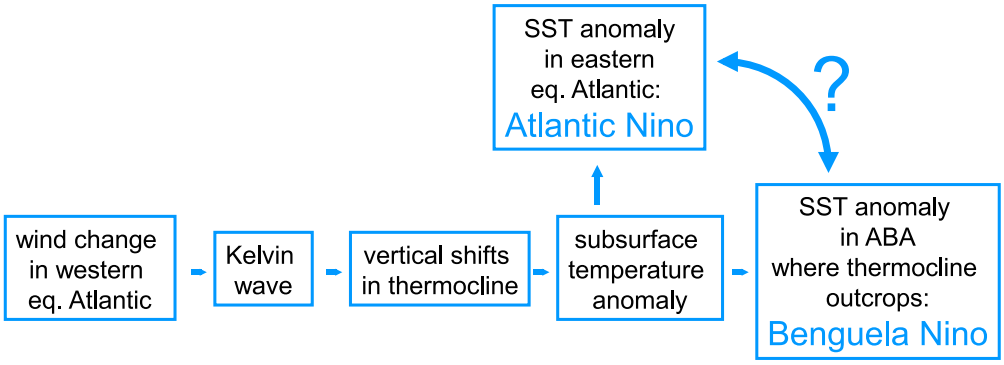

Figure 1.3: Schematic representation of the mechanism suggested for the generation of Atlantic and Benguela Niños

EUC, indicated by a blue arrow in Fig. 1.1, is an eastward flowing zonal current centered on the equator around the depth of the thermocline, driven by the wind-induced zonal pressure gradient (*McCreary*, 1981; *McPhaden*, 1981). It shoals on its way to the east and feeds the equatorial upwelling (*Hazeleger and de Vries*, 2003), thereby impacting eastern equatorial SST. On interannual time scales, *Hormann and Brandt* (2007) found boreal summer variations of near-surface temperatures in the cold tongue region to be anticorrelated with thermocline EUC transport anomalies.

Interaction between Tropical Atlantic and Pacific

SST variability in the Tropical Atlantic is not only determined by processes within the Atlantic, but is also influenced remotely from interannual variations in the Tropical Pacific, i.e. the El Niño - Southern Oscillation (ENSO): *Enfield and Mayer* (1997) showed that Tropical Pacific SST anomalies modulate the Atlantic northeasterly trade winds leading to a warming of the northern Tropical Atlantic 4 - 5 months after an El Niño event. Also, *Latif and Grötzner* (2000) found that ENSO events in the Pacific change the Atlantic trade winds. They suggested that this modulation of the Atlantic zonal surface winds together with local coupled feedbacks results in a modulation of western and eastern Atlantic heat content, which might contribute to induce the Atlantic zonal mode. According to *Sutton et al.* (2000) there are two mechanisms by which ENSO may influence the Tropical Atlantic region: first via changes of the Walker and Hadley circulation and second via Rossby wave like disturbances propagating through the extratropics (related to Pacific North American teleconnection pattern). *Colberg et al.* (2004) suggest that ENSO induced anomalies might also play an important role for upper ocean temperature variations in the Southern Atlantic Ocean and thus Benguela Niños by altering the net surface heat flux, the meridional Ekman heat transport and Ekman pumping. In spite of the many studies addressing that issue, the importance of ENSO forcing for Tropical Atlantic variability is still controversial. There is no robust response in eastern equatorial Atlantic temperatures to El Niño events. While e.g. *Latif and Grötzner* (2000) find warm conditions 6 months after an El Niño in the in their cross-spectral analysis, composite analysis by *Huang et al.* (2004) indicate that El Niño events lead to cold SST anomalies in the Tropical Atlantic. Harmonic analysis of composite ENSO response in SST shows Tropical Atlantic cold anomalies in the first half of an ENSO cycle and warming in the second phase (*Nicholson*, 1997). Consistent with the disagreement between the different studies, the in-phase correlation between Niño3 and Atl3 SST anomalies is very low. *Chang et al.* (2006a) suggested that the inconsistent relationship between Pacific El Niños and Atlantic Niños might be

due to destructive interference between the tropospheric-temperature-induced warming (*Chiang and Sobel*, 2002; *Chiang and Lintner*, 2005) and Bjerknes type ocean dynamics induced by the change in trade winds. Recent studies by, e.g., *Jansen et al.* (2009) and *Rodríguez-Fonseca et al.* (2009) propose that not only Tropical Pacific variability influences the Tropical Atlantic, but that variabilty in the Tropical Atlantic has an impact on ENSO as well.

1.2 Objectives

The major goal of the present study is to investigate the relationship between Equatorial Atlantic and Benguela Niños in a combined analysis of observational data and a set of simulations utilizing a global ocean model. Despite their similar assumed forcing mechanisms (as described in the previous section and shown schematically in Fig. 1.3) and the fact that representations of the zonal mode show a SST maximum not only in the cold tongue region, but also off Angola (e.g. *Ruiz-Barradas et al.*, 2000, Fig. 1.2a), until recently Atlantic and Benguela Niños have been viewed as separate events and have been addressed in separate studies. In recent years, however, a few studies indicated that Benguela and Atlantic Niños are physically connected and should rather be viewed as parts of the same mode. *Reason and Rouault* (2006) suggested that the interannual SST variability of the ABA and the eastern equatorial Atlantic are strongly related. *Hu and Huang* (2007) considered the SST variability in the cold tongue and off Angola as two centers of the southern Tropical Atlantic (STA) pattern (*Huang et al.*, 2004) and described the connection between SST anomalies in the two regions as one dynamical air-sea coupled mode. *Rouault et al.* (2009) noted that some Atlantic Niños were preceded by Benguela Niños and also *Polo et al.* (2008b) found a connection between warming off Angola and at the equator. They describe the Atlantic Niño mode to extend from the western African coast to the equatorial region. In this study, it will be examined to which extent and by which mechanisms equatorial Atlantic and Benguela Niños are linked and whether they are part of the same eastern Tropical Atlantic Niño. For a systematic analysis of the sequence of events in the eastern Tropical Atlantic correlation/regression analysis is used as well as a composite analysis of warm Benguela years.

Interestingly and seemingly inconsistent with the forcing mechanism proposed by *Florenchie et al.* (2003, 2004) there are suggestions in all the studies mentioned above that warming in the equatorial Atlantic tends to lag warming off Angola by one season; *Rouault et al.* (2009) pointed out that so far there is no satisfactory explanation for this relationship. The air-sea coupled mode

described by *Hu and Huang* (2007) is initiated at the Angolan coast between March and May and peaks at the equator in June to August, and the equatorial SST mode discussed by *Polo et al.* (2008b) begins in the Angola Benguela region as well. Thus, a special focus of this thesis is to understand the cause of the time-lag between SST anomalies off Angola and in the eastern equatorial Atlantic. The interpretation of the observational analysis is aided by a series of model experiments studying the oceanic response to atmospheric variability utilizing a comprehensive forcing data set recently developed for Co-ordinated Ocean-ice Reference Experiments ("CORE", *Large*, 2007; *Griffies et al.*, 2009). Specific perturbation experiments allow to revisit the forcing mechanism for Benguela Niños with respect to the relative roles of local upwelling and remote forcing from the equator in order to find an explanation for the (direction of the) time lag between warm events in the Angola Benguela area and in the cold tongue region.

Regarding the influence of local versus remote wind stress forcing on SST variability, the role of the South Atlantic Anticyclone (SAA) will be brought into the focus of attention. The SAA is the dominant wind system over the South Atlantic Ocean and consists of the midlatitude westerlies, equatorward winds along the west coast of Southern Africa and the Southeasterly Trade Winds (Fig. 1.1). The question arises whether temperature anomalies off Angola and in the cold tongue region might both be linked to variations of this large-scale atmospheric circulation.

Complementary to the analysis of Atlantic and Benguela Niños, further factors that impact SST variability in the eastern Tropical Atlantic on interannual to decadal time scales will be briefly discussed in the latter part of the study. As interannual to decadal EUC variability is tied to variations in wind stress (*Kröger et al.*, 2005; *Hüttl and Böning*, 2006), the wind changes that induce Atlantic and Benguela Niños might lead to EUC transport variations as well and thus contribute to the SST anomalies in the cold tongue region. Along these lines *Góes and Wainer* (2003) showed the EUC to be stronger in cold event years and weaker in warm event years. Their results will be revisited using the ORCA ocean model simulations. Regarding the potential influence of the subtropical - tropical cells, a special configuration of the Kiel Climate Model will be used to isolate the effect of off-equatorial wind forcing.

With respect to the interaction between interannual variability in the Tropical Pacific and Atlantic ocean, perturbation experiments from an intermediate complexity model are analyzed in order to address the question whether the

conditions in one of the tropical oceans favour the developement of a subsequent warm or cold event in the other one. The main focus lies on the dynamical response of eastern equatorial Atlantic SST to remote ENSO forcing and its seasonal dependency, while the impacts that Atlantic Niños might have on the Tropical Pacific are only touched on.

This thesis is organized as follows: In Chapter 2 the models and observational data used in this study are described. In Chapter 3 the ability of the ocean model to capture major aspects of the mean circulation and seasonal cycle in the Tropical Atlantic is discussed before turning to an analysis of the interannual variability in Chapter 4 which is divided in seven subsections: Section 4.1 elucidates the link between Benguela and Equatorial Atlantic Niños; Section 4.2 focusses on the forcing mechanism of Benguela Niños; Section 4.3 discusses the time lag between warm events in the Angola Benguela area and in the cold tongue region; Sections 4.4, 4.5 and 4.6 examine the roles of the South Atlantic Anticyclone, the Equatorial Undercurrent and the subtropical-tropical cells; and section 4.7 summarizes the main results. Chapter 5 focusses on the interaction with interannual variability in the Tropical Pacific. Chapter 6 provides the conclusions and a discussion of their implications.

2 Models and data sets

Never trust anything that can think for itself if you can't see where it keeps its brain.

(Joanne K. Rowling, Harry Potter and the chamber of secrets)

In order to address the questions that were raised in the introduction, observational data sets as well as output from three different types of numerical models are analyzed. First and foremost a global ocean model is used to investigate the spatio-temporal sequence of events in the ocean. Regarding the potential influence of the subtropical cells on equatorial SST coupled model simulations are additionally looked at. For idealized experiments with respect to the issue of Atlantic-Pacific interaction an ocean model of intermediate complexity is used. It can either be run as an ocean only model or coupled to a statistical atmosphere. The models and observations used in this study are described in the following sections.

2.1 Ocean model

The model mainly used in this study is the global ocean-sea ice model NEMO-ORCA05 with 0.5° horizontal resolution forced by a prescribed interannually varying atmosphere spanning the period 1958–2000. The model configuration (referred to as ORCA05) is based on the "Nucleus for European Modelling of the Ocean" (NEMO, *Madec*, 2008) numerical framework, implemented by the European DRAKKAR collaboration (*DRAKKAR Group*, 2007). The ocean model is coupled to the dynamic-thermodynamic sea ice model LIM2 (*Fichefet and Morales-Marqueda*, 1997).

2.1.1 Configuration

The model is based on the primitive equations (*Bryan*, 1969) that are solved on an Arakawa-C grid (*Arakawa and Lamb*, 1977) in which the tracer point is located in the middle of the grid box and the velocity components are staggered in space such that the zonal (meridional, vertical) component falls on the interface between tracer grid boxes in the zonal (meridional, vertical) direction. In the configuration used here, the nominal grid size is 0.5° with a horizontal resolution of 0.5° in longitude and values in the range between 0.5° at the equator to 0.1° close to the poles in latitude. To overcome the north pole singularity, ORCA utilises a tripolar grid with two northern poles situated on North America and Eurasia (*Madec and Imbard*, 1996). In the vertical, the water column is divided into 46 geopotential levels of variable thickness with 20 levels in the top 500m and a resolution of 6m at the surface. The thickness of the upper-most layer can vary due to the implementation of an implicit free surface in a volume conserving formulation. Bottom topography and coastlines are derived from *ETOPO5* (1988) and interpolated on the model grid. Topographic slopes are represented by a partial step formulation (*Adcroft et al.*, 1997), which improves the representation of bottom-near flow in regions with steep and narrow topography (*Barnier et al.*, 2006). Regarding the temporal resolution, a time step of 2400s is used.

2.1.2 Physics

ORCA05 does not resolve mesoscale eddies but the effect of eddies is parameterized using a GM scheme (*Gent and McWilliams*, 1990) with coefficients depending on the internal Rossby Radius, effectively rendering a non-eddying solution. Vertical mixing is achieved using the Turbulent Kinetic Energy (TKE) scheme of *Blanke and Delecluse* (1993). Mixing coefficients, computed from a characteristic turbulent velocity and a mixing length scale, are high above the thermocline and low in stratified regions. Lateral mixing of tracers is oriented along isopycnals and MUSCL (Monoton Upstream-Centered Scheme for Conservation Laws, *Hourdin and Armengaud*, 1999) is used as the tracer advection scheme. The momentum advection scheme is conserving both energy and enstrophy (EEN scheme, an adaption of *Arakawa and Hsu*, 1990), and viscosity is parameterized by a biharmonic scheme. Free-slip is used as the boundary condition at the coastlines, i.e. there is no lateral friction. At the bottom linear friction is used.

2.1.3 Atmospheric surface forcing

In ocean-only model experiments an atmospheric forcing at the sea surface has to be prescribed. Here momentum, heat and freshwater fluxes are implemented according to the protocol suggested for Co-ordinated Ocean-ice Reference Experiments ("CORE" *Griffies et al.*, 2009), Version 1, utilising the bulk forcing methodology for global ocean-ice models developed by *Large and Yeager* (2004) and *Large* (2007). It is based on NCEP/NCAR reanalysis products for the atmospheric state during 1958 – 2004, merged with various observational (e.g., satellite) products for radiation, precipation and continental run-off fields, and adjusted to provide a globally balanced diurnal to decadal forcing ensemble (*Large*, 2007). For the experiments analyzed in this study, daily data for incoming shortwave and outgoing longwave radiation, specific humidity and and wind (u_{10}, v_{10}) as well as monthly precipitation and runoff-data are used.

The model integrations were initialized with the annual mean temperature and salinity distributions of the Levitus climatology (*Levitus et al.*, 1998) for low and mid-latitudes, and from the data set of the Polar Hydrographic Center (PHC 2.1) for high latitudes (*Steele et al.*, 2001).

In order to avoid drifting of water mass properties, a relaxation of sea surface salinity towards initial conditions is applied. For all experiments used here the restoring is rather weak with a time scale of 180 days. In the polar region, salinity and temperature restoring is three-dimensional in all experiment besides FRESH, which uses a strong surface salinity restoring there. No further temperature restoring is used, but the bulk formulation for the turbulent heat flux causes an implicit damping of SST towards the prescribed surface air temperature values. Prescribed surface specific humidity acts as a strong Newtonian cooling towards air temperature variability as well. Thus, SST ceases to be a fully prognostic variable. This problem will be addressed by additionally analyzing temperature variations below the mixed layer (temperature in 40m depth) where the direct influence of the thermal boundary condition is small. As shown in more detail in *Lübbecke et al.* (2008), the impact of wind-driven circulation changes on the near-surface temperature (NST) variability is reflected in the temperature response below the mixed layer.

2.1.4 Experiments

Several experiments are considered in this study. All of them are (partly) interannually forced and build on a climatological spin-up of 20 years. The reference experiment **REF** (as introduced in *Biastoch et al.*, 2008) is a hindcast of the period 1958 – 2000 investigating the oceanic response to interannual CORE forcing. In order to explore dynamical causes of the ocean variability, perturbation experiments (as described in *Lübbecke et al.*, 2008) are analyzed. They use the same initial conditions and span the same integration period as REF, but are subject to different, artificial changes in the forcing set-up. In **WIND**, an experiment designed to examine the relative importance of changes in the wind-driven circulation, the interannual variability is restricted to the momentum fluxes (wind stress) only, while the thermohaline fluxes are based on a climatological, repeated annual cycle. In **EQ**, an experiment aiming at identifying the contribution from equatorial forcing, the interannual forcing variability (both thermohaline and momentum fluxes) is restricted to the equatorial band of 3°S to 3°N, whereas poleward of 7°N/S the forcing is climatological. There is a smooth transition from 3° to 7° latitude so that the interannual forced band covers the major part of the equatorial wave guide. Case **NO EQ** uses the opposite forcing configuration, i.e., interannual forcing poleward of 7° latitude. From **FRESH**, an experiment with effectively increased fresh water input in high northern latitudes (*Lorbacher et al.*, 2010), the response of the subtropical cells to a weakened meridional overturning stream function can be studied. An overview over the experiments that are used in this study is given in Table 2.1.

Experiment	internal name	interannually varying forcing
REF	KAB042	full
WIND	KAB047	for momentum fluxes only
EQ	KJL001	only between 3°N and 3°S (transition until 7°N/S)
NO EQ	KSH003	only outside 7°N/S (transition until 3°N/S)
FRESH	KAB110	full, additional fresh water input in high northern latitudes

Table 2.1: Overview over the different NEMO-ORCA05 experiments

2.2 Coupled ocean-atmosphere model

In order to account for ocean-atmosphere feedbacks and to allow SST to evolve less constraint by the boundary conditions of prescribed forcing variability, output from special configurations of the coupled ocean-atmosphere Kiel Climate Model (KCM) is also analyzed. The KCM simulations are used here to investigate the possible connection between subtropical cell variability and SST, and the Tropical Pacific's response to remote Atlantic Niño forcing. A detailed model descripton can be found in *Park et al.* (2009).

The Kiel climate model consists of the NEMO-ORCA2 ocean model, which is a coarse resolution version of NEMO-ORCA05 described above, and ECHAM5 (European Centre for Medium-Range Weather Forecasts (ECMWF) Hamburg atmospheric general circulation model version 5, *Roeckner et al.*, 2003) as the atmospheric component. They are coupled once per day via the Ocean Atmosphere Sea Ice Soil Version 3 (OASIS3 *Valcke et al.*, 2006). The horizontal

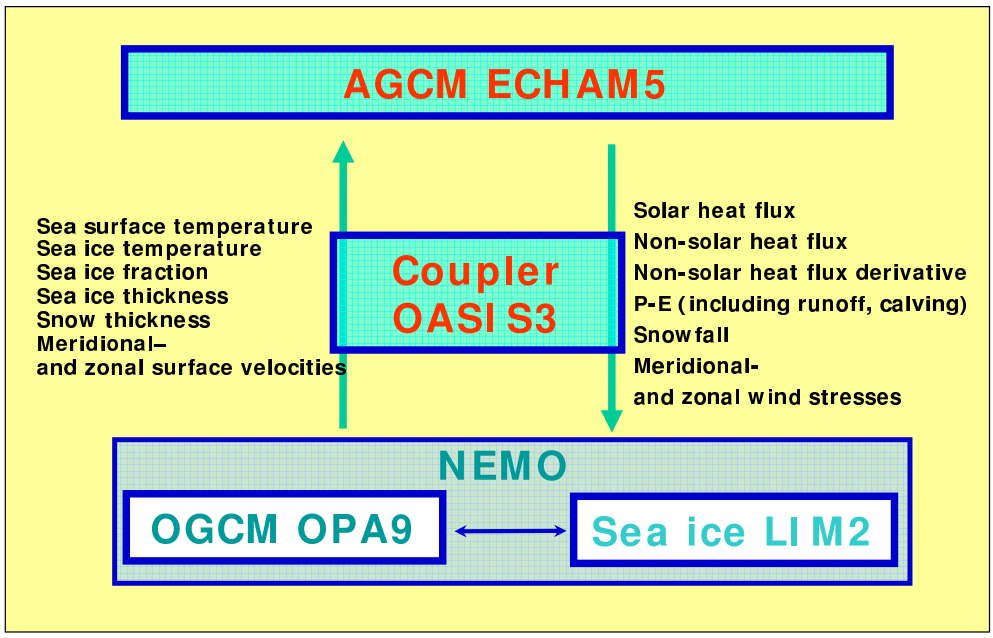

Figure 2.1: *Components of the Kiel Climate Model (adopted from Park et al., 2009)*

resolution is T31 (which equates to about 3.75° by 3.75°) for the atmospheric component and 2° for the ocean component. Near the equator the latitudinal resolution of the ocean model increases to 0.5°. In the vertical, ECHAM5 has 19 vertical levels and extends up to 10hPa, and ORCA2 has 31 depth levels. A schematic of the model components and the exchange parameters is provided by Fig. 2.1. No flux correction is used in the standard configuration.

As almost all of the current state-of-the-art coupled general circulation models (CGCMs), the standard KCM simulations exhibits a strong warm SST bias in the eastern tropical Atlantic ocean (*Davey et al.*, 2002; *Wahl et al.*, 2009). The deviations from observed SST peak in boreal summer and even lead to a reversed SST gradient along the equator. Due to the strong bias, the Atlantic zonal mode is basically absent from coupled models (*Deser et al.*, 2006). Thus, the conclusions that can be drawn from standard coupled model simulations regarding Tropical Atlantic variability are rather limited.

Instead, output from two modified runs (provided by Sebastian Wahl and described in detail in *Wahl et al.*, 2009) is used in this study:

1. **FLX**: A common approach to overcome model biases and to prevent model drift is to correct the fluxes that are exchanged between the different components of the coupled model. FLX is such a flux corrected run. A flux correction climatology is calculated from a run with restoring towards climatological SST and then applied on a daily basis between 40°S and 40N°. Poleward of 40° the flux corrections are linearly reduced towards zero. As shown in *Wahl* (2009), the flux corrections at the surface, which effectively remove the errors in the mean seasonal cycle of SST in the Tropics, significantly reduce the subsurface temperature bias compared to the reference case in all seasons. Also, this run shows a seasonality of the interannual SST variability in agreement with observations with Atlantic Niños peaking in boreal summer and Pacific El Niño and La Niña events taking place in boreal winter.

2. **WIND4**: In the sensitivity experiment WIND4 climatological wind stress is prescribed between 4°S and 4°N in the tropical Atlantic, while the ocean-atmosphere coupling is active everywhere else. This set-up allows to study the impact of off-equatorial wind variations on equatorial variability.

2.3 Intermediate complexity ocean-atmosphere model

As a third model, an ocean model of intermediate complexity (IOM) developed by *Keenlyside* (2001) and applied in studies by *Keenlyside and Kleeman* (2002), *Zhang et al.* (2005) and *Ding et al.* (2009) is used in a version provided by Stéphane Raynaud (pers. comm.). It can either be run as a forced ocean model or coupled to a statistical atmosphere (in this case referred to as Intermediate Coupled Model, ICM). It is simple enough to isolate certain effects and make artificial changes, but sophisticated enough to agree to a certain extent with observations and results from real GCMs. The model domain covers the subtropical-tropical Atlantic and Pacific from 30°S to 30°N with a horizontal resolution of 2° zonally, and in the meridional direction 0.5° within 10° about the equator to 3° close to the boundaries. Realistic coastlines are taken into account, but no bottom topography. The IOM is derived from equations describing wind-induced dynamical pertubations about a resting background state. Its dynamical part consists of linear and nonlinear components. The dominant linear component is based on the model of *McCreary* (1981) with the extension of horizontally varying background stratification. It solves the equations of motion in terms of 10 baroclinic modes plus two surface layers that are governed by Ekman dynamics, representing the effects of the higher baroclinic modes from 11 to 30. The nonlinear component is a simplified model of the residual nonlinear momentum equation that is applied within the two surface layers. SST variability in the IOM is derived from a SST anomaly model coupled to the dynamical component. It is driven by ocean horizontal advection and vertical advection associated with (prescribed) mean and (simulated) anomalous currents. The heat flux is parameterized by thermal damping based on latent heat being controlled by anomalous SST. Thus SST anomalies are damped towards zero, i.e. SST is damped towards the climatology. A detailed descripton of the IOM is given in *Keenlyside* (2001).

2.4 Observational data sets

Monthly maps of the NOAA Optimum Interpolation Sea Surface Temperature (SST) data are used, provided by NOAA/OAR/ESRL PSD, Boulder, Colorado, USA, with a spatial resolution of 1°. These data sets consist of a blend of satellite and in-situ observations (*Reynolds et al.*, 2002) and span the period from December 1981 to present. Here, data for the period January 1982 to December 2007 are analyzed and, to be consistent with the model, from January 1982 to December 2000, whenever observational data are compared

to model results. For comparison, data from the Tropical Rainfall Measuring Mission (TRMM) Microwave Imager (TMI) are used. This satellite is able to see through clouds and the SST product has a higher horizontal resolution of 0.25°. The data are available for the comparatively short period from 1999 to present. TMI data are produced by Remote Sensing Systems and sponsored by the NASA Earth Science MEASURES DISCOVER Project. Data are available at www.remss.com.

Observations of sea surface height (SSH) produced and distributed by AVISO (www.aviso.oceanobs.com) are used for the period January 1993 until December 2006. Sea Level Pressure (SLP) data are taken from the CDC (Climate Diagnostics Center) derived NCEP reanalysis product (*Kalney et al.*, 1996) for the period January 1982 to December 2007. Monthly data with a horizontal resolution of 2.5° are used.

3 Mean circulation and seasonal cycle

All water has a perfect memory and is forever trying to get back to where it was.

(Toni Morrison, The Site of Memory)

Before discussing the interannual to decadal variability, it is useful to look at the salient features of the mean subtropical-tropical circulation and the seasonal cycle, as both play an important role in the Tropical Atlantic variability. It is also examined how well they are captured by the NEMO-ORCA05 ocean model. The representation of the equatorial current system and of the subtropical-tropical cells (STCs) is particularly relevant, as both potentially influence SST in the eastern equatorial Atlantic.

3.1 Mean circulation

In a zonally-integrated sense, the upper-ocean circulation in the Tropical Atlantic can be described as a superposition of the northward warm-water branch of the large-scale meridional overturning circulation (MOC, *Ganachaud and Wunsch*, 2001) and the shallow wind-driven subtropical-tropical overturning cells (STCs; *McCreary and Lu*, 1994; *Malanotte-Rizzoli et al.*, 2000; *Schott et al.*, 2004). The STCs involve equatorward geostrophic transport of water in the main thermocline, its upwelling at the equator, and return to the subtropics in the surface Ekman layer. The cool water from the subtropics that reaches the equator is required to maintain the tropical thermocline. According to the model study by *Liu et al.* (1994) there exist three different pathways water masses subducted in the subtropics can take. First, waters subducted in the western part of the subduction region recirculate in the subtropical gyre and do not reach the equator. Water parcels which take the second path move to the Equatorial Undercurrent (EUC) via the western boundary currents. In the Atlantic these would be the Guiana Undercurrent in the northern hemisphere (*Schott et al.*, 1998) and the North Brazil (Under)current (NBC) in the

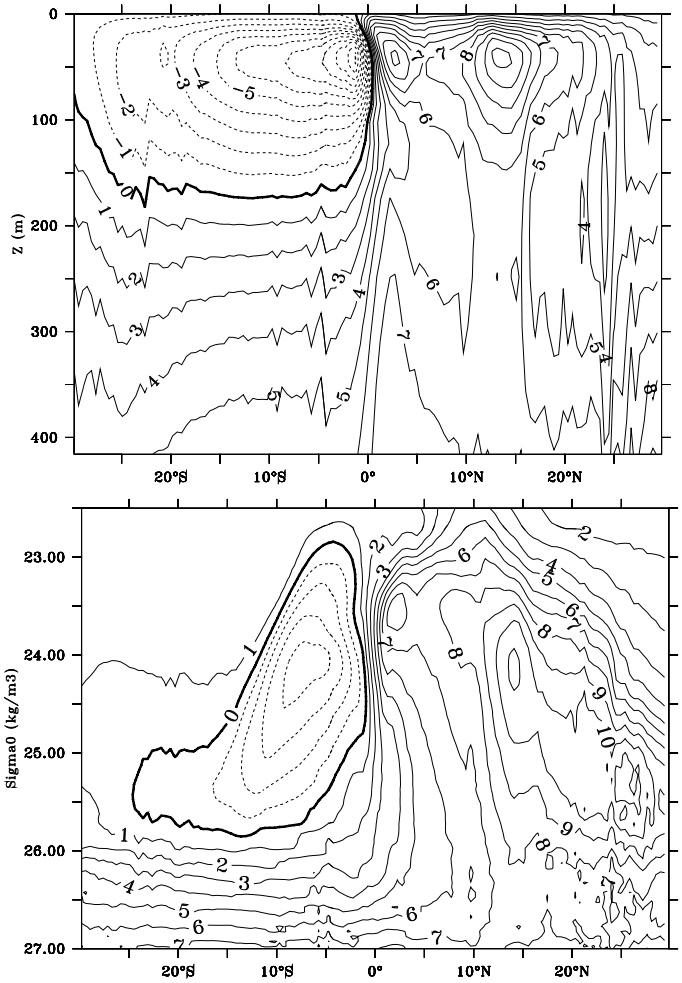

Figure 3.1: Mean Atlantic meridional overturning stream function from REF as a function of depth (upper panel) and as a function of potential density σ_0 (lower panel)

southern hemisphere. Finally, there is an exchange window in the interior of the ocean through which water subducted in the eastern subtropics enter the Tropics in a zigzag pattern. *Inui et al.* (2002) showed that the existence of such an interior exchange window in models is dependent on the wind forcing.

Figure 3.1 shows the mean Atlantic meridional overturning stream function from REF, both as a function of depth and of potential density from 30°S to 30°N for the upper 500m and $\sigma_0 = 22.5 kg/m^3$ to $27.0 kg/m^3$, respectively. Shallow tropical cells (TCs) that are associated with downwelling driven by the latitudinal decrease of the poleward Ekman transport (*Schott et al.*, 2004)

exist in both hemispheres confined to 5° around the equator in the depth-integrated stream function. As shown by *Hazeleger et al.* (2001), they are not associated with diapycnal transports and thus are considerably weakened if the overturning is considered in density coordinates.

In the Southern Hemisphere a closed subtropical cell exists in the upper 200m with maximum meridional transports of about 6 Sv. The equatorward flow spans the σ_0-range of about $24.2kg/m^3$ to $25.8kg/m^3$. In contrast, there is no connection between suptropical subduction and equatorial upwelling in the Northern Hemisphere, i.e. no mean northern STC, but a strong recirculation cell centered around 13°N. There are, however, periods in which a closed northern STC can be found in the model, (i.e. in the mid-80s), indicating that northern subtropical water might contribute to the equatorial upwelling from time to time. In a sensitivity experiment with effective additional fresh water input in high northern latitudes (FRESH) and an accordingly decreasing MOC strength a closed northern STC connected to the equator is found. This is in agreement with the results by *Fratantoni et al.* (2000) who found the asymmetry of the Atlantic STCs (in contrast to the Pacific where the cells are more symmetric) to be caused by the overlying northward flowing warm water path of the MOC that was mentioned above. In their model the EUC was fed symmetrically from both hemispheres when forced with winds only, while the southern source clearly dominated when the MOC was taken into account. Also *Jochum and Malanotte-Rizzoli* (2001) showed that the northward return flow of the MOC inhibits the connection between the northern subtropical gyre and the Tropics. Consistent with that, *Snowden and Molinari* (2003) note that there is no observational evidence that water from the northern subtropics reaches the equator. *Zhang et al.* (2003), however, found one third of the total equatorward STC layer transport to originate from the northern hemisphere. They estimated a pycnocline transport of 15Sv across 6°S and 10°N associated with the STC from hydrographic data. Of these, 5 Sv originates in the north, with 3 Sv from the western boundary and 2 Sv taking a zigzag pathway through the interior. In the Southern Hemisphere the interior pathway (4Sv) is more direct. The remaining 6Sv reach the equator via the NBC. The NBC pathway including the recirculation north of the equator is indicated schematically in Fig. 1.1.

The North Brazil (Under)current is the most important pathway for subtropical waters to supply the EUC. In Figure 3.2 a section of the meridional velocity at 5°S from REF shows the strong NBC directly along the coast. In agreement with observations (e.g. *Schott et al.*, 1998, 2002, 2005), the NBC

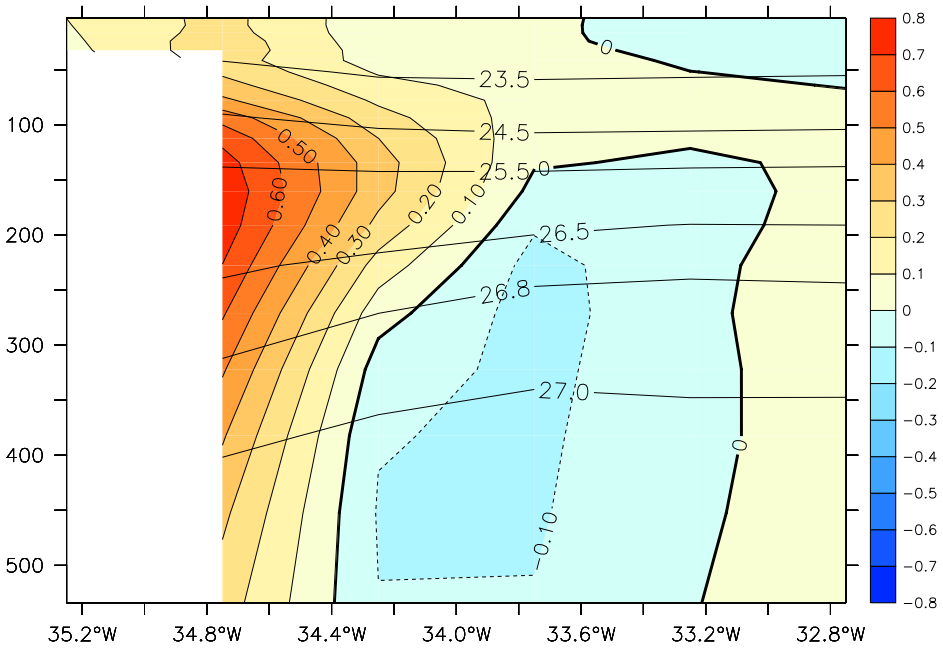

Figure 3.2: Mean meridional velocity (in m/s) and isopycnals (in kg/m^3) as a function of depth (in m) at 5°S from REF (1958 to 2000)

core with a maximum velocity of 80cm/s is located in 150 to 200m depth and within the density range of $\sigma = 24.5kg/m^3$ to $26.8kg/m^3$. Its mean transport calculated between these density surfaces amounts to 10.7 Sv in REF, slightly lower than the observational value of 13.4 ± 2.7Sv estimated by *Schott et al.* (2002) from shipboard profiles. The isopycnals that span the NBC core are usually selected to divide the surface water layer ($\sigma \leq 24.5kg/m^3$) from the thermocline layer ($24.5kg/m^3 \leq \sigma \leq 26.8kg/m^3$) that supplies the equatorial branch of the STCs, i.e. mainly the EUC (e.g. *Schott et al.*, 1998).

For an examination of the zonal current system, Fig. 3.3 provides sections of the mean zonal velocity, both meridional at 23°W and zonal along the equator. The general picture is consistent with observations (*Brandt et al.*, 2006; *Hormann and Brandt*, 2007) showing the EUC centered around the equator, two branches of the westward South Equatorial Current (SEC) as well as the eastward North Equatorial Countercurrent (NECC). There are weak eastward velocities around 4-5°S incidating the existence of the South Equatorial Undercurrent (SEUC) which is not simulated well by the model at this resolution. The EUC spans the density range of $\sigma = 23.5kg/m^3$ to $26.5kg/m^3$ with a maximum eastward velocity of about 70 cm/s in the western part of the basin. Its

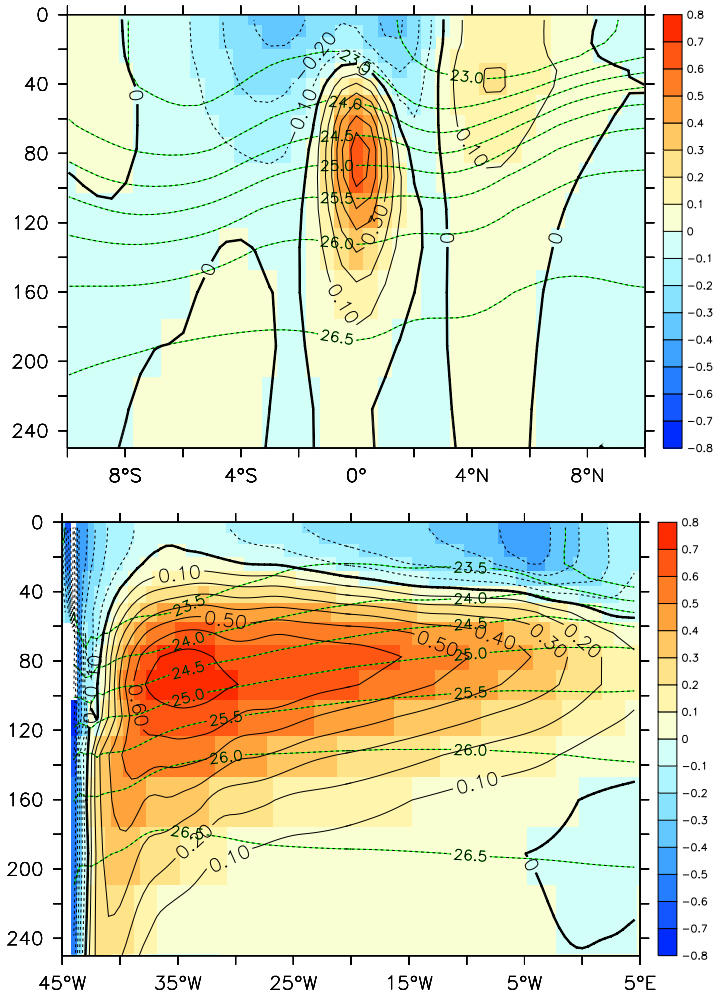

Figure 3.3: Mean zonal velocity (in m/s) and isopycnals (in kg/m^3) as a function of depth (in m) at 23°W (upper panel) and along the Equator (lower panel) from REF (1958 to 2000)

core slightly shoals from about 90m near the western boundary to 70m in the east. The mean transport of the EUC from REF, calculated by integration of all eastward velocities in the density range of the mean core ($23.5 \leq \sigma \leq 26.5$) between 3°N and 3°S for 1961 to 2000, is about 16Sv at 35°W and 15Sv at 23°W. To compare with observations the transport was also calculated over the upper 300m resulting in 23Sv at 35°W and 19Sv at 23°W. These values are somewhat higher than the observations by *Schott et al.* (2003); *Brandt et al.* (2006) and *Hormann and Brandt* (2007) of about 20Sv at 35°W and 14Sv at 23°W but show a similar reduction in transport towards the east. If, as

common in observational studies, only velocities within the thermocline layer ($24.5kg/m^3 \leq \sigma \leq 26.8kg/m^3$) are taken into account, the transport values are lower (14Sv at 35°W, 13Sv at 23°W) and closer to observations (14Sv at 35°W, 11Sv at 23°W).

One can conclude that ORCA05 provides a realistic simulation in key measures of the Tropical Atlantic mean circulation. The model captures the basic structure of the subtropical-tropical overturning cells and the current field. The NBC as well as the major zonal currents are present and display transport values close to observations. The main weakness lies in the absence of the off-equatorial undercurrents (NEUC and SEUC), probably due to insufficient resolution. Apart from this deficiency, ORCA05 simulations appear to be well suited to investigate upper ocean Tropical Atlantic variability.

3.2 Seasonal cycle

As interannual Tropical Atlantic variability is phase-locked to the dominating seasonal cycle (*Xie and Carton*, 2004), seasonal variations will play an important role in the discussion of interannual SST anomalies in the next section. Here, the seasonal cycles of SST, SSH and EUC transport are thus briefly introduced and some of the difficulties in obtaining a robust seasonal signal from both models and observations are touched on.

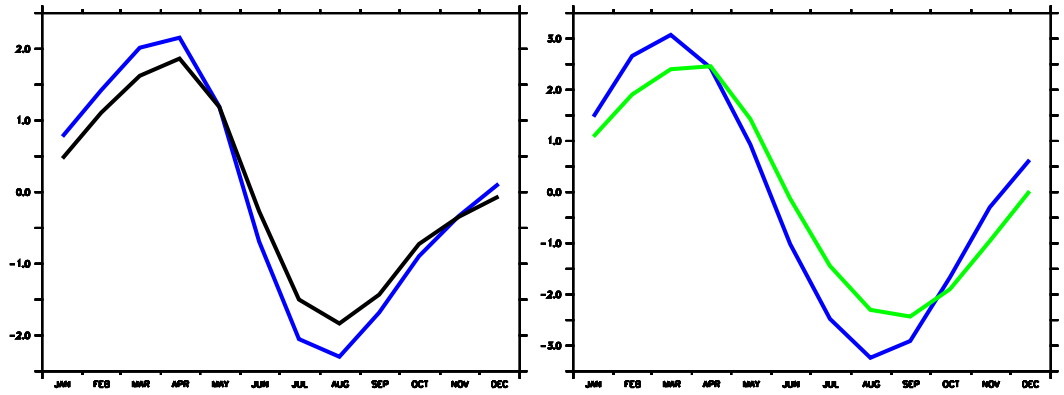

Figure 3.4: Mean seasonal cycle of SST anomalies (in °C) averaged over (left) Atl3 region and (right) Angola Benguela area from NOAA observations (blue) and REF (black, green)

3.2.1 SST

SST in the Atl3 region and the Angola Benguela area (ABA; both regions indicated by lightblue boxes in Fig. 1.1) display an annual cycle – shown in Fig. 3.4 from both the model and observations – with highest temperatures in austral fall and minimum values in late austral winter. While the seasonal cycle in the eastern equatorial Atlantic is represented well by the model, the simulated maximum and minimum lag the observed ones by one month in the ABA. As mentioned in section 2.1.3 model SST is damped towards prescribed atmospheric temperatures by the bulk formulation of the surface heat flux. Thus the correspondence between observed and simulated seasonal variations basically reflects the ability of the CORE forcing to realistically represent the seasonal cycle in the region. Amplitudes are slightly higher in the ABA reaching $\pm 3°$ compared to about $\pm 2°$ in the Atl3 region. As described in the introduction the annual cycle at the equator can be explained by continental monsoon forcing and air-sea interaction. Along the African coast the late austral winter minimum is thought to result from intensified coastal upwelling (*Xie and Carton*, 2004).

3.2.2 SSH

The seasonal cycle of equatorial Atlantic observed sea surface height (SSH) from altimeter data has been described by *Schouten et al.* (2005) as a cycle of consecutive Kelvin and Rossby waves. Eastward propagating equatorial waves (free and forced) are obvious both in the climatology of observed monthly SSH and the depth of the 23°C isotherm (as a measure of the thermocline depth)

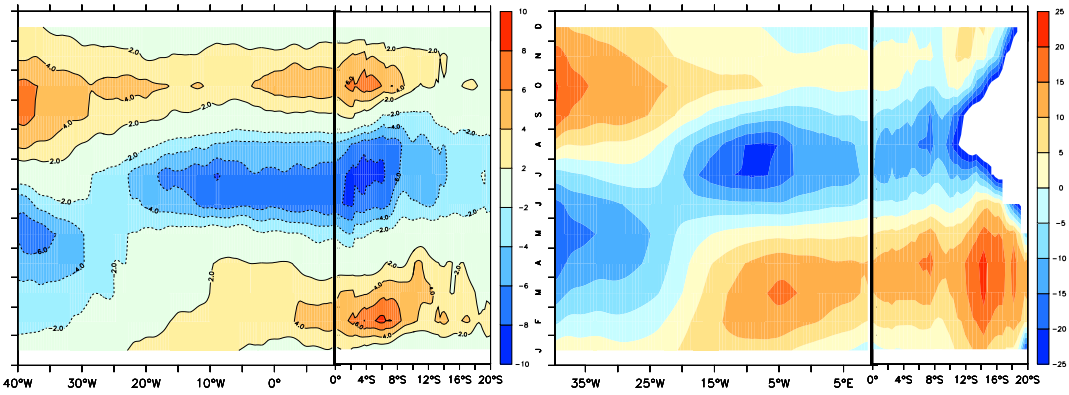

Figure 3.5: Mean seasonal cycle of (left) observed monthly SSH anomalies (in cm) for 1993 to 2006 and (right) anomalies of the depth of the 23°C isotherm (in m) from REF along the equator and southward along the African coast

from REF as shown in Fig. 3.5 in a Hovmoeller diagram along the equator and continuing southward along the African coast. Two downwelling Kelvin waves occur in February-March and in October-November. After encountering the coast the February-March SSH maximum as well as the boreal summer SSH minimum propagate poleward along the African coast (*Schouten et al.*, 2005; *Polo et al.*, 2008a) while a coastal propagation is less clear for the October-November maximum. As analyzed in detail in a recent study by *Ding et al.* (2009) both Kelvin and Rossby waves contribute to the seasonal SSH signal at the equator, but the Kelvin waves dominate leading to eastward propagation. As illustrated by Fig. 3.5 seasonal variations in thermocline depth and SSH display annual cycles in the western and semiannual cycles in the eastern equatorial Atlantic. *Ding et al.* (2009) showed that the boreal spring downwelling Kelvin wave consists of both annual and semiannual components that occur in phase of each other. Although the semiannual cycle in zonal winds is much weaker than the annual cycle the semiannual component in SSH is shown to be quite strong. Both components are partly forced directly by the wind and partly by reflection processes with the latter being more important for the semiannual component. As a result about 25% of the boreal spring Kelvin wave can be attributed to wave reflection.

3.2.3 EUC

Seasonal current variability along the equator is dominated by two processes: local wind forcing and the propagation and reflection of equatorial waves (*Philander and Pacanowski*, 1986). As a result, the seasonal cycle of the Atlantic EUC transport is not constant throughout the basin but depends on the longitude. In addition, longitudinal differences might also be due to instability wave variability and further modulated by local processes like wind-induced upwelling variability in the eastern part of the basin and the annual cycle of inflow from the NBC in the west (*Hüttl*, 2006).

There is a large range of variability between different observational snap shots as shown by *Hormann and Brandt* (2007). Also models differ considerably (e.g. *Hüttl*, 2006), probably due to the fact that small differences in the state of Rossby and reflected waves in a certain longitude can result in very different EUC strength. Thus the seasonality of the EUC transport is still afflicted with uncertainties. There is, however, general agreement that the seasonal cycle reveals two maxima, one in boreal summer/fall and the other in boreal winter/spring (e.g. *Philander and Pacanowski*, 1986; *Hazeleger et al.*, 2003; *Hüttl and Böning*, 2006). The boreal summer/fall maximum is understood as a near-equilibrium response to the equatorial easterly trades in the central

and western equatorial Atlantic (*Philander and Pacanowski*, 1986). Fig. 3.6 shows the seasonal cycle of the EUC transport at 35°W and 23°W from REF calculated for the different density and depth ranges, respectively, for which the mean transport was given in section 3.1. At 35°W the differences are quite large but for all three EUC definitions the seasonal cycle shows maximum values in May and August/September and minimum values in July and December/January. At 23°W the transport is clearly highest in August/September and lowest in May/June. The shape of the seasonal variations at both longitudes are in agreement with the results by *Hormann and Brandt* (2007).

Since the EUC feeds the equatorial upwelling (e.g. *Hazeleger and de Vries*, 2003) its transport variability has a direct impact on eastern equatorial SST. Besides this $w' \frac{\delta \bar{T}}{\delta z}$ mechanism that changes SST via the anomalous strong upwelling of water with a rather constant temperature, eastern equatorial SST is also effected by subsurface temperature anomalies (corresponding to a shallower or deeper thermocline) reaching the surface with the mean upwelling ($\bar{w} \frac{\delta T'}{\delta z}$). While interannual eastern Atlantic SST variability and a possible influence of EUC transport variations will be discussed in section 4.5, a connection on seasonal time scales is suggested by Fig. 3.7 showing the seasonal cycles of the thermocline EUC transport and Atl3 SST. They are clearly anti-correlated at -0.96 indicating a strong relationship between EUC transport and surface temperatures in the equatorial upwelling region on the annual time scale. It is, however, not clear which of the mechanisms mentioned above dominates. The high correspondence could be either due to an enhanced transport of cold water from the subtropics in boreal summer contributing to the seasonal cool-

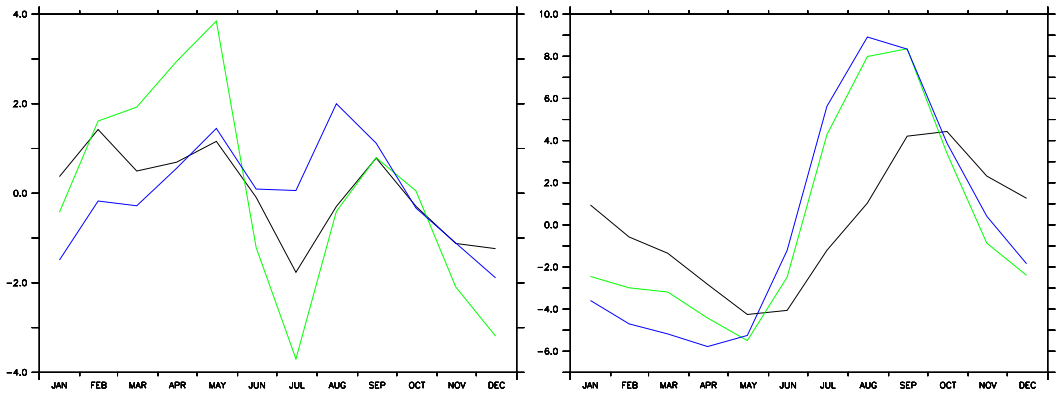

Figure 3.6: Mean seasonal cycle of EUC transport anomalies (in Sv) at 35°W (left panel) and 23°W (right panel) from REF calculated for different density/depth ranges: $\sigma = 23.5 - 26.5 kg/m^3$ ("EUC core", black), $\sigma = 24.5 - 26.8 kg/m^3$ ("thermocline layer", blue) and $z = 0 - 300m$ (green)

ing in the eastern equatorial Atlantic or both EUC transport and SST could rather reflect the seasonal variation of the zonal wind stress. Local wind variations would both increase the EUC transport and enhance local upwelling, leading to cooler SST. The latter interpretation is supported by the fact that the seasonal cycle of the zonal wind stress in the central equatorial Atlantic (30°W to 10°W and 3°S to 3°N) is correlated well with the ones of Atl3 SST ($r = 0.93$) and thermocline EUC transport ($r = -0.84$) as shown in Fig. 3.7.

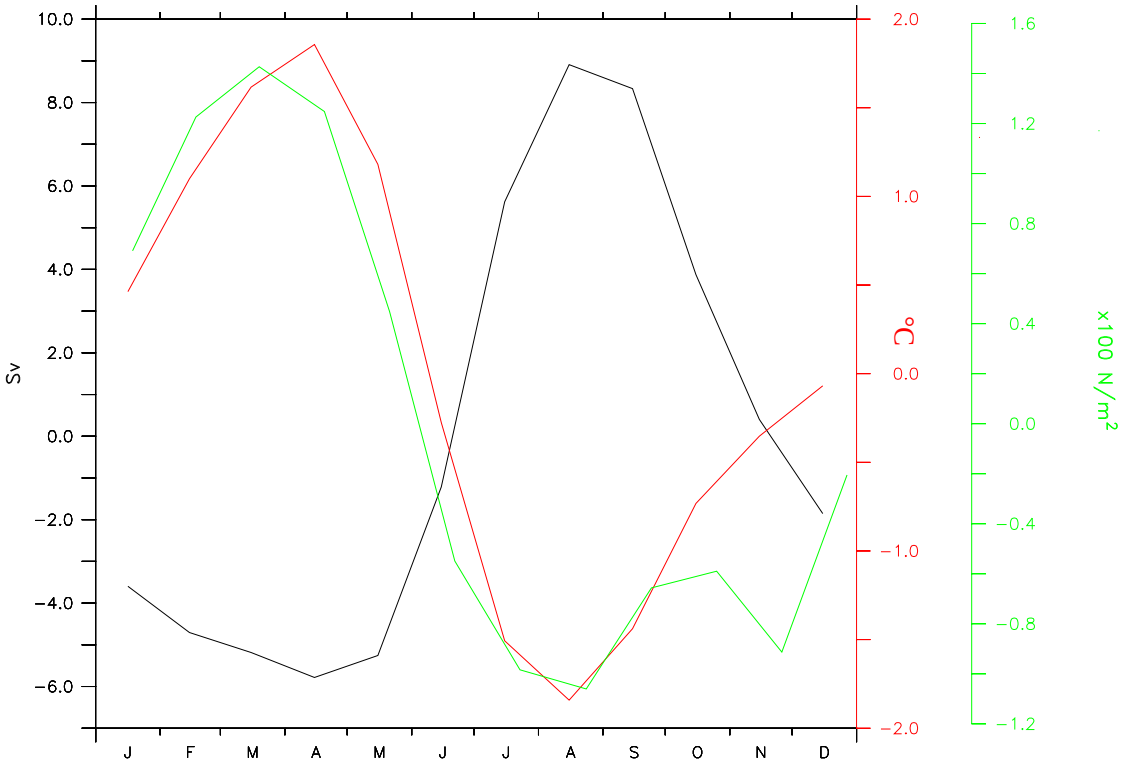

Figure 3.7: Seasonal cycle of thermocline layer EUC transport at 23°W (black) and Atl3 SST (red) from REF (curves are correlated at $r = -0.96$) as well as seasonal cycle of NCEP zonal wind stress averaged over 30°W to 10°W and 3°S to 3°N (green)

4 Interannual variability

But time went on, as it will, and the seasons changed.
(Ann Brashares, The last summer)

The seasonal cycle that dominates SST in the Tropical Atlantic is modulated by year-to-year variations that are of particular importance with respect to rainfall anomalies over the adjacent land masses. In this chapter mechanisms governing the interannual variability of southeastern Tropical Atlantic SST are investigated with ocean model simulations, as well as observational data sets. The main focus is on the recurring events with high SST anomalies off Southwest Africa - the so called Benguela Niños - and their connection to the Atlantic zonal mode.

4.1 Link between Benguela Niños and Equatorial Atlantic Niños

The analysis begins with a comparison between observational SST data and model output for the two regions of interest here: Monthly SST time series from which the mean seasonal cycle was subtracted – in the following referred to as interannual anomalies – from the reference experiment of ORCA05 and NOAA Optimum Interpolation data for the ABA and the Atl3 region are shown in Fig. 4.1. Since the NOAA OI SST product is suspected of involving issues with clouds, which can be problematic off the coast of Angola and Namibia where clouds are present frequently they were compared with data from the Tropical Rainfall Measuring Mission (TRMM) Microwave Imager (TMI) that is able to see through clouds and has a higher horizontal resolution of 0.25°. For the overlapping period of 1999 to 2007, NOAA and TMI SST anomalies averaged over the ABA are correlated well at 0.86 and the agreement is especially good for the maximum/minimum values. The model captures most of the observed interannual SST variability including, e.g., the Benguela and

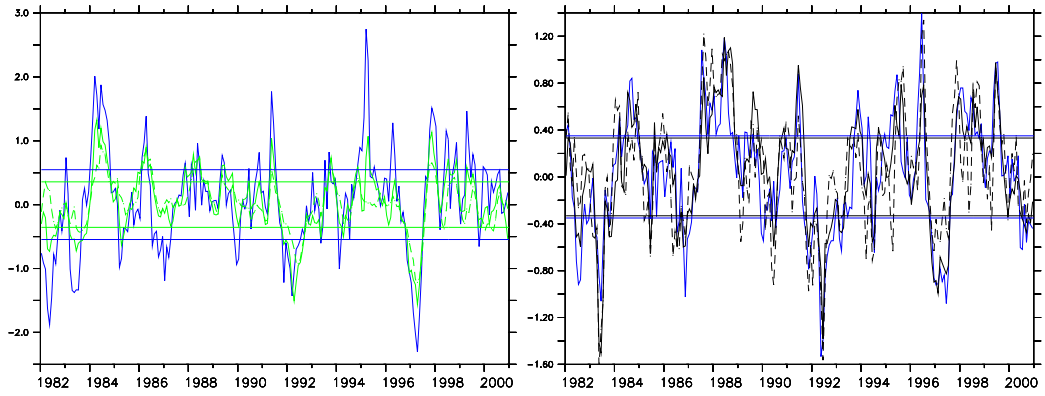

Figure 4.1: Time series of (a) interannual SST (solid lines) and NST (temperature at 40m depth, dashed) anomalies (in °C) averaged over ABA from REF (green) and observed NOAA SST anomalies (blue); (b) interannual SST (solid lines) and NST (temperature at 40m depth, dashed) anomalies averaged over Atl3 from REF (black) and observed NOAA SST anomalies (blue); horizontal lines indicate standard deviation times (-)0.7, used for the definition of Niño and Niña events in this study

Atlantic Niño of 1984 and the Benguela Niña of 1997. The variability in the ABA is, however, underestimated by the model. The standard deviation of the interannual SST anomalies averaged over the ABA region is 0.78 °C in the NOAA observations but only 0.51 °C in the reference experiment. This is apparent for example in 1995 where the observed amplitude is not simulated well, as it was also the case in the model simulation analyzed by *Florenchie et al.* (2004) forced with ECMWF re-analysis wind stress. Since the interannual SST variability in the ABA is higher in a model simulation with increased horizontal resolution of 0.25°, its underestimation in ORCA05 might be related to the representation of coastal upwelling. For the Atl3 region observed (0.50 °C) and simulated (0.47 °C) standard deviations agree very well. Correlations between interannual SST anomalies from the model and observations are 0.83 (ABA) and 0.84 (Atl3), respectively. As discussed in section 2.1.3, one has to be cautious to use SST as a diagnostic of remote forcing mechanisms in an ocean-only model where the ocean surface temperature is damped toward the given atmospheric temperature. Thus NST (temperature below the mixed layer, in 40m depth) will be used in addition to SST to explore the cause of temperature anomalies in the ABA in the next section. As demonstrated in Fig. 4.1 it captures a large fraction of the SST variability, but is below the immediate influence of the local constraint imposed by the thermal boundary condition. Correlations between SST and NST are 0.83 (ABA) and 0.80 (Atl3).

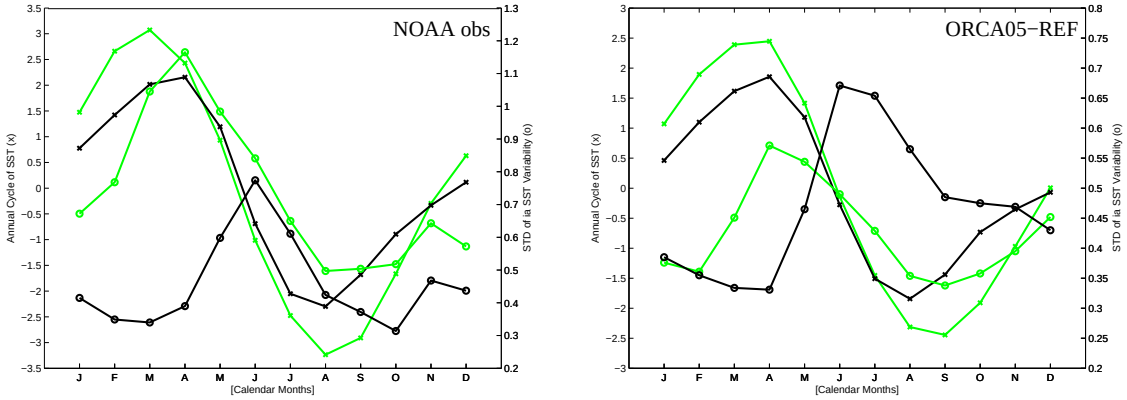

Figure 4.2: Mean annual cycle (crosses) of SST (left axis; in °C) and standard deviation (dots) of interannual SST anomalies (right axis; in °C) in ABA (green) and Atl3 (black) from (a) NOAA observations and (b) from REF; please note the different scales used

The pronounced interannual variability in both the ABA and the Atl3 region displays anomalies that in some cases even reach the magnitude of the dominant annual cycle, as shown in Fig. 4.2 for observations as well as from the model simulation. As noted already in section 3.2.1, the seasonal cycle is very similar for both regions with SST reaching its maximum in March/April and its minimum in August/September. In addition to the seasonal cycle in SST, Fig. 4.2 shows the seasonal variations of interannual SST variability depicted here as the standard deviation of the interannual SST time series for different calendar months. It is striking that in both model and observational data, interannual variability peaks in the cold season in the eastern equatorial Atlantic, while the maximum occurs as an amplification of the seasonal cycle in the ABA. This different phase-locking to the seasonal cycle will be discussed later.

In the literature, there is no agreed criterion for classifying Benguela or Equatorial Atlantic Niños and Niñas, respectively. Here, Benguela (Equatorial Atlantic) Niño and Niña events are defined as periods in which SST anomalies averaged over the ABA (Atl3 region) exceed the standard deviation of the time series multiplied by (-)0.7 for at least 3 months in a row. The threshold is indicated by horizontal lines in Fig 4.1. It is obvious that there are Niño and Niña conditions that co-occur in both regions, e.g. warm events in 1984, 1988, 1991 and 1995 and cold events in 1982, 1983, 1992 and 1997. As shown by the

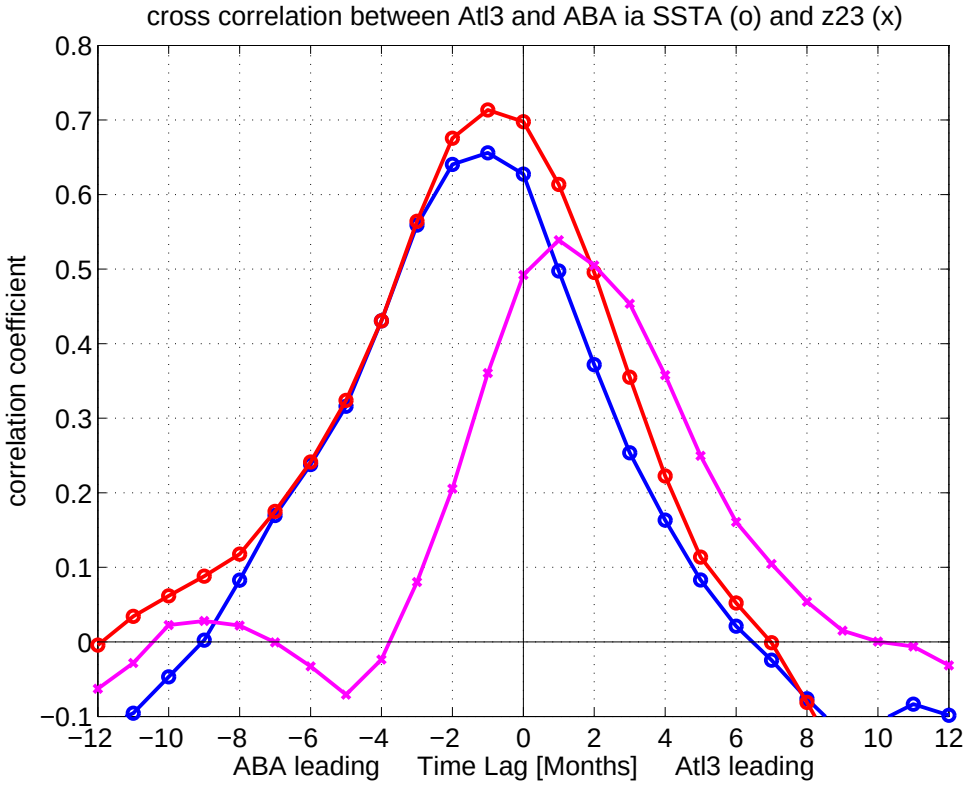

Figure 4.3: Cross correlation between Atl3 and ABA interannual variability of the depth of the 23 °C isotherme (magenta) and SST from REF (red) and NOAA obs (blue) for the time period of 1982 to 2000

cross correlation function, interannual SST variability in Atl3 and ABA are correlated with a value of about 0.7 in both the model and observations (Fig. 4.3). The correlation is highest when the ABA region leads by 1 month indicating that warming in the ABA occurs prior to a warm event at the equator. This behaviour is consistent with the findings of *Reason and Rouault* (2006), *Hu and Huang* (2007), *Polo et al.* (2008b) and *Rouault et al.* (2009), but rather surprising in view of the remote forcing generation mechanism suggested by *Florenchie et al.* (2003, 2004) that was described in Chapter 1. In order to find out why the warming off Angola leads the one at the equator the generation mechanism for SST anomalies in the ABA will be the focus of the next section.

4.2 Forcing of Benguela Niños

In this section model simulations with special focus on the perturbation experiments are used to elucidate the forcing of SST variations in the ABA. For the developement of Benguela Niños there are basically two scenarios discussed in the literature. *Florenchie et al.* (2003, 2004) propose a mechanism based on Kelvin wave propagation from the western equatorial Atlantic, shown schematically in Fig. 1.3. In contrast *Polo et al.* (2008b) suggest that SST anomalies off Angola are due to upwelling anomalies caused by local winds and then might reach the cold tongue region via westward Rossby wave propagation.

If equatorial (and subsequent coastal) Kelvin waves were important for the generation of SST anomalies off Angola, subsurface anomalies should be closely related to anomalies in SST. The connection between the depth of the 23°C isotherm (z23) as a proxy of the thermocline depth (following *Florenchie et al.*, 2003) and SST is investigated in Fig. 4.4. Correlations between interannual

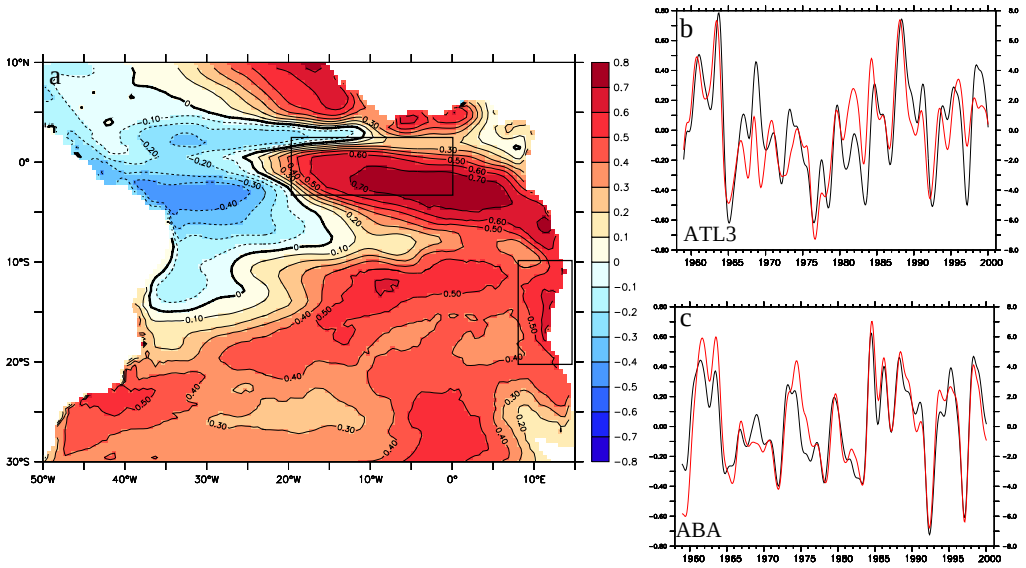

Figure 4.4: (a) Correlation between interannual anomalies of SST and depth of 23 °C isotherm (z23) from REF; boxes indicate ABA and Atl3 region; (b) and (c) Timeseries of smoothed interannual SST (in °C, black, left axes) and z23 (in m, red, right axes) anomalies averaged over Atl3 region (b) and ABA (c)

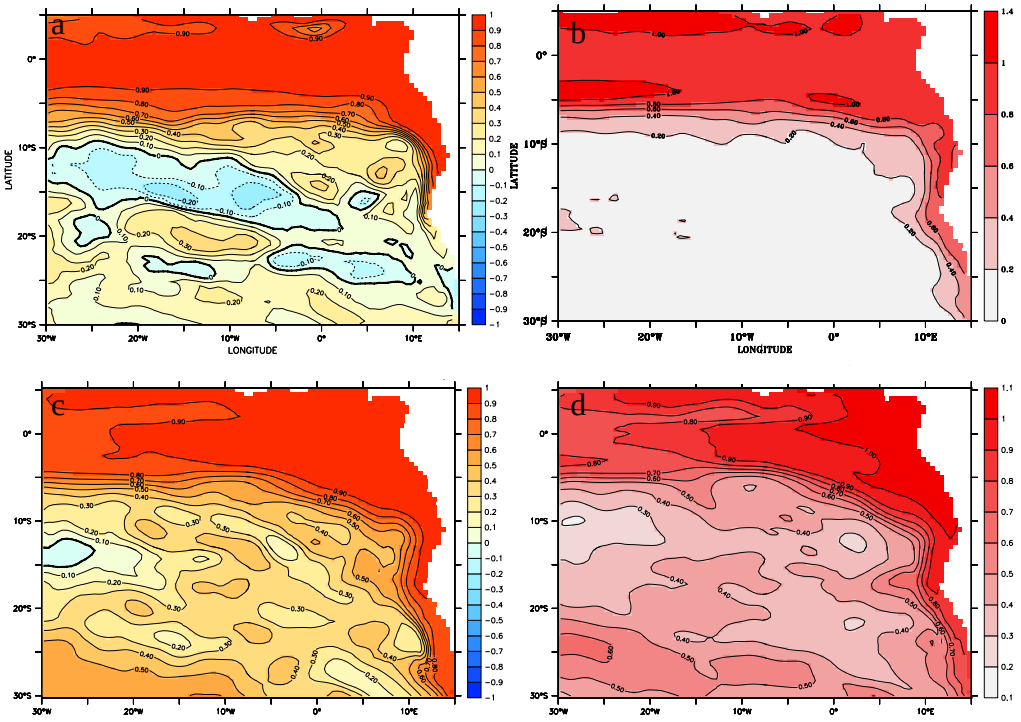

Figure 4.5: Interannual NST anomalies for 1958–2000: (a) Correlation between REF and EQ; (b) Ratio between standard deviation from REF and EQ; (c) Correlation between REF and WIND; (d) Ratio between standard deviation from REF and WIND

anomalies of z23 and SST are highest in the cold tongue region but good correspondence is also found along the southern African coast and particularly in the ABA (Fig. 4.4a). Time series of interannually smoothed SST and z23 anomalies (Fig. 4.4b, c) are correlated at 0.91 (ABA) and 0.77 (Atl3) for zero lag. The correlation in the Atl3 region goes up to 0.80 for variations in z23 leading SST anomalies by one month. The results indicate that ABA and Atl3 SST anomalies are tied to thermocline variations, and hence could be remotely forced.

There are two aspects of the forcing that are of particular interest here. The first one concerns the relative importance of remote forcing from the equatorial region and the second one deals with the role of dynamical vs. thermodynamical forcing for interannual NST variability in the ABA. To address these points the two perturbation experiments EQ (with interannually varying forcing con-

fined to an equatorial band) and WIND (with interannually varying forcing restricted to momentum fluxes while thermohaline fluxes are based on a climatological annual cycle) are analyzed. As discussed in the previous section the analysis below will focus on NST rather than SST.

The correlation between interannual NST anomalies from EQ and REF as well as the ratio between their standard deviations are shown in Fig. 4.5a, b. Values are naturally highest in the equatorial band where EQ is forced interannually, but beyond that there is a tongue of high correspondance reaching from the equator southward into the ABA. Especially in the ratio of the standard deviations, the southward extension along the coast is clearly visible. The correlation between time series of NST anomalies from REF and EQ averaged over the ABA is 0.52. This indicates that a significant part of the interannual NST variability in the Benguela region in REF is of equatorial origin, i.e. remotely forced, which is consistent with the mechanism proposed by *Florenchie et al.* (2003, 2004).

The correlation map between interannual NST anomalies from REF and WIND (Fig. 4.5c) shows high correlations in the whole eastern equatorial Atlantic, especially in the cold tongue region, and along the African coast demonstrating that NST variability in these areas is nearly completely attributable to wind stress variations. This is supported by the ratio between the standard deviation of interannual NST anomalies from REF and WIND (Fig. 4.5d) showing that eastern tropical NST variability in WIND is almost as high as in REF. Time series of NST anomalies from REF and WIND averaged over the ABA are correlated at 0.79. This is consistent with *Carton et al.* (1996) finding that on interannual time scales eastern equatorial SST variability is driven by wind stress variations. The higher correlations between REF and WIND than between REF and EQ indicate that in addition to the remote forcing also local wind variations are in general important for the ABA SST variability, as suggested by *Richter et al.* (2010).

The composite difference in SST, z23 and wind stress from REF between years with Benguela warm events taking place in March-April-May (MAM warm event years, defined as years in which an interannual ABA SST anomaly exceeds 0.7∗Std in MAM and peaks in one of these months: 1963, 1974, 1984, 1986, 1988 and 1995) and the climatological mean for different calendar months (Fig. 4.6) shows that especially the southeasterly trade winds in the central equatorial Atlantic are weakened in the months prior to a Benguela warming. The Benguela SST anomaly peaks in April, followed by a warming in the east-

ern equatorial Atlantic that reaches its maximum in June, in agreement with the cross correlation between ABA and Atl3 SST anomalies (Fig. 4.3) and the seasonality of the interannual variability (Fig. 4.2). In contrast to the clear relaxation of the trades, there is no significant wind stress change directly at the African coast, indicating that remote forcing is more important than local upwelling anomalies for the generation of warm events. Consistent with the idea of Kelvin waves being responsible for temperature anomalies off Angola and the correlation map between z23 and SST shown in Fig. 4.4, there is a thermocline signal in the ABA when the SST anomaly shows up.

In total, the perturbation experiments in combination with the composite analysis and the close relationship between subsurface and SST anomalies confirm the results by *Florenchie et al.* (2003, 2004) and *Rouault et al.* (2007) that warm events off Angola are remotely forced from the equator via Kelvin wave propagation. While local winds play an important role for the general SST variability of the region they are not responsible for the generation of strong warm events.

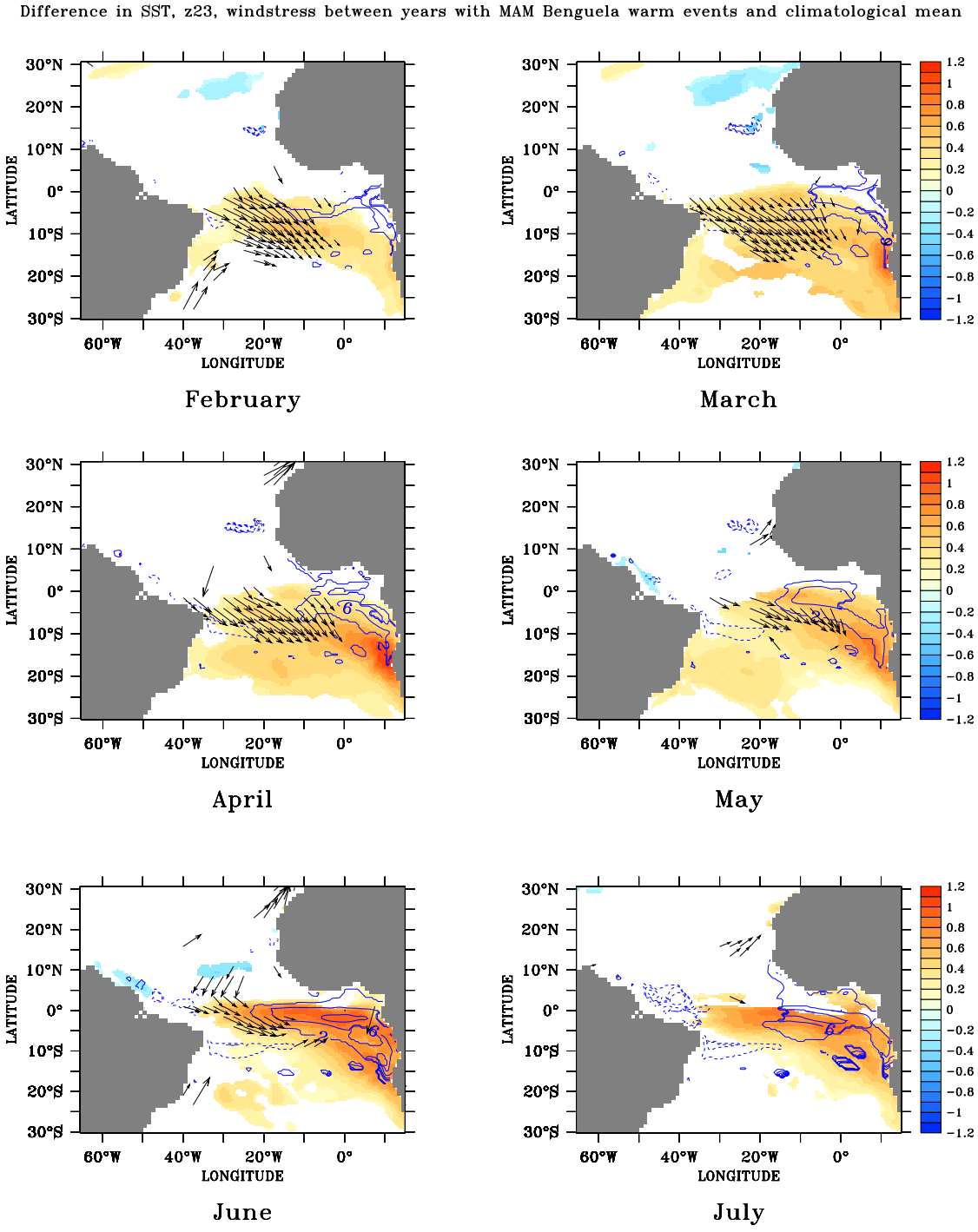

Figure 4.6: Composite difference in SST (°C, color), z23 (m, contour lines) and wind stress (N/m^2, vectors) from REF between years with MAM Benguela warm events (years in which interannual ABA SST anomaly exceeds 0.7 x Std in MAM and peaks in one of these months) and climatological mean for different calendar months; only values significant at the 95% level are shown

4.3 Cause of the direction of the time lag between the warming in the ABA and in the eastern equatorial Atlantic

As shown in the previous section, Benguela Niños appear to be primarily forced remotely from the equator via Kelvin wave propagation. Thus one might expect a warming (cooling) to take place first at the equator and then at the African coast. So why does the warm events in the ABA occur prior to those at the equator (Atl3 region)?

Three possibilities are considered in order to explain the lead-lag relationship in the occurence of SST anomalies off Angola and in the eastern equatorial Atlantic. First the difference in mean thermocline depth will be investigated, followed by a discussion of the importance of the seasonality. Last, the role of an atmospheric feedback that was suggested by *Hu and Huang* (2007) will be touched on.

4.3.1 Mean thermocline depth

Since subsurface temperature anomalies associated with the Kelvin waves propagate along the thermocline the time it takes for them to affect the temperature at the surface depends on the depth of the thermocline. Fig. 4.7 shows a map of the mean depth of the 23°C isotherm (z23) as a measure of the thermocline. In the ABA the thermocline is very shallow - with a box average of 30m - which allows for a close coupling between subsurface anomalies and SST variations. In the Atl3 region, however, the mean thermocline is 63m deep, so that subsurface anomalies must be lifted – by upwelling and vertical mixing – to affect SST (cf. "upwelling pathway" described in *Zelle et al.*, 2004, for the eastern Tropical Pacific). Following the estimate by *Zelle et al.* (2004) (their equation 2), the difference in mean thermocline depth alone would cause a time lag of about two weeks in the response between subsurface temperature anomalies and SST between the two regions. The mean thermocline depth might, however, be of limited significance since the thermocline depth in the southeastern Tropical Atlantic as well as SSH and SST variability exhibits pronounced seasonality.

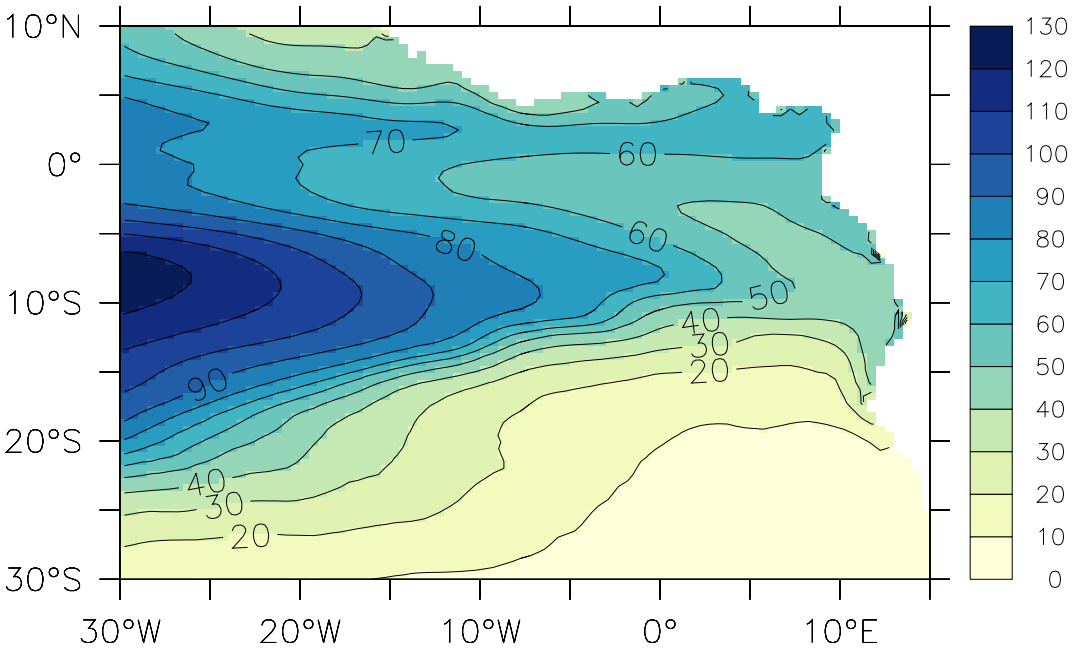

Figure 4.7: Mean depth of the 23 °C isotherm in REF (1958 – 2000)

4.3.2 Seasonality

Concerning the seasonality of the interannual SST variability (Fig. 4.2) the lag between Benguela and equatorial Atlantic Niños appears to be reflected by the lag between the seasons of highest interannual variations. While SST variability in the ABA is highest in March and April, it peaks in June/July in the Atl3 region. Thus to understand the lag between warm (cold) events off Angola and in the eastern equatorial Atlantic it is necessary to understand the different phase relationship of the events to the seasonal cycle. When compared to the seasonal cycle in SST, it is striking that while interannual warm events at the equator take place during the cold season (cf. e.g. *Carton and Huang*, 1994), Benguela warm events occur mainly as an amplification of the seasonal cycle. Figure 4.2 shows that both in observations and the model simulation, interannual SST variability in the ABA is highest in March/April when the climatological SST is at its maximum. It is interesting to note that in the Pacific the ENSO warming at the Peruvian coast also occurs as an amplification of the regular seasonal cycle, while the largest SST anomalies in the eastern equatorial Pacific take place during the cold season (*Xie*, 1995).

For the Atl3 region, the period of high SST anomalies is consistent with the

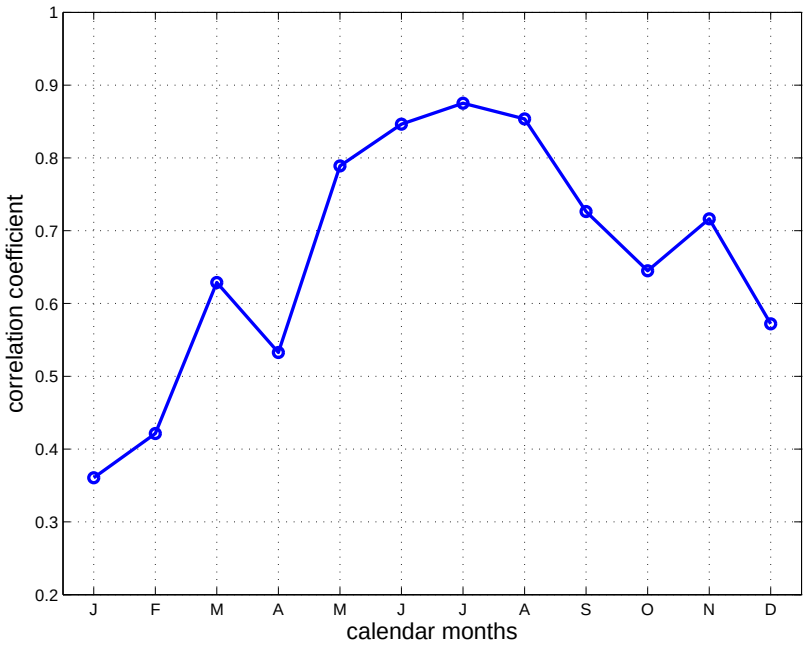

Figure 4.8: Seasonality of the correlation between interannual anomalies of SST and z23 in the Atl3 region from REF as a measure of subsurface - surface coupling

season of the shallowest thermocline (e.g. *Xie and Carton*, 2004). *Keenlyside and Latif* (2007) showed that a coupling between subsurface and surface in the eastern Tropical Atlantic is strongest in austral winter as a result of both a shallow thermocline and a peak in upwelling. This is illustrated by the correlation between interannual anomalies of SST and z23 from the Atl3 region as a function of calender months which peaks in JJA (Fig. 4.8). The phase locking of the subsurface-surface coupling in the eastern equatorial Atlantic to austral winter, in combination with the year-round shallow thermocline in the ABA, renders the possibility that subsurface temperature anomalies arrive first in the Atl3 region but are visible at the surface only later, after they outcropped in the ABA. This idea is supported by the fact that, in contrast to the cross correlation function for SST anomalies, the one for the depth of the thermocline is shifted towards "Atl3 leading" (Fig. 4.3). Consistent with this *Hormann and Brandt* (2009) found that equatorial Kelvin waves in austral fall precondition the upper layer stratification and thereby significantly influence the strength of the cold tongue in austral winter, while the direct influence of equatorial Kelvin waves on cold tongue SST in austral fall is small.

In contrast to the eastern equatorial Atlantic, a seasonal shallowing of the thermocline is obviously not required as a precondition for the occurence of Benguela warm events. In the months of highest SST variance in the ABA the thermocline is actually deepest. This relation might be due to the fact that only in austral fall the thermocline is deep enough for Kelvin wave signals to propagate down the coast all the way to the ABA while the thermocline outcrops north of the ABA in austral winter. The period of highest interannual SST variability in the ABA thus appears to be phase locked to the seasonal migration of the Angola Benguela Front (ABF). As described by *Shannon et al.* (1987) and *Meeuwis and Lutjeharms* (1990), the ABF is located furthest to the south in January to March and furthest to the north in July to September. In agreement with that the seasonal cycle of the latitude in which SST equals 23°C from NOAA observations (Fig. 4.9 a) shows the southernmost position in March and the northernmost postion in August. Consistent with the northward shift of the ABF from austral fall to winter, the maximum of interannual SST variability along the west African coast migrates northward, peaking in April in the ABA but in May/June closer to the equator (Fig. 4.9 b). This indicates that even if Kelvin waves were propagating along the coast all year long they might outcrop in the ABA only in austral fall and thus not influence SST in the other seasons.

Seasonality may not only be due to local variations in the mean state, but also due to remotely forced Kelvin waves, which are known to be subject to interannual variations. As described in section 3.2.2 the climatology of observed SSH in the equatorial Atlantic reveals two downwelling Kelvin waves, one in February-March and one in October-November. After encountering the African coast the February-March SSH maximum propagates poleward as far as 22°S (*Schouten et al.*, 2005; *Polo et al.*, 2008a) while a coastal propagation is not as clear for the October-November maximum. Following *Polo et al.* (2008a) the coastal signal propagation will be referred to as coastal Kelvin wave although it might be mixed with a shelf wave signal. Similar to the climatology by *Schouten et al.* (2005), Fig. 4.10a shows the seasonal cycle of observed SSH along the equator and continuing southward along the African coast. A manifestation of the two downwelling Kelvin waves is clearly visible, both travelling down the coast with the maximum of the February-March wave reaching the ABA in March-April. An interannual variation in the annual February-March-April (FMA) Kelvin wave would thus result in a concentration of SST variability in the Angola Benguela area in these months. Accordingly, the seasonal cycle of the standard deviation of interannual SSH anomalies (Fig. 4.10b) shows variations in February-March in the eastern equatorial Atlantic connected to strong variability off the African coast all the way southward

to the ABA where the maximum variability occurs in April. Enhanced interannual SSH variations along the equator also occur in austral winter and some minor variations close to the eastern boundary in austral spring, but the only continuous signal from the equatorial Atlantic to the ABA takes place in February-March-April. The signal is weakened if also the years 2000 to 2007 are taken into account. The strong variability in austral fall is in agreement with the description of the interannual SSH variability given by *Schouten et al.* (2005) who reported that the strength of the February-March Kelvin wave is subject to strong interannual variations in contrast to the October-November wave. We conclude that the combination of the FMA Kelvin wave propagating down the coast as a coastal Kelvin wave, the high interannual variability of this wave, and the southernmost position of the ABF at that season allowing the Kelvin wave to reach the ABA and impact SST there, is behind the maximum in interannual SST variations off Angola in March and April. Consistent with this explanation *Rouault et al.* (2007) argue that the Benguela Niño in 2001 was forced by a SSH anomaly that occured as an amplification of the seasonal cycle in SSH.

Since equatorial Kelvin waves are forced by wind stress variations on the equator it is puzzling that there is no peak in the interannual variability of the equatorial winds in late austral summer (not shown). There may, however, be large atmospheric stochastic variability at that time of the year related to the weak mean wind stress due to the ITCZ being closest to the equator. According to results by *Ding et al.* (2009), variations of the FMA Kelvin wave signal might actually be related to the weaker semiannual component of the wind field. In view of the semiannual cycle of the zonal winds being comparatively weak the cause for interannual variability of the FMA Kelvin wave is difficult to assess.

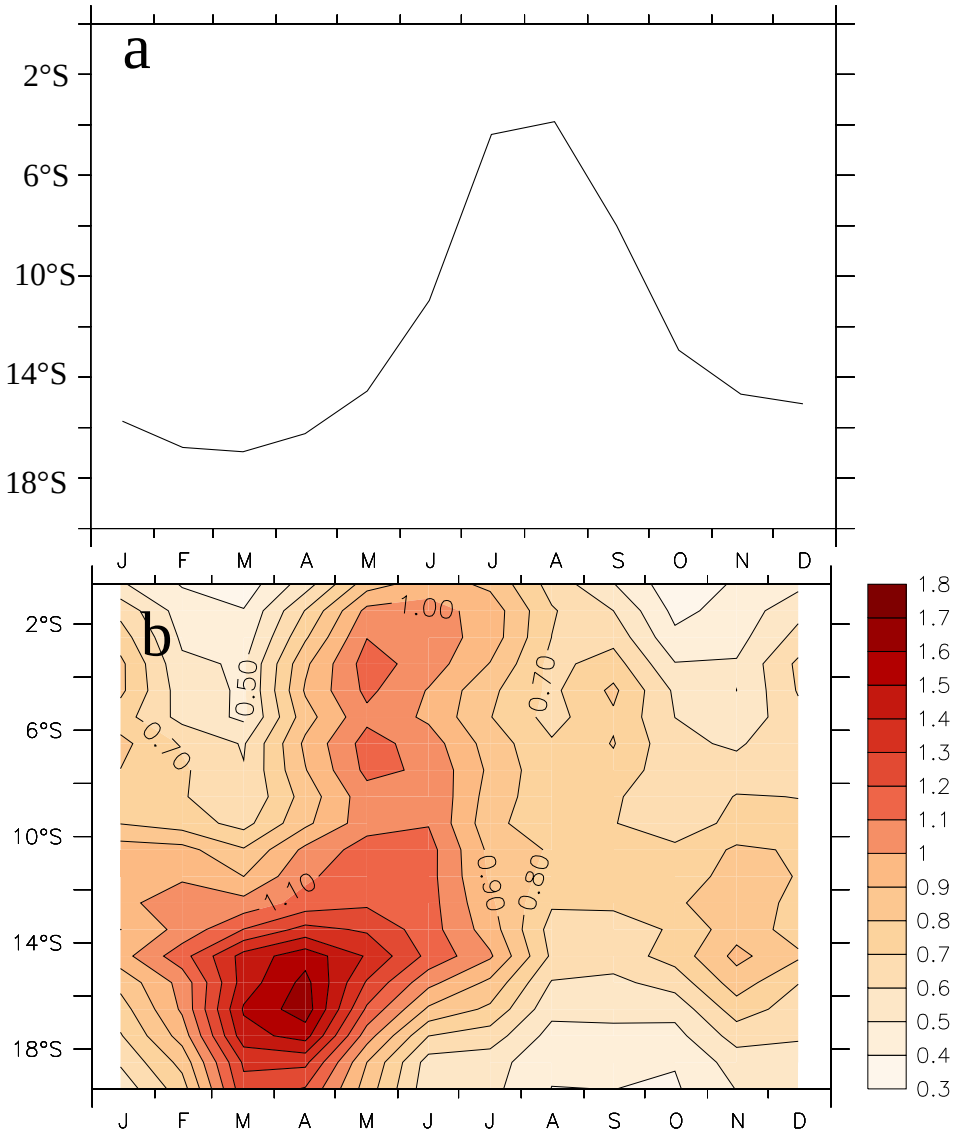

Figure 4.9: Seasonal cycle of (a) latitude in which SST (averaged over 10°S to 15°S) equals 23°C (b) standard deviation of interannual SST anomalies (in °C) along West African coast from NOAA observations (1982 to 2007)

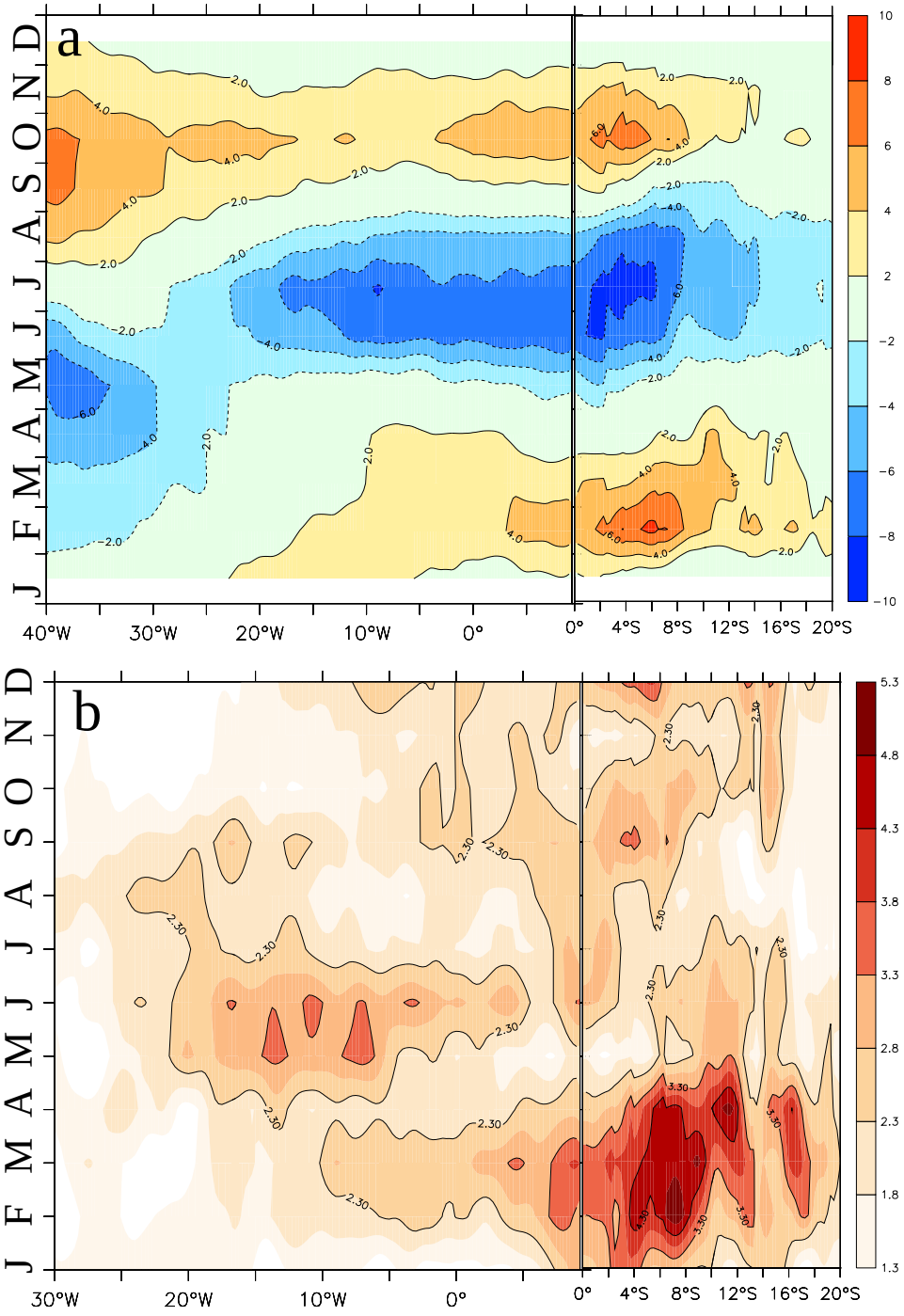

Figure 4.10: Seasonal cycle of (a) observed SSH (in cm) and (b) standard deviation of interannual SSH anomalies (in cm, from weekly data 1993 to 2000) along the equator and southward along the African coast

4.3.3 Coupled ocean-atmosphere mode

Another potentially important aspect in the relation between the ABA and Atl3 SST anomalies is the feedback of the coupled ocean-atmosphere system discussed by *Hu and Huang* (2007). A local SST anomaly occuring in the ABA may have an impact on the atmosphere that then in turn leads to SST changes at the equator by changing the local upwelling of cold water or the zonal pressure gradient (*Carton and Huang*, 1994). *Hu and Huang* (2007) described the connection between SST anomalies along the Angolan coast and near the equator in austral winter as a dynamical air-sea coupled mode. They suggest that coastal warming in austral fall induces a wind convergence over the basin that causes westerly wind anomalies in the southern tropical and equatorial Atlantic. The equatorial warming is then intensified by local positive Bjerknes and Ekman feedbacks. This idea is not pursued further here. In a correlation map between April ABA SST and wind stress fields for different calender months, however, equatorial westerly wind anomalies that are associated with ABA SST anomalies occur prior to a Benguela warming (Fig. 4.11), not supporting the idea of wind changes forced by ABA SST. Nevertheless, there are also wind anomalies occuring after the warm event, suggesting that the wind stress at the equator might respond to a Benguela warming.

In summary we conclude that two factors contribute to the direction of the lag between Benguela and Equatorial Atlantic Niños: the difference in thermocline depths in the two regions, and a different phase locking of the interannual SST variability to the seasonal cycle. In the eastern equatorial Atlantic SST variability is highest in austral winter when subsurface-surface coupling is strong due to the shallow thermocline and maximum upwelling. Off Angola the seasonality of the interannual SST variability is determined by the seasonal migration of the ABF and the seasonal variations in coastal wave variability. The ABF reaches its southernmost position in austral fall allowing the annual Kelvin wave that takes place in February-March to reach the ABA and impact the SST. Furthermore, consistent with the peak in interannual SST variability, the strength of this wave displays high interannual variability. As a result Benguela Niños tend to peak in March-April-May while Equatorial Atlantic warm events reach their maximum a few months later in June-July.

Together with the high correlation between interannual SST variability in the ABA and the cold tongue region (Fig. 4.3) and the remote forcing mechanism, the explanation of the order of events in terms of a lagged response in the Atl3 region suggests that Benguela and Equatorial Atlantic warm events are part

of one phenomenon (cf. *Hu and Huang*, 2007) and can be traced back to the same forcing event. Towards this end the question of the connection between eastern tropical SST anomalies and variations of the large-scale atmospheric circulation is the focus of the next section.

4.4 Role of the South Atlantic Anticyclone

Near surface temperature anomalies in the eastern Tropical Atlantic have been shown to be mainly driven by wind stress variations (Fig. 4.5c and d, e.g. *Carton et al.*, 1996). In order to elucidate what triggers the joint eastern Tropical Atlantic Niños, we will have a closer look at the wind stress. A long-term mean of NCEP wind stress over the southern (sub)tropical Atlantic is shown in Fig. 1.1. The tropical region is dominated by the Southeastern Trade Winds. Together with the midlatitude westerlies and the equatorward winds along the west coast of Southern Africa they form the South Atlantic Anticyclone (SAA) that is indicated by a black ellipse in Fig. 1.1.

Since the interannual SST variability in the Angola Benguela area peaks in

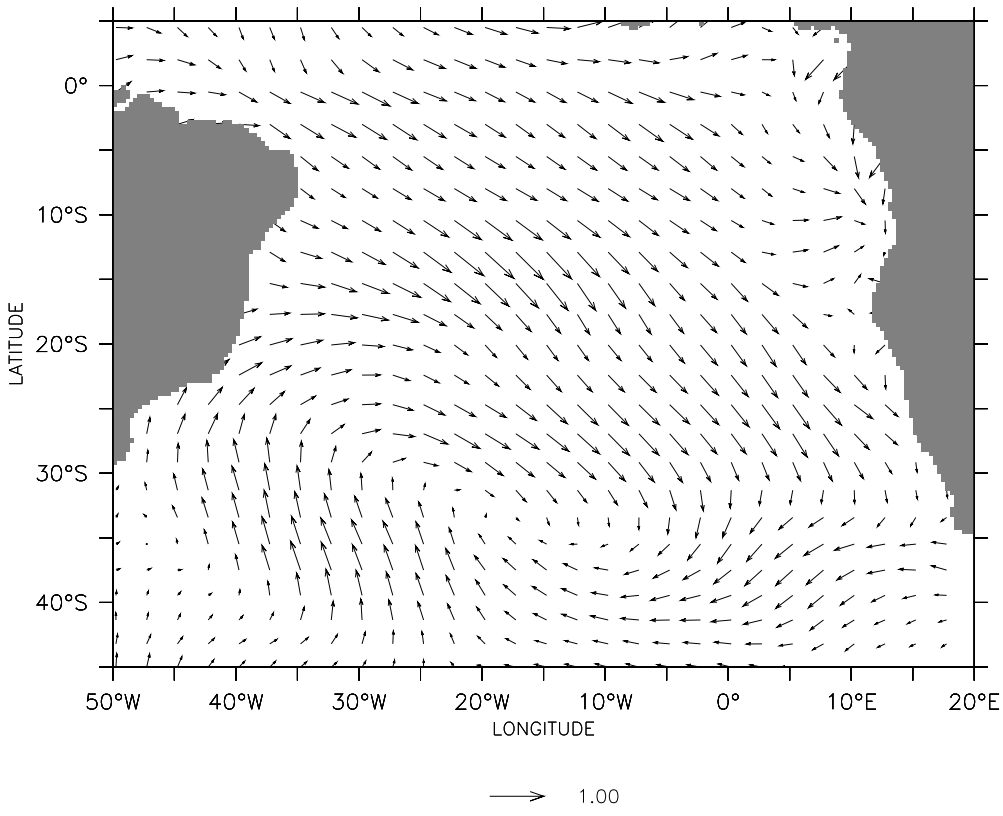

Figure 4.11: Correlation between a time series of April SST averaged over the ABA and a field of February wind stress (the x and y component of the vectors are correlation with zonal and meridional wind stress, respectively) from REF for the time period 1958 – 2000

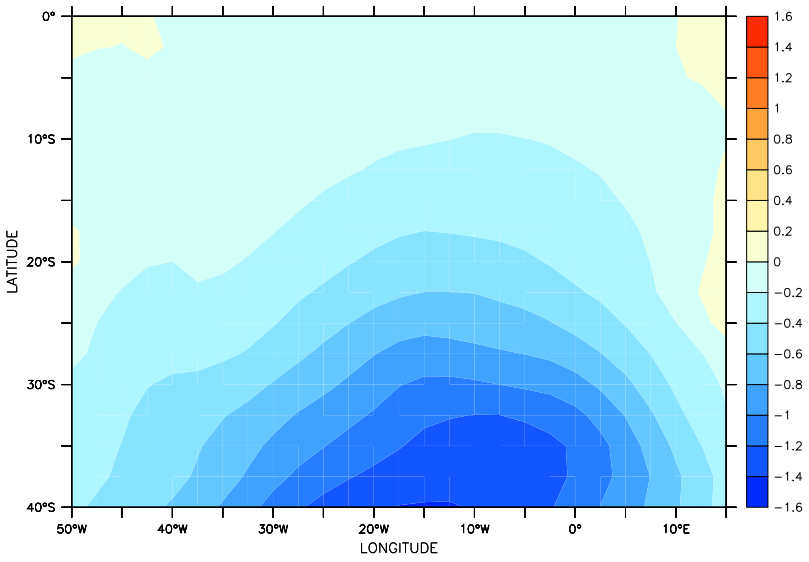

Figure 4.12: First EOF of the total Sea Level Pressure (SLP) variance for 1982 to 2007 austral summer (DJF) from the NCEP reanalysis product

April (Fig. 4.2), it is instructive to examine the relation between April SST averaged over the ABA and the wind field in the preceding months. The correlation map between April ABA SST and February wind stress (Fig. 4.11) clearly shows a weakening not only of the trade winds (as described in *Florenchie et al.*, 2004) but of the whole South Atlantic Anticyclone prior to the the Benguela warming. Variations in the strength of the subtropical high are one possibility to alter the southeasterly trade winds (the other would be variations in the intertropical convergence zone (ITCZ)). They can therefore directly influence the equatorial Atlantic (*Robertson et al.*, 2003). The variability of the SAA actually turns out to be the first EOF (shown in Fig. 4.12). It explains 56% of the austral summer (DJF) Sea Level Pressure (SLP) variance for the period 1982 to 2007 and over the South Atlantic basin (40°S to 0°S, 50°W to 15°E). This mode is significantly correlated with the March/April SST in the ABA at $r = -0.57$. A possible connection between changes in the subtropical high and SST anomalies in the southeastern Tropical Atlantic has been discussed by *Hu and Huang* (2007). They found the evolution of SLP patterns to be consistent with the ones of SST and wind stress. Also, in a anomaly coupled GCM study, *Bates* (2008) found a weakening of the subtropical high affecting SST along the Angolan coast.

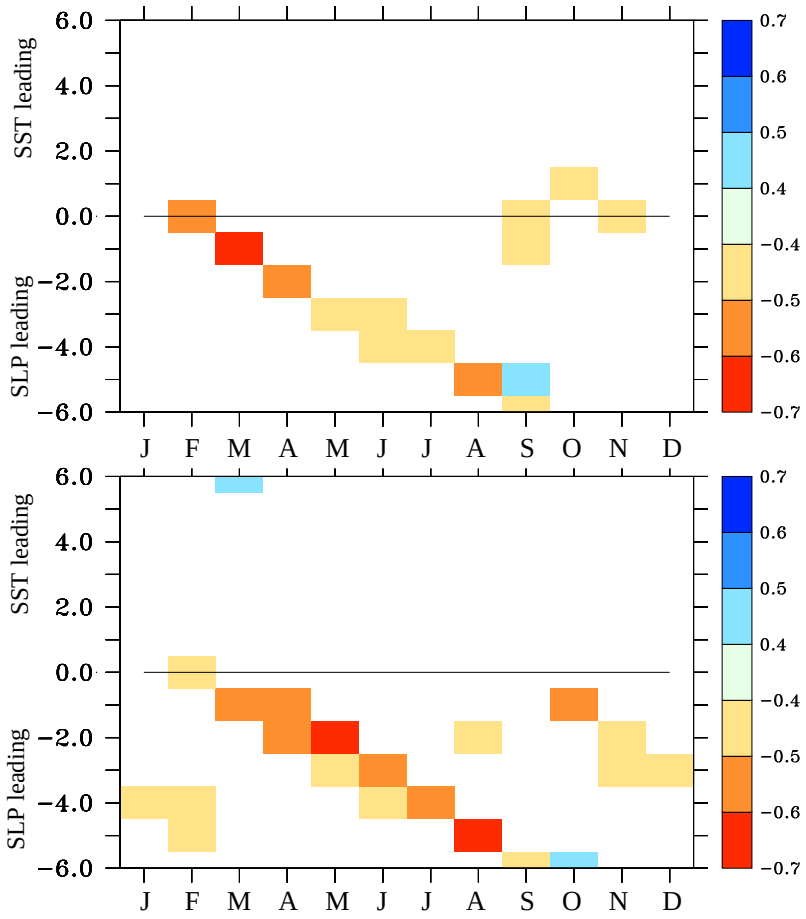

Figure 4.13: Monthly stratified cross correlation between interannual anomalies for 1982 to 2007 of SAA index (SLP averaged over 40°S to 20°S and 30°W to 10°W) and a) NOAA ABA SST (correlations greater than 0.36 are significant at the 95% level); b) NOAA Atl3 SST (correlations greater than 0.43 are significant at the 95% level); months on lower axis indicate the month for SST

In order to examine the connection between the South Atlantic Anticyclone and SST variability in the ABA and Atl3 region in more detail, a simple index for the strength of the SAA is defined by averaging SLP over 40°S to 20°S and 30°W to 10°W. This index is then decomposed into indices for every month of the year and correlated with interannual anomalies of observed ABA and Atl3 SST for different calendar months. The resulting monthly stratified cross correlation functions are shown in Fig. 4.13. The one for the ABA (Fig. 4.13a) shows a good correlation of about 0.65 in March with SLP leading by one month. There is a band of high correlation indicating that the strength of

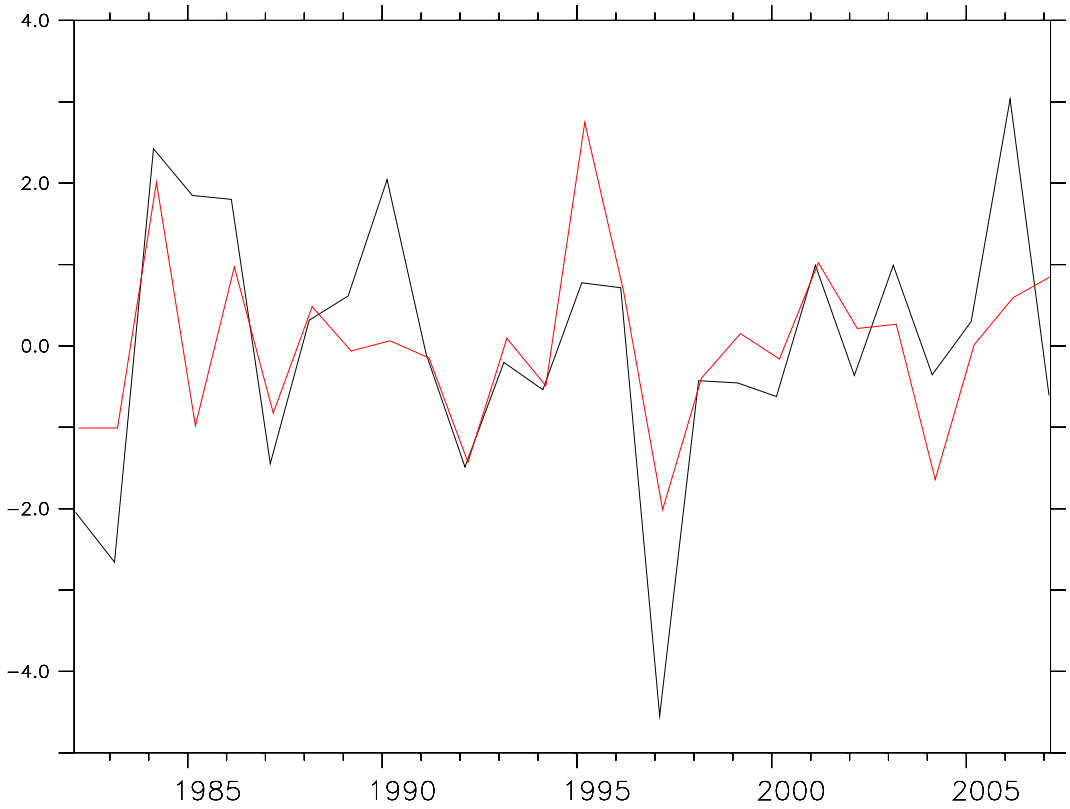

Figure 4.14: Time series of interannual anomalies of February SAA index (SLP averaged over 40°S to 20°S and 30°W to 10°W in millibars, inverted, black) and March ABA SST (in °C, red) from observations; correlation between time series is -0.65

the SAA in February is linked to ABA SST variability in the following austral fall (especially March and April). This connection is confirmed by time series of February SLP anomalies and March ABA SST anomalies (Fig. 4.14) that clearly show positive SLP anomalies in Benguela Niña years (e.g. 1997) and negative SLP anomalies for years with Benguela Niño events (e.g. 1984). Also the SST variability in the eastern equatorial Atlantic is linked to variations in the strength of the SAA. The monthly stratified cross correlation between interannual anomalies of Atl3 SST and the SAA index (Fig. 4.13b) show highest correlation of about 0.6 in May and August with SLP leading by two and five months, respectively. A diagonal band of negative correlations, reminiscent of the one seen for the ABA, reaches from March to August.

To conclude, the austral fall/winter SST variability in the eastern Tropical

Atlantic appears to be influenced by variations in the strength of the South Atlantic Anticyclone in the preceding late austral summer. The restriction of the SAA influence to February and March is reflected in the correlation between the SAA index and zonal wind anomalies in the western and central equatorial Atlantic being high only in these months (not shown).

4.5 Connection to EUC variability

The wind stress variations whose role have been discussed in the last sections, in particular the relaxation of the trade winds in the western equatorial Atlantic, do not only excite Kelvin waves but also have a direct impact on the zonal currents. These may also affect the SST in the eastern equatorial Atlantic by transporting more or less cold water eastwards.

In a composite analysis from 40 years of NCOM model data, *Góes and Wainer* (2003) showed that SEC and EUC are strengthened in equatorial Atlantic cold event years and weakened in warm event years. Using output from the high resolution Atlantic ocean model FLAME, *Hormann and Brandt* (2007) also found that interannual boreal summer variations of near-surface temperatures in the cold tongue region are anticorrelated with thermocline EUC transport anomalies.

In agreement with their results, composite analysis of Benguela Niño and Niña phases from REF show that the zonal currents are weakened during warm phases and strengthened during cold phases, consistent with the change in wind stress (not shown). Time series of interannual anomalies in thermocline EUC transport at 23°W and Atl3 SST (Fig. 4.15) confirm that a high EUC transport is related to colder surface temperatures in the eastern equatorial Atlantic on interannual time scales. The time series are anti-correlated at -0.61. As discussed in section 3.2.3 with respect to the seasonal cycle, the connection may not only be due to the advection of more or less cold water within the EUC supplying the upwelling, but also related to changes in subsurface temperatures (remotely driven) and local winds that will both influence SST as well as the EUC transport. A thorough budget analysis would be necessary to distinguish between the different terms, in particular $w' \frac{\delta \bar{T}}{\delta z}$ versus $\bar{w} \frac{\delta T'}{\delta z}$ but is beyond the scope of this study.

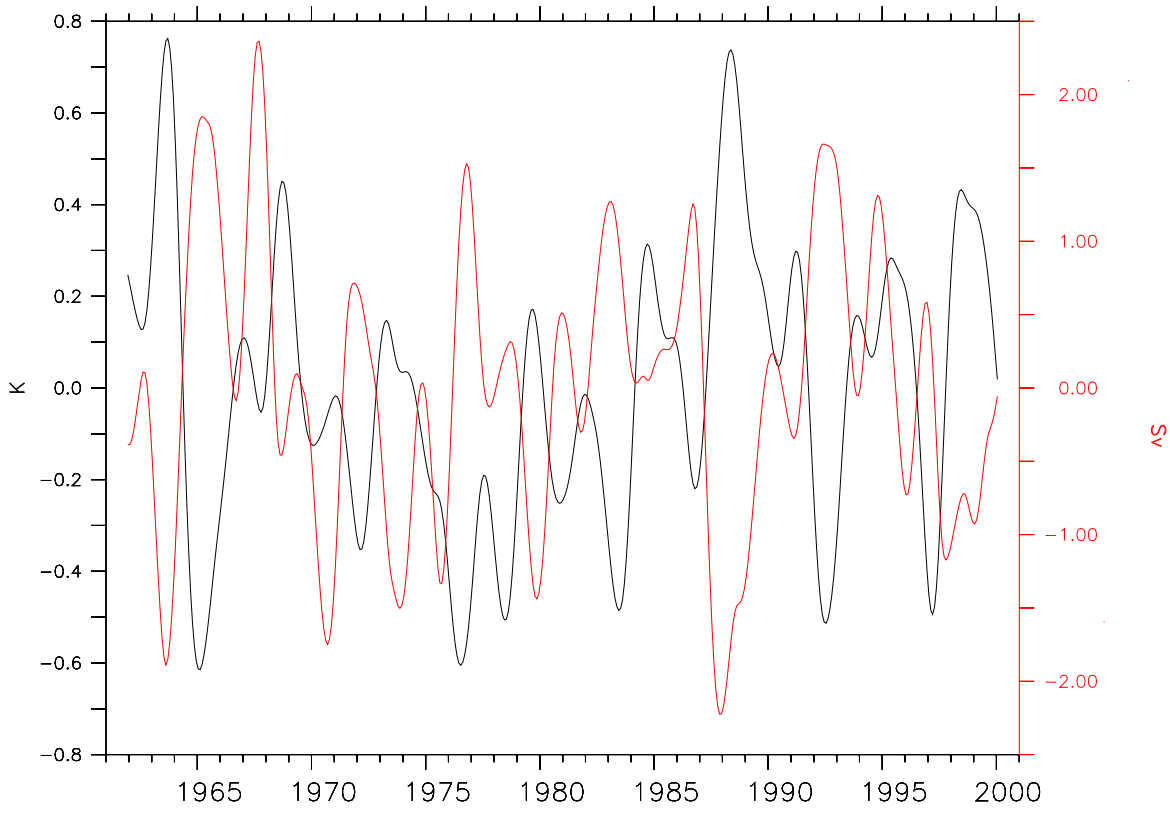

Figure 4.15: Interannually smoothed anomalies of thermocline layer ($24.5kg/m^3 \leq \sigma \leq 26.8kg/m^3$) EUC transport at 23°W (red) and Atl3 SST (black) from REF

4.6 Impact of the subtropical-tropical cells

While interannual SST and NST variability in the eastern equatorial Atlantic is predominantly driven by equatorial forcing, on decadal time scales forcing from outside the equatorial band has an impact as well.

This is illustrated by time series of Atl3 SST and NST anomalies smoothed both interannually and decadally (Fig. 4.16). Comparison between NST variability from sensitivity experiments forced climatologically outside (inside) the equatorial region (EQ and NO EQ) shows that on interannual time scales the variability from REF can be mainly simulated by EQ. On decadal time scales, however, a significant part of the REF variations is due to off-equatorial forcing. The ratio between the standard deviation of Atl3 NST variability between the experiments EQ and NOEQ changes from about 67:33% on interannual time scales to 53:47% on decadal time scales.

Part of this off-equatorial influence on decadal NST variability is likely to be connected to changes in the subtropical-tropical cells (STCs, *Snowden and Molinari*, 2003; *Schott et al.*, 2004) that have already been described in the introduction and in chapter 3.1. For the Pacific there is evidence from both models and observations that low-frequency changes in STC transport contribute to the modulation of SST in the eastern equatorial region (*Kleeman et al.*, 1999; *Nonaka et al.*, 2002; *McPhaden and Zhang*, 2002). For the Atlantic this connection is less clear. There are, however, studies indicating that also in the Atlantic STC variability might affect equatorial SST. *Kröger et al.* (2005) used ocean model sensitivity experiments to study decadal variations in the STC strength, which exhibited different phases in the Northern and Southern Hemisphere. The variability of both hemispheres had a time-lagged influence on equatorial SST, but due to different mechanisms. While the spin-up and spin-down of the cell ($v'\bar{T}-$mechanism, *Kleeman et al.*, 1999) dominated for the northern hemisphere, both $v'\bar{T}-$ and $\bar{v}T'-$ mechanism (*Gu and Philander*, 1997) appeared to play a role for the southern STC (see also *Lazar et al.*, 2001). *Rabe et al.* (2008) analyzed the output of the GECCO assimilation model and found a cycle involving the STC on pentadal and longer timescales that is initiated by increased wind stress at 10°S-N, followed by an enhanced EUC transport at 23°W and an increased STC layer convergence at 10°S-N about a year later.

In the ORCA ocean-only model no clear connection between eastern equatorial SST anomalies and STC variations could be found, neither on interannual nor longer time scales. In view of decadal SST variability in the Tropical Atlantic being small in general – the standard deviation of 1870 to 2006 HADISST

variability decadally filtered with a 119 point Hanning filter amounts to values of about 0.15K – it might be masked by the damping towards prescribed atmospheric temperatures in forced ocean model simulations. Thus a special simulation from the coupled Kiel Climate Model (KCM) is used here to investigate the connection between STC strength and eastern equatorial SST variability. In the so called WIND4 experiment the wind stress derived from the atmospheric model is replaced by climatological wind forcing between 4°S and 4°N in the Atlantic. This configuration allows to look specifically at the impact of off-equatorial wind variations on equatorial variability since all wind-driven interannual and decadal variability must stem from poleward of 4° latitude. The mean overturning stream function from WIND4 (not shown) displays a structure similar to the one from the ocean-only model (Fig. 3.1). There is a closed southern STC with a maximum meridional transport of 5 Sv at about 12°S and a strong recirculation cell of about 15 Sv in the northern subtropics that is not connected to the equator. Time series of the strength of the cells are derived from the transport maxima between 8° and 15° and the upper 500m at each time step (following *Lohmann and Latif*, 2005). Significant correlation between Atl3 SST variations and STC strength is found only for the southern cell on decadal time scales (Fig. 4.17) but neither for the northern cell nor the total cell strength. Decadal anomalies of the southern STC strength and Atl3 SST are anti-correlated at $r = -0.54$, and the correlation coefficient is significant at the 90% level. The cross correlation function is shifted towards a leading southern STC with identical correlation values for zero lag and for STC leading by 1 year. This indicates that variations in the strength of the southern STC might indeed have some influence on SST in the equatorial Atlantic upwelling regions. However, the impact appears to be quite weak and usually masked by local processes.

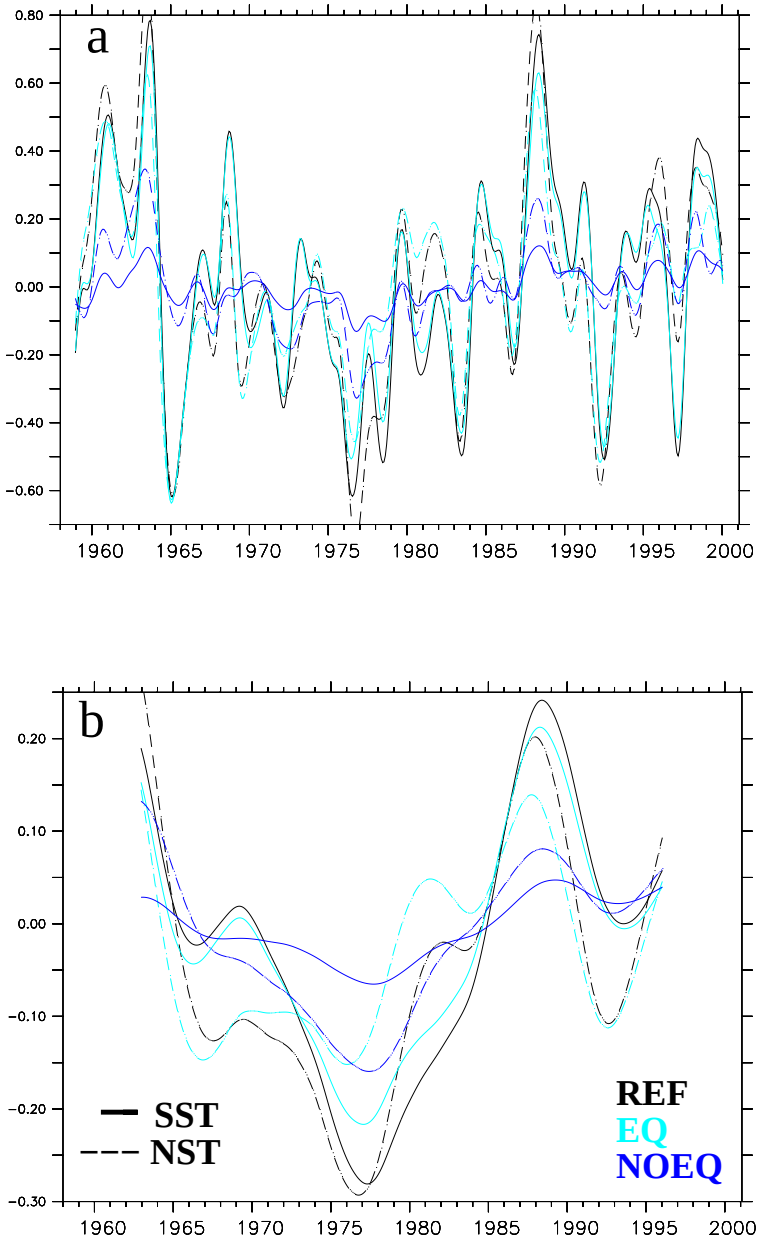

Figure 4.16: Interannual (a) and decadal (b) anomalies of Atl3 SST (solid lines) and NST (dashed lines) in °C from REF (black), EQ (lightblue) and NOEQ (blue)

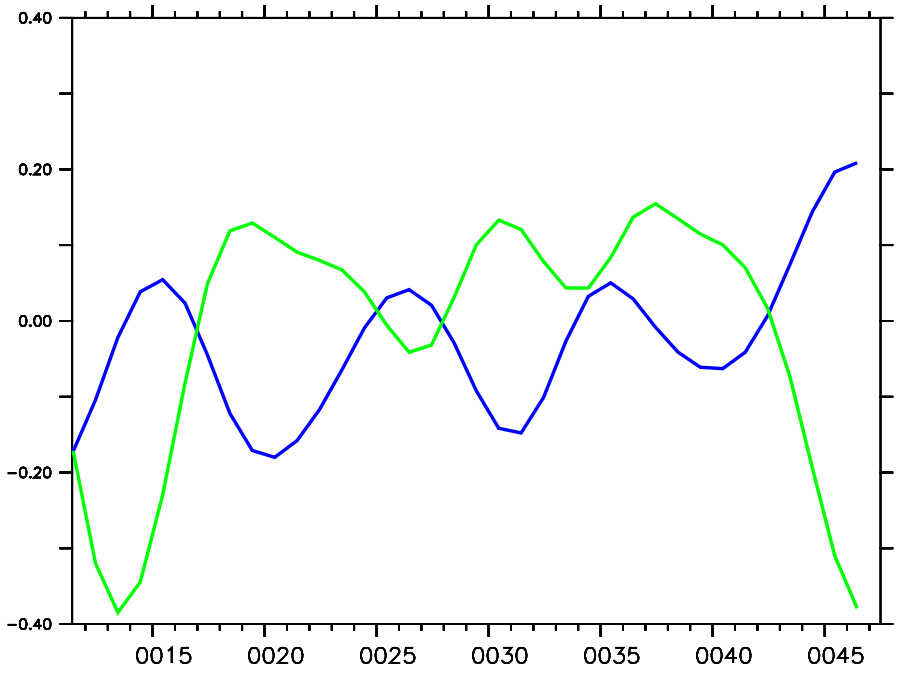

Figure 4.17: Decadal anomalies of southern STC strength (in Sv, green) and Atl3 SST (in K, blue) from KCM WIND4; correlation between detrended time series is $r = -0.54$

4.7 Summary

In this chapter the eastern Tropical Atlantic SST variability, with special focus on the connection between Benguela and Equatorial Atlantic Niños, has been investigated in a combined analysis of observational data sets and ocean model simulations.

The analysis confirms indications from previous studies which suggested that interannual SST variability in the Angola Benguela area and in the eastern equatorial Atlantic are linked. More specifically, warm (cold) events in the ABA in austral fall appear to be closely related to warm (cold) events in the eastern equatorial Atlantic in austral winter. Thus surface warming (cooling) off Angola tends to lead warming (cooling) at the equator by one to three months. As a main result, the direction of the lag is shown to be caused by the difference in thermocline depths between the two regions and a different phase-locking of the interannual SST variations to the seasonal cycle. While the subsurface-surface coupling in the cold tongue region can only be effective in June/July when the thermocline is shallowest, SST anomalies off Angola reach their maximum when the forcing effect due to Kelvin waves is strongest; they are therefore phase-locked to the season in which the Angola Benguela Front is at its southernmost position and the interannual variability in the strength of equatorial and subsequent coastal Kelvin waves is highest in February-March-April.

The specific role of different aspects of the atmospheric forcing was addressed by sensitivity experiments with artificial perturbations in the forcing set-up. They showed that near surface temperature variability in both regions can be understood as a dynamic response to atmospheric wind stress anomalies. Further analysis revealed that the temperature fluctuations are linked to variations in the strength of the South Atlantic Anticyclone that includes both the equatorward winds along the African coast and the southeastern trade winds. The literature is divided on the question whether SST anomalies off Angola are driven mainly by variations in local winds (*Polo et al.*, 2008b; *Richter et al.*, 2010) or are remotely forced from the equator via Kelvin wave propagation (e.g. *Florenchie et al.*, 2003, 2004; *Rouault et al.*, 2007). Results from a perturbation experiment aiming at identifying the relative contributions from equatorial vs. off-equatorial atmospheric forcing and from the composite analysis of Benguela Niño years support the latter idea: Subsurface temperature anomalies propagating to the ABA from the equator appear to be of major importance for the generation of Benguela warm events, while local upwelling

variations play a minor role.

As additional influences on eastern equatorial Atlantic SST the Equatorial Undercurrent and the Subtropical Cells were briefly discussed. In agreement with previous studies in the ORCA model the EUC is weaker during warm and stronger during cold phases. On decadal time scales the southern STC might have a weak impact on the cold tongue as well. Results from a KCM sensitivity experiment that allows to look specifically at the impact of off-equatorial wind variations on equatorial variability shows positive STC strength anomalies leading low surface temperatures.

5 Interaction with the tropical Pacific

Whatever there is, there is always more. Whatever is happening, something else is going on, too.

(Susan Sontag, At the same time)

From a global perspective, climate variations on interannual time scales are dominated by the El Niño-Southern Oscillation (ENSO) phenomenon in the Tropical Pacific. ENSO is supposed to have an impact on Tropical Atlantic variability by driving atmospheric circulation changes (e.g. *Hastenrath et al.*, 1987; *Klein et al.*, 1999; *Sutton et al.*, 2000; *Chiang et al.*, 2000; *Huang*, 2004) that manifest themselves for instance in changes of the Atlantic trade winds (*Latif and Barnett*, 1995; *Enfield and Mayer*, 1997; *Latif and Grötzner*, 2000; *Münnich and Neelin*, 2005). However, correlations between Niño3 (150°W to 90°W, 5°S to 5°N) and Atl3 SST anomalies are very low and the interaction between interannual SST variability in the Tropical Pacific and Atlantic is still a controversial issue. The cross correlation function between Niño3 and Atl3 SST is shown in Fig. 5.1 from both model and observational data. For Niño3 leading, the values do not exceed $r = 0.15$. It is interesting to note that the highest correlation values occur for the Atlantic leading the Pacific by 6 to 12 months (cf. also *Keenlyside and Latif*, 2007), which would correspond to anomalous cold SST in the eastern Tropical Atlantic in the summer prior to El Niño and vice versa. In agreement with this, a number of recent studies suggest that conditions in the Tropical Atlantic might affect SST variability and thus ENSO in the Tropical Pacific as well (*Wang*, 2006; *Jansen et al.*, 2009; *Rodríguez-Fonseca et al.*, 2009; *Losada et al.*, 2009).

In this chapter, first the role remote forcing from the Tropical Pacific might play for the Atlantic zonal mode will be discussed before turning to the potential influence from the Tropical Atlantic on ENSO in the Pacific. While the cross correlation function suggests that the latter is the dominant effect (Fig. 5.1), the former has potentially stronger implications for predictability. It has

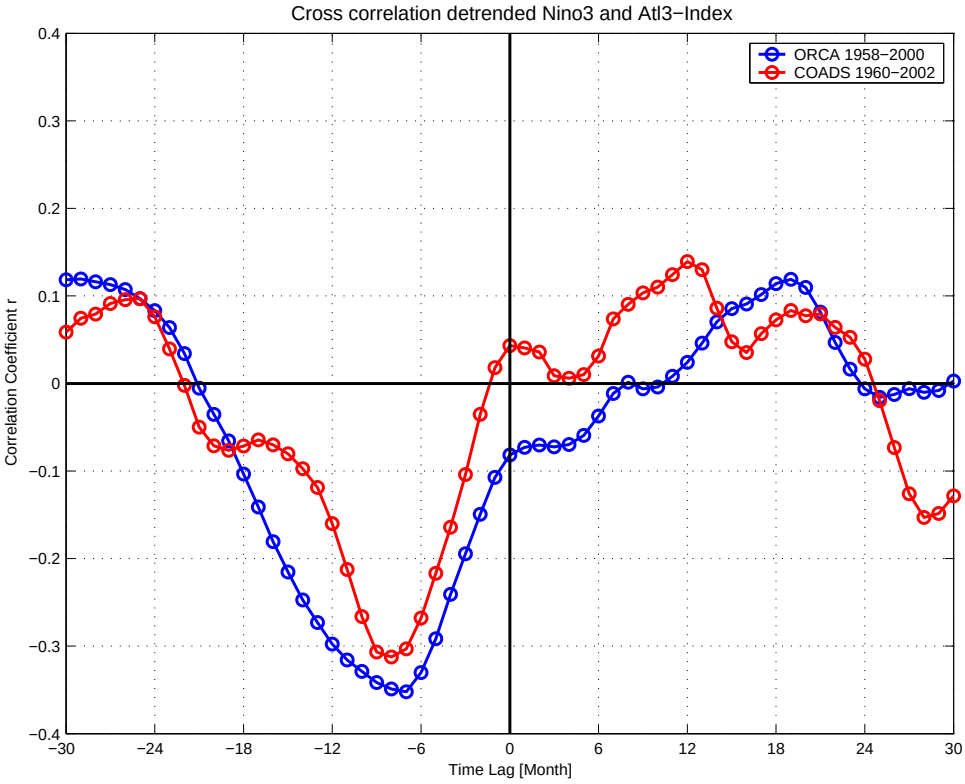

Figure 5.1: Cross correlation between interannual SST anomalies averaged over Niño3 and Atl3 regions from ORCA05-REF model simulation (blue) and COADS observations (red); positive lag corresponds to Niño3 index leading

thus received more attention in the past and will also be the one discussed in more detail here.

5.1 Tropical Pacific influence on the Tropical Atlantic

For the Tropical Pacific influence on the Tropical Atlantic a robust response in SST is predominantly found in the northern Tropical Atlantic (NTA, *Enfield and Mayer*, 1997; *Huang et al.*, 2002; *Alexander and Scott*, 2002). Analyzing output from a regionally coupled model, *Huang et al.* (2002) found that weakened northeasterly Atlantic Trades in an El Niño winter lead to warmer NTA SST in the following spring, while variability in the southern Tropical Atlantic (STA) was determined mainly by interactions within the Atlantic. In contrast, *Colberg et al.* (2004) showed that ENSO induced anomalies play an important role for upper ocean temperature variations in the southern Atlantic ocean by altering the net surface heat flux, the meridional Ekman heat transport and

Ekman pumping. A connection between ENSO and the Tropical South Atlantic was also suggested by *Hu and Huang* (2007) who noted that cold SST anomalies prevail in the eastern Tropical Pacific during the devolement of a STA warm phase. In contrast, results of composite analysis indicate that warm Niño3 SST are followed by a warming of the entire Tropical Atlantic, apart from a weak cooling in the eastern equatorial Atlantic (*Lohmann and Latif*, 2007). According to a study by *Chang et al.* (2006a) the inconsistent relationship between Pacific El Niños and Atlantic Niños can be explained by destructive interference between atmospheric and oceanic processes in the equatorial Atlantic in response to El Niño. While the tropospheric-temperature-induced warming (*Chiang and Sobel*, 2002; *Chiang and Lintner*, 2005) favors a basinwide temperature increase, the Bjerknes feedback induced by the change in Trade Winds produces a cooling signal in the eastern equatorial Atlantic (*Latif and Barnett*, 1995). In order to improve the predictability of warm events in the Tropical Atlantic, it is necessary to better understand the destructive interference between the dynamical and the thermodynamical responses. Here, the focus will be on the dynamical part, in particular addressing the questions of how eastern equatorial Atlantic SST responds to the Trade Winds changes associated with ENSO and whether this relation is dependent on the season and the forcing period.

5.1.1 Dynamical response to ENSO forcing

To investigate the dynamical response of the Tropical Atlantic to interannual variations in the Tropical Pacific, the wind anomaly over the Tropical Atlantic that is associated with ENSO is used to force an ocean model of intermediate complexity (IOM, described in section 2.3). The output of these model runs is analyzed with respect to SST anomalies in the eastern equatorial Atlantic. Then, the IOM is weakly coupled to a statistical atmosphere over the Atlantic and the response to an added ENSO-like wind anomaly is studied.

In hindcast simulations forced with NCEP wind stress the IOM captures the most important features of the tropical circulation in the Atlantic and Pacific including the position and strength of surface currents and the EUC as well as the seasonal cycle of SSH (*Keenlyside and Kleeman*, 2002; *Ding et al.*, 2009). Here it is used to isolate the effect of wind stress forcing associated with ENSO on the Tropical Atlantic.

The wind stress forcing used for the perturbation experiment is calculated as follows:

$$\tau_{forcing} = \alpha \, \tau_{ENSO} \, cos(\omega \, t) \tag{5.1}$$

in which τ_{ENSO} is the Tropical Atlantic wind stress pattern associated with ENSO. It is derived from regressing Niño3 SST anomalies against zonal and meridional wind stress from NCEP over the Tropical Atlantic. The regression patterns (Fig. 5.2) basically show a strengthening of the southeasterly Trade Winds, particularly over the western Atlantic, while the northeasterly Trade Winds are reduced. The regression is performed for zero lag but the wind stress response is very similar for the months following (*Fang*, 2005). The scaling factor α is chosen to result in $\tau_{forcing}$ values equal in magnitude to that of the composite difference of Atlantic wind stress for El Niño minus La Niña phases. With an α of 1×10^{-5} the amplitude of the ENSO associated zonal wind stress anomaly is about $6 \times 10^{-3} N/m^2$ in the central Tropical Atlantic, which is in the order of 20% of the seasonal cycle and in the order of the interannual variability in that region. Experiments are performed for different forcing frequencies ω and for the wind stress anomaly peaking in different calendar months. All simulations used here were run for 13 years of which the last 10 years are analyzed.

Simulations performed with the ENSO associated wind stress forcing show thermocline and SST variability with periods corresponding to the forcing variations. The response in SST from a run with a forcing period of 4 years and wind stress anomalies peaking in December is shown in Fig. 5.3. As illustrated by the standard deviation, the largest SST anomalies of about 0.3°C occur in the southeastern Tropics (Fig. 5.3, left panel), which corresponds to the region

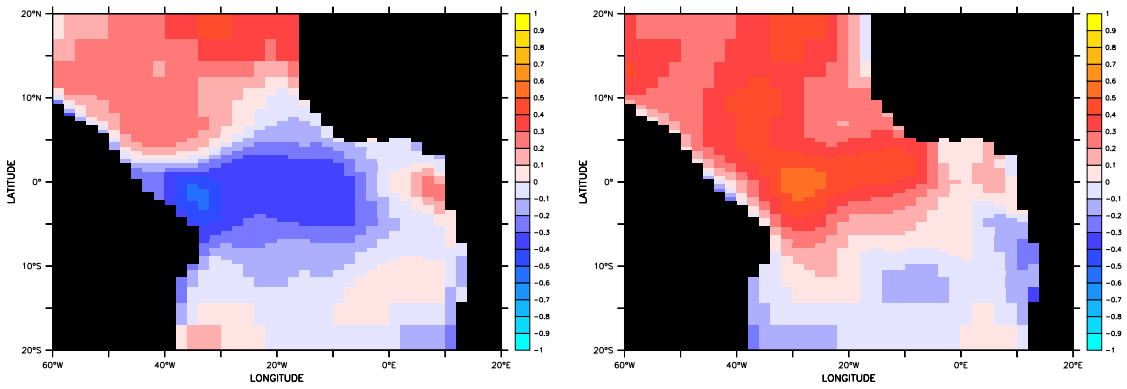

Figure 5.2: Regression of Niño3 SSTA against (a) τ_x and (b) τ_y

where the zonal mode manifests itself (e.g. *Kushnir et al.*, 2006). A time series of SST anomalies averaged over the cold tongue region (defined as 6°S to 2°N and 20°W to 5°E, following *Hormann and Brandt*, 2007) and central Tropical Atlantic zonal wind stress anomalies (Fig. 5.3, right panel) reveals that easterly (westerly) wind anomalies are accompanied by cold (warm) water. The SST variations reach their maximum and minimum values about one month after the peak in wind stress. The fast adjustment of the ocean to the wind anomalies is consistent with equatorial Kelvin waves crossing the equatorial Atlantic in about a month. Variations in the depth of the 20°C isotherm, a measure of the thermocline and thus upper ocean heat content, appear to be in balance with the wind stress forcing (not shown). This is in agreement with *Katz et al.* (1995) who showed from the first 2 years of TOPEX/POSEIDON data that there is a quasi-stationary linear relationship between the basin-wide, averaged zonal wind stress and the zonal pressure gradient in the equatorial Atlantic. The thermocline and SST responses are consistent with Bjerknes-type dynamics and indicate that wind anomalies triggered by ENSO might contribute to the interannual SST variability in the southeastern Atlantic.

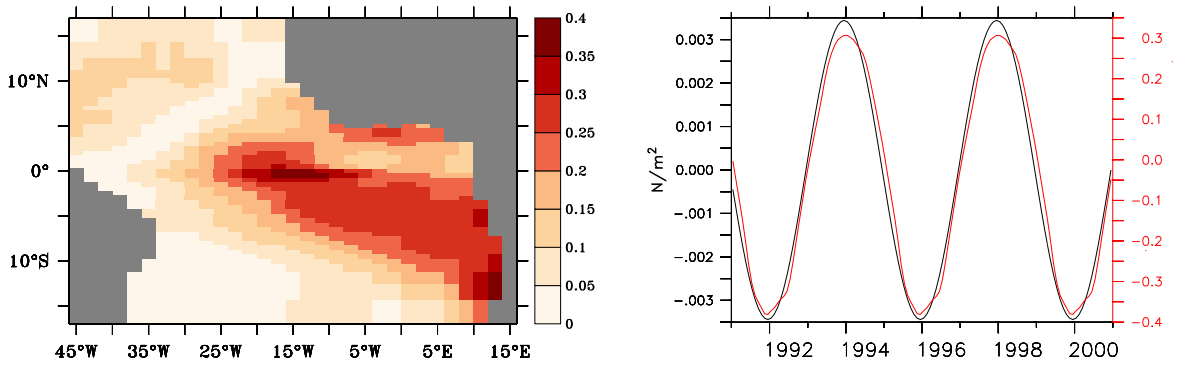

Figure 5.3: *SST response from IOM experiment with forcing period $p = 4$ years and wind stress anomaly peaking in December: a) Standard deviation of SST anomaly in °C; b) time series of SST averaged over the cold tongue region (6° S to 2° N and 20° W to 5° E, in °C, red) and taux averaged over 3° S to 3° N and 35° W to 15° W (in $\frac{N}{m^2}$, black)*

5.1.2 Seasonality of the response

For a Bjerknes type response to the Trade Wind changes associated with ENSO, the strength of the SST response in the cold tongue region is dependent on the depth of the thermocline and thus on the season (*Keenlyside and Latif*,

2007). The strongest subsurface-surface coupling in the model occurs in June, as illustrated by the correlation between anomalies of SST and the depth of the 20°C isotherm from an IOM run forced with NCEP wind stress (Fig. 5.4).

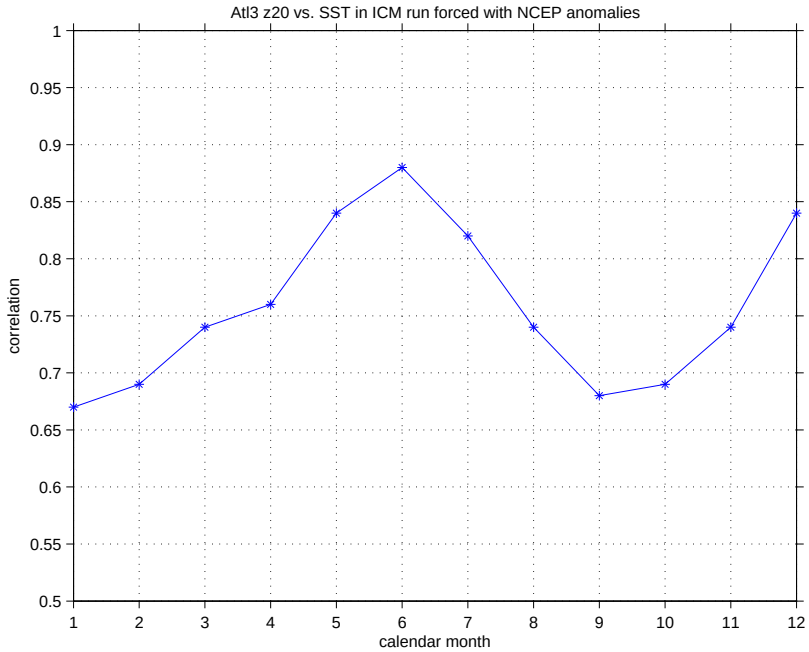

Figure 5.4: *Seasonality of the correlation between interannual anomalies of SST and z20 in the Atl3 region from NCEP forced ICM run as a measure of subsurface - surface coupling*

To address the role of seasonality, twelve IOM experiments with the ENSO associated wind stress anomaly peaking in the different calendar months are analyzed. They all have a forcing period of 4 years. Consistent with the season of strongest subsurface-surface coupling (Fig. 5.4), the strongest SST response in the cold tongue region occurs in the runs in which the wind stress anomaly peaks in boreal summer (Fig. 5.5). The differences between the experiments are, however, quite small with maximum SST anomalies ranging between 0.304°C for the run in which the wind stress anomaly peaks in January and 0.332°C for the run with the wind stress anomaly peaking in June.

While Figure 5.5 shows that wind stress anomalies in June give rise to the highest cold tongue SST anomalies, it does not provide any information about the lag between the wind stress forcing and the SST response, i.e. in which

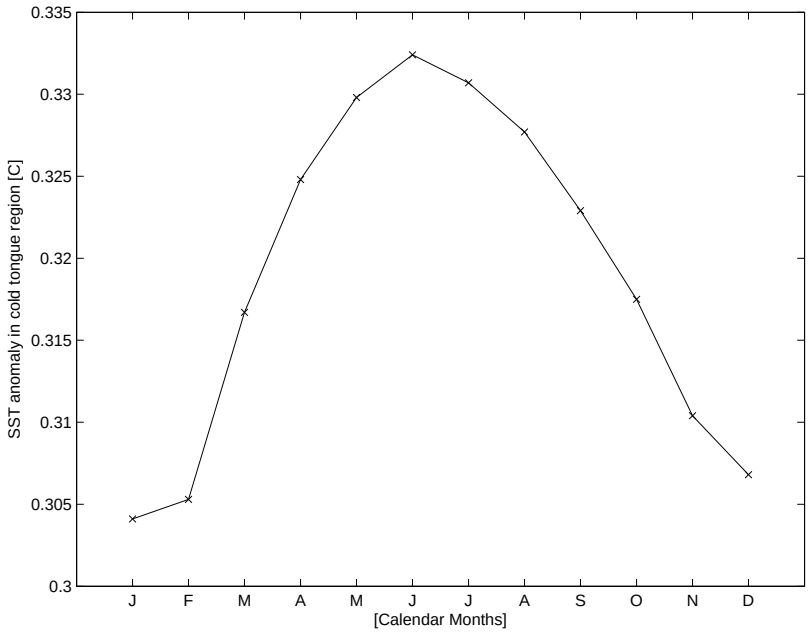

Figure 5.5: *Maximum SST anomaly in cold tongue region in °C from IOM experiments with ENSO associated wind stress anomalies peaking in different calendar months (indicated on x-axis)*

month the SST anomaly reaches its maximum. The experiment discussed in the previous section indicated that there is a lag of about one month between the maximum in the wind stress forcing in the western equatorial Atlantic and the SST response in the eastern equatorial Atlantic. In Fig. 5.6 the values of the maximum SST anomaly in the cold tongue region are displayed not only as a function of the month in which the ENSO associated wind stress anomalies peak (as in Fig. 5.5), but also as a function of calendar month in which the SST anomaly occurs. It shows that the SST response is in general lagging the wind stress but also that the lag is seasonally dependent. Most experiments reveal a lag of one month, but lags of up to three months are found for the runs in which the wind stress anomaly peaks in boreal spring.

While a lag of about one month is consistent with the time equatorial Kelvin waves need to cross the basin, the longer time lags seen for the spring runs likely result from two key factors. First, subsurface temperature anomalies in spring need longer to reach the surface in the cold tongue region than in summer, because of the deeper thermocline and weaker upwelling, following the arguments in chapter 4.3. Second, a stronger response in the summer months to the (albeit weaker) wind anomaly at that time could create the impression

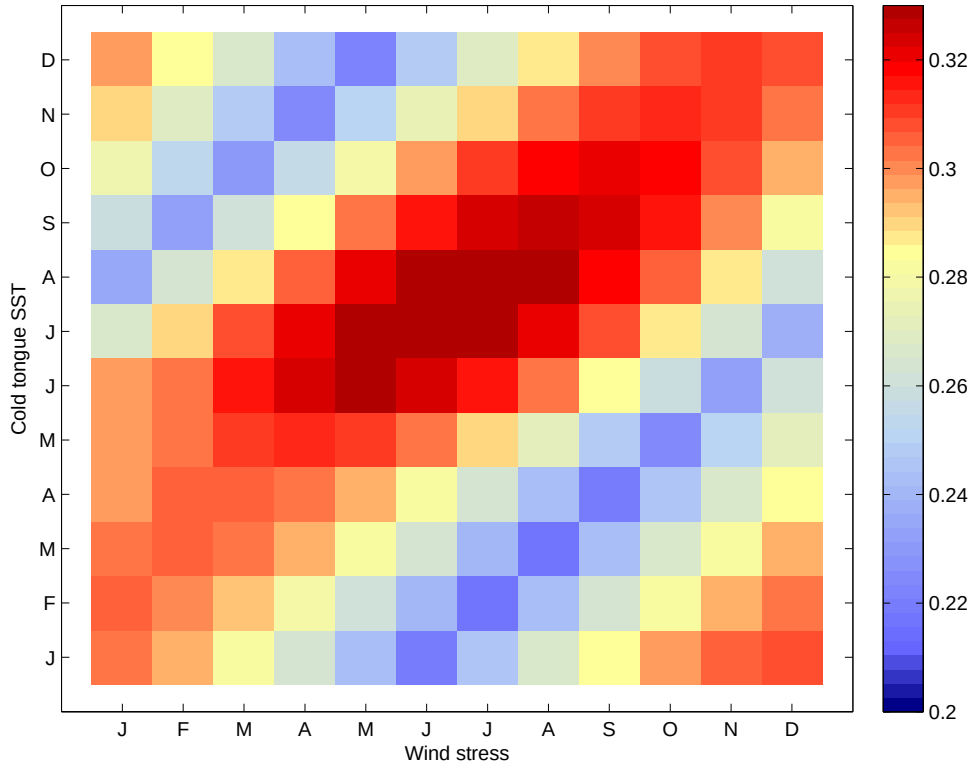

Figure 5.6: *Maximum SST anomaly in cold tongue region in °C (color) for different months (indicated on y-axis) from IOM experiments with ENSO associated wind stress anomalies peaking in different calendar months (indicated on x-axis)*

of a longer lag between wind forcing peaking in spring and the SST response. Since the wind anomaly forcing is applied using a cosine function, the wind forcing in the months directly before and after the peak is only slightly lower than the maximum. This implies that if the SST response to a certain wind stress anomaly is much higher in month A than in month $(A-2)$, the maximum SST response to a wind forcing peaking in month $(A-2)$ might seem to occur at a greater lag although the response occurs instantaneously (or within one month) to the slightly weaker wind forcing in month A. The cold tongue SST response per unit wind stress change as a function of calendar months is shown in Fig. 5.7 for the individual experiments with the wind stress anomalies peaking in the different months as well as the ensemble mean. The impact of a wind stress anomaly on SST in the eastern equatorial Atlantic is clearly highest in JJA and lowest in FMA, in agreement with the seasonality of the subsurface-surface coupling (Fig. 5.4). The spread of the curves is quite small

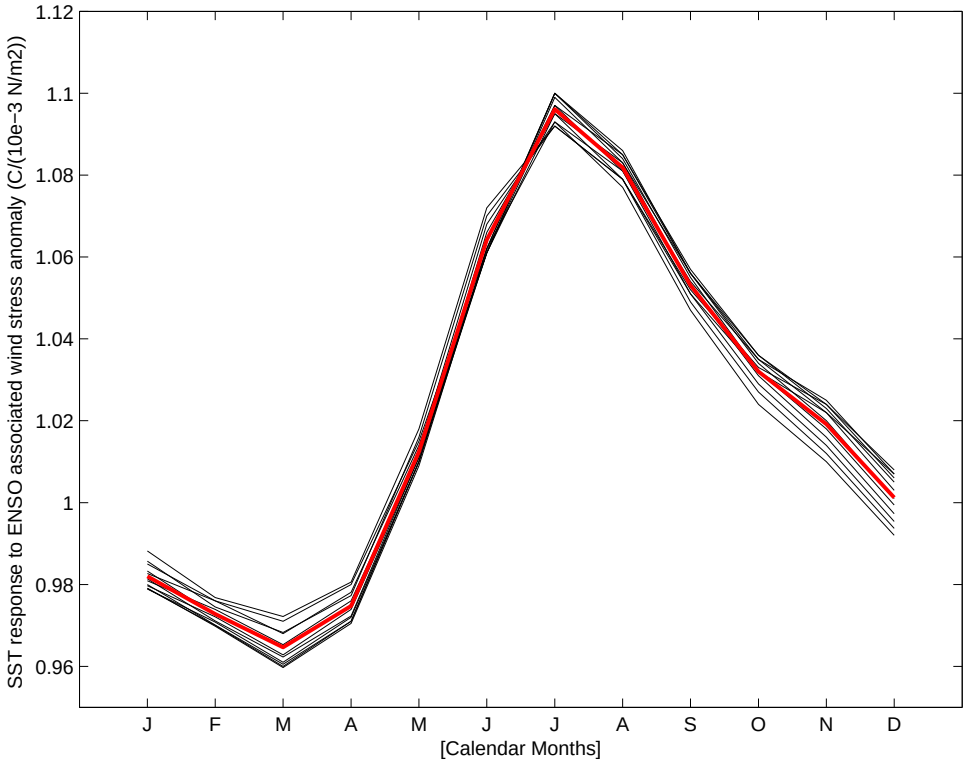

Figure 5.7: *Cold tongue SST response to ENSO associated wind stress anomaly (in °C per* $10^{-3}\frac{N}{m^2}$*) as a function of calendar month; individual black curves represent different experiments with wind stress peaking in different months, red curve represents the ensemble mean*

compared to the seasonal amplitude, indicating that the response in °C per $\frac{N}{m^2}$ is almost independent of the actual value of the wind stress anomaly. The difference between boreal spring and summer months in combination with the response being rather linear could contribute to the larger lags seen for the runs with wind stress anomalies peaking in spring (Fig. 5.6). The high SST anomalies in June and July in the runs in that the wind stress forcing peaks in March, April and May could thus be understood as a combination of a lagged response to the spring wind stress peak and a faster but stronger response to the slightly weaker summer wind stress forcing.

To conclude, the perturbation experiments forced with ENSO associated wind stress anomalies show a response reminiscent of the Atlantic zonal mode with equatorial thermocline changes and SST anomalies in the southeastern tropical region. The response is very fast (about one month), consistent with

Kelvin wave propagation speed, but shows a seasonal dependency. In agreement with the season of the shallowest thermocline and the correspondingly strong subsurface-surface coupling, the largest response occurs for wind anomalies peaking in boreal summer while smaller SST anomalies and longer lags (up to three months) are found for winds peaking in boreal spring.

5.1.3 Coupled response: Remote forcing by ENSO as a method to sustain the zonal mode

As shown in the previous section, wind anomalies over the Atlantic that are associated with ENSO in the Pacific can induce zonal mode like SST variations in the eastern Tropical Atlantic. According to the study by *Zebiak* (1993) the Atlantic zonal mode is strongly damped and not self-sustained. ENSO is thought to be one of the external forces sustaining the oscillation (e.g., *Latif and Barnett*, 1995), another is the North Atlantic Oscillation NAO via its influence on the meridional mode. The role of ENSO in exciting SST variability in the eastern equatorial Atlantic is studied using the IOM coupled to a statistical atmosphere (in the following referred to as ICM) in order to allow for feedbacks between ocean and atmosphere to take place. The statistical atmospheric model is based on a joint Singular Value Decomposition (SVD) analysis of SST and surface winds. Wind stress anomalies are calculated from SST anomalies at each time step.

ICM runs are performed with a low coupling strength of 1.2, i.e. a very weak coupling between oceanic and atmospheric components. A time series of Atl3 SST anomalies from such a run does not show any oscillations at all. If, however, an ENSO associated wind anomaly as described in the last section (Eq. 5.1) is added to the wind stress derived from the atmospheric model, SST in the Tropical Atlantic displays variability with period and amplitude depending on the forcing frequency. The strongest response is obtained with a forcing period of 2.5 years, as demonstrated by the standard deviation of the Atl3 SST anomalies as a function of forcing period (Fig. 5.8). In this case SST anomalies of O(0.8°C) occur in the cold tongue region. Thus the experiments support the idea that external forcing associated with Pacific ENSO can excite SST variability in the equatorial Atlantic ocean and may therefore contribute to the developement of warm and cold events in the eastern Tropical Atlantic.

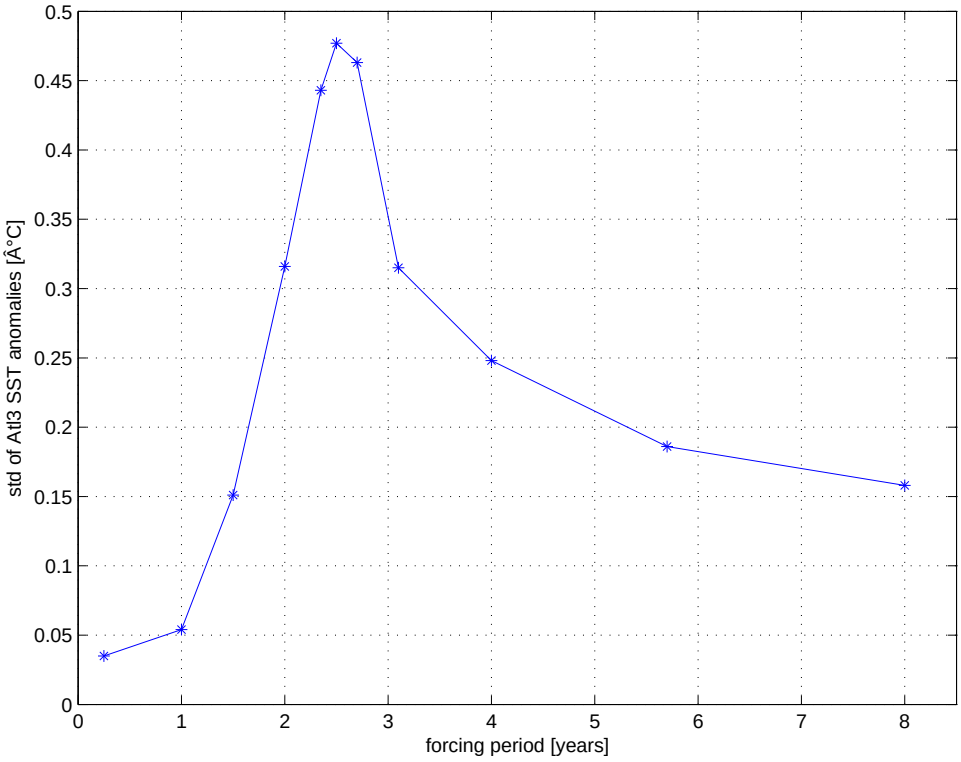

Figure 5.8: *Coupled response to the periodic wind forcing as a function of forcing period*

5.1.4 Summary

In this chapter the connection between Pacific ENSO and the Atlantic zonal mode has been investigated with focus on the Tropical Atlantic's dynamical response to remote ENSO forcing. In summary, El Niño conditions in the Tropical Pacific affect Tropical Atlantic winds by reducing the Northeasterly Trades and enhancing the Southeasterly Trade Winds. Here, the response to such ENSO related wind anomalies was studied using an ocean model of intermediate complexity, both stand alone and coupled to a statistical atmosphere. In weakly coupled experiments, added wind anomalies associated with ENSO are shown to induce eastern equatorial Atlantic SST variations, supporting the idea that ENSO is an important factor in sustaining the Atlantic zonal mode. The response to the Trade Wind changes seen in both the ocean-only and the coupled perturbation experiments is consistent with Bjerknes dynamics, i.e. stronger Southeasterly Trades result in a shallower equatorial thermocline and a subsequent cooling in the cold tongue region. The strength of the SST anomalies as well as the time-lag between peak wind and SST anomalies

is dependent on the season. Highest anomalies occur in boreal summer, in agreement with the subsurface-surface coupling being strongest at that season. Longest lags are found for wind stress anomalies peaking in boreal spring when the eastern equatorial thermocline is deepest.

Compared to previous studies (e.g., *Huang et al.*, 2004; *Hu and Huang*, 2007) the lags between SST variations in the Tropical Pacific and the Atlantic cold tongue SST response found here are rather short. This might be due to the fact that the seasonality in the subsurface-surface coupling in the IOM is not as pronounced as in observations and other models. While, e.g., the correlation values between anomalies in thermocline depth and SST range between 0.35 and 0.9 in NEMO-ORCA05 (Fig. 4.8), they are above 0.65 throughout the entire year in the IOM with values in December almost reaching the summer maximum (Fig. 5.4). Thus, in the real world, the lags introduced by the dependency on thermocline depth and upwelling strength can be expected to be larger.

5.2 Tropical Atlantic influence on the Tropical Pacific

As shown at the beginning of this chapter, the cross correlation function between Niño3 and Atl3 SST anomalies from both model and observational data shows highest values (-0.34) when the Atlantic leads the Pacific by 6-12 months, rather than when it lags. This indicates that Atlantic forcing of the Tropical Pacific might be as strong as or possibly even stronger than the ENSO influence on the Atlantic zonal mode.

There are a number of recent studies addressing this issue. *Wang* (2006) put forward a mechanism in which an inter-basin SST gradient between the equatorial Atlantic and Pacific induces zonal wind anomalies over equatorial South America and some areas of both ocean basins. The zonal wind anomalies then act as a bridge linking the Tropical Atlantic and Pacific and reinforce the inter-basin SST gradient through an anomalous Walker circulation in the Pacific and ocean dynamics in the Atlantic. *Jansen et al.* (2009) used a conceptual model based on the delayed oscillator model by *Burgers et al.* (2005) to analyze the effect of Atlantic variability on ENSO predictions. They find that a feedback from the Atlantic on ENSO appears to exist, and that taking the Atlantic into account slightly improves the retrospective forecast skill of the conceptual model. *Rodríguez-Fonseca et al.* (2009) found summer Atlantic Niños act to strengthen the Walker circulation, which favors the develope-

ment of a Pacific La Niña event in the following-winter and vice versa. Along the same lines *Losada et al.* (2009) showed that for a warm phase of the Atlantic equatorial mode the associated southward displacement of the ITCZ with rising motion over equatorial Atlantic leads to subsidence over the rest of the tropics favouring La Niña conditions in the Tropical Pacific. Partial coupled GCM experiments in which Atlantic SST is prescribed from observations, but elsewhere the model is fully coupled, confirm the mechanism proposed by *Rodríguez-Fonseca et al.* (2009) (Hui Ding, pers. comm.).

A thorough analysis of the interaction between the Atlantic zonal mode and ENSO in the Pacific is beyond the scope of this study and will be addressed in future work. It should, however, be mentioned that results from a composite analysis of NOAA SST and NCEP wind stress for years with Atlantic Niños peaking in JJA (Fig. 5.9) are consistent with the studies cited above. It shows eastward wind anomalies in the western Tropical Pacific and a strong cooling signal in the eastern part of the basin in the (boreal) fall and winter following the peak phase of the eastern Tropical Atlantic warm events. First results from a flux corrected run of the Kiel Climate Model (described in section 2.2) also support the idea that an eastern Tropical Atlantic warm event during boreal summer favors the development of a Pacific La Niña event in the following winter. Composite differences between Atlantic Niño and Niña phases show no clear SST signal at zero lag but an overall cooling in the Tropical Pacific when the Pacific lags the Atlantic by half a year (not shown).

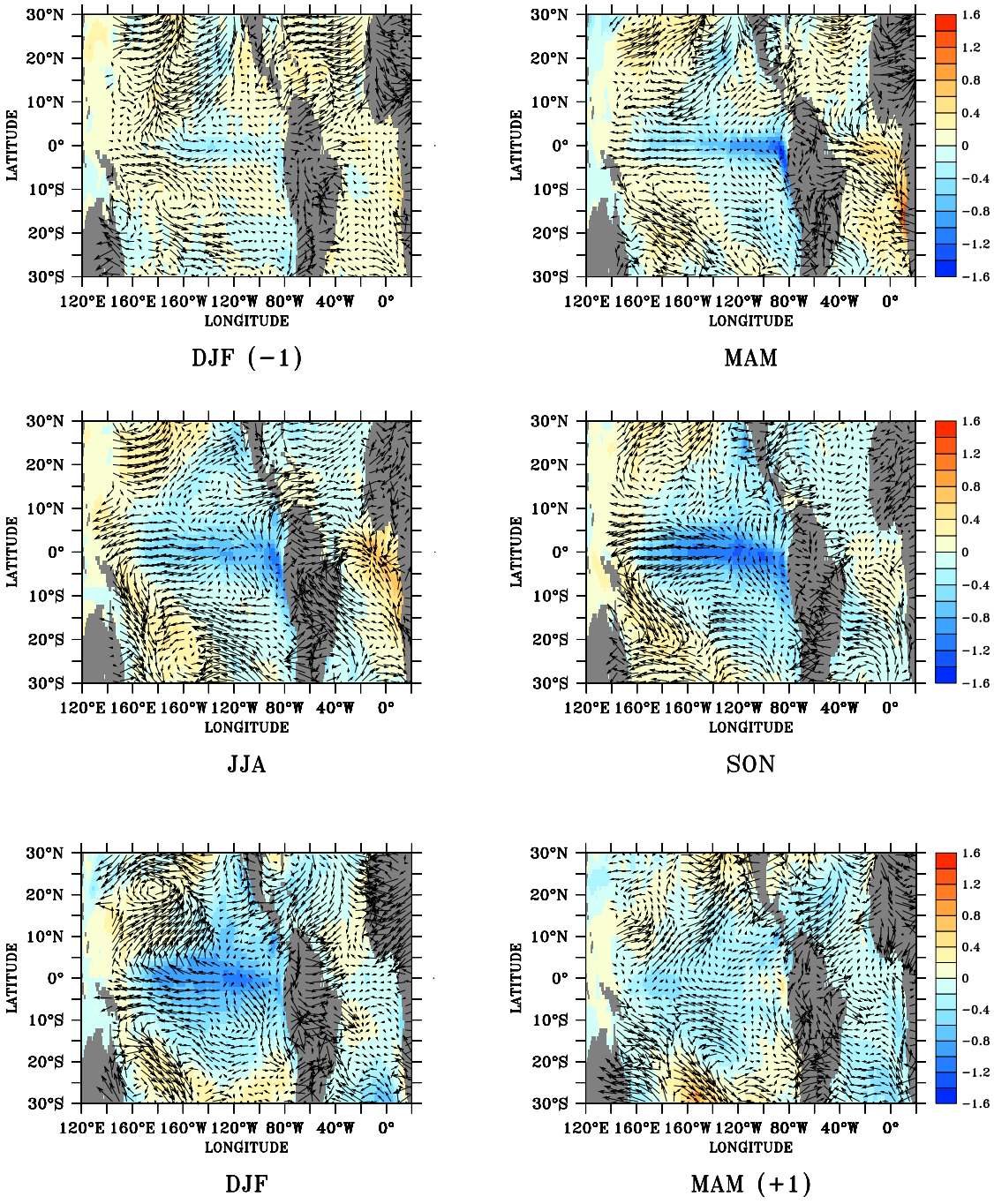

Figure 5.9: *Composite difference in NOAA SST and NCEP wind stress between years with Atlantic warm events peaking in JJA (1984, 1988, 1991, 1995, 1996, 1999, 2007) and the climatological mean (1982 to 2007)*

6 Conclusions and Discussion

Enough research will tend to support your conclusions.

(Arthur Bloch)

The main goal of this work was to better understand the connection between Equatorial Atlantic and Benguela Niños with special focus on their temporal relationship. Eastern Tropical Atlantic SST variability in this study has been investigated in a combined analysis of observational data sets and ocean model experiments. In a hindcast simulation with interannual CORE forcing, the global NEMO-ORCA05 ocean model has been shown to capture the basic features of the mean circulation in the Tropical Atlantic ocean and its seasonal variations as well as most of the interannual SST variability in the region.

Eastern Tropical Atlantic Niño

The main findings regarding interannual SST variability in the eastern Tropical Atlantic are:

- Benguela and Atlantic Niños are linked:
  Interannual SST variability in the Angola Benguela area and the eastern equatorial Atlantic is shown to be well correlated at r=0.7. Also composite analysis of Benguela warm events peaking in May-April-May show eastern equatorial SST anomalies to be associated with the Benguela warming.

- Benguela Niños are mainly driven by remote forcing from the equator:
  The relative roles of local wind anomalies (*Polo et al.*, 2008b; *Richter et al.*, 2010) versus remote forcing from the equator via Kelvin wave propagation (*Florenchie et al.*, 2003, 2004; *Rouault et al.*, 2007) for the generation of Benguela Niños is still a controversial issue. Here, the idea that warm events off Angola are generated by a wind stress relaxation in the western equatorial Atlantic inducing Kelvin waves that then propagate to the Angola Benguela area is supported by:

  - a close correspondence between thermocline depth and SST anomalies in the eastern equatorial Atlantic and southward along the West African coast
  - perturbation experiments with artificial changes in the forcing set-up that demonstrate that eastern equatorial near surface temperature (NST) variability is governed by wind stress variations and that a significant part of ABA NST variations is of equatorial origin
  - a composite analysis of Benguela Niño years showing a weakening of the southeasterly trades but no significant wind stress change along the Angolan coast prior to the warming

- Warming off Angola occurs prior to warming at the equator. This is mainly due to different linkages to the seasonal cycle:
  The cross correlation function between Atl3 and ABA interannual SST variability is shifted towards ABA leading. Also composite analysis shows SST anomalies at the equator following those off Angola. This behaviour, which seems to be counterintuitive in view of the forcing mechanism discussed above, can be explained by the deeper thermocline at the equator in combination with the interannual SST variations being phase-locked to the seasonal cycle in different ways. At the equator, SST variations are strongest in June/July when the subsurface-surface coupling in the cold tongue region reaches its maximum due to the seasonal shallowing of the thermocline. SST anomalies off Angola appear to be phase-locked to the season in which the forcing effect due to Kelvin waves is strongest, i.e. to February-March-April when the Angola Benguela Front is at its southernmost position and the interannual variability in the strength of equatorial and subsequent coastal Kelvin waves is highest.

- Near surface temperature anomalies in the eastern Tropical Atlantic are linked to variations in the strength of the South Atlantic Anticyclone:
  A correlation between a time series of April ABA SST and February wind stress fields shows a weakening of the whole South Atlantic Anticyclone (SAA) prior to the Benguela warming. The connection is confirmed by the monthly stratified cross correlation function between interannual ABA and Atl3 SST anomalies and a sea level pressure index representing the SAA. It shows that austral fall/winter SST variability in the eastern Tropical Atlantic is related to variations in the strength of the South Atlantic Anticyclone in the preceding late austral summer.

In summary, the results shown here provide a new interpretation of the Atlantic zonal mode in terms of a combination of Benguela and Atlantic Niños and offer new possibilities, e.g. with respect to predictability of eastern Tropical

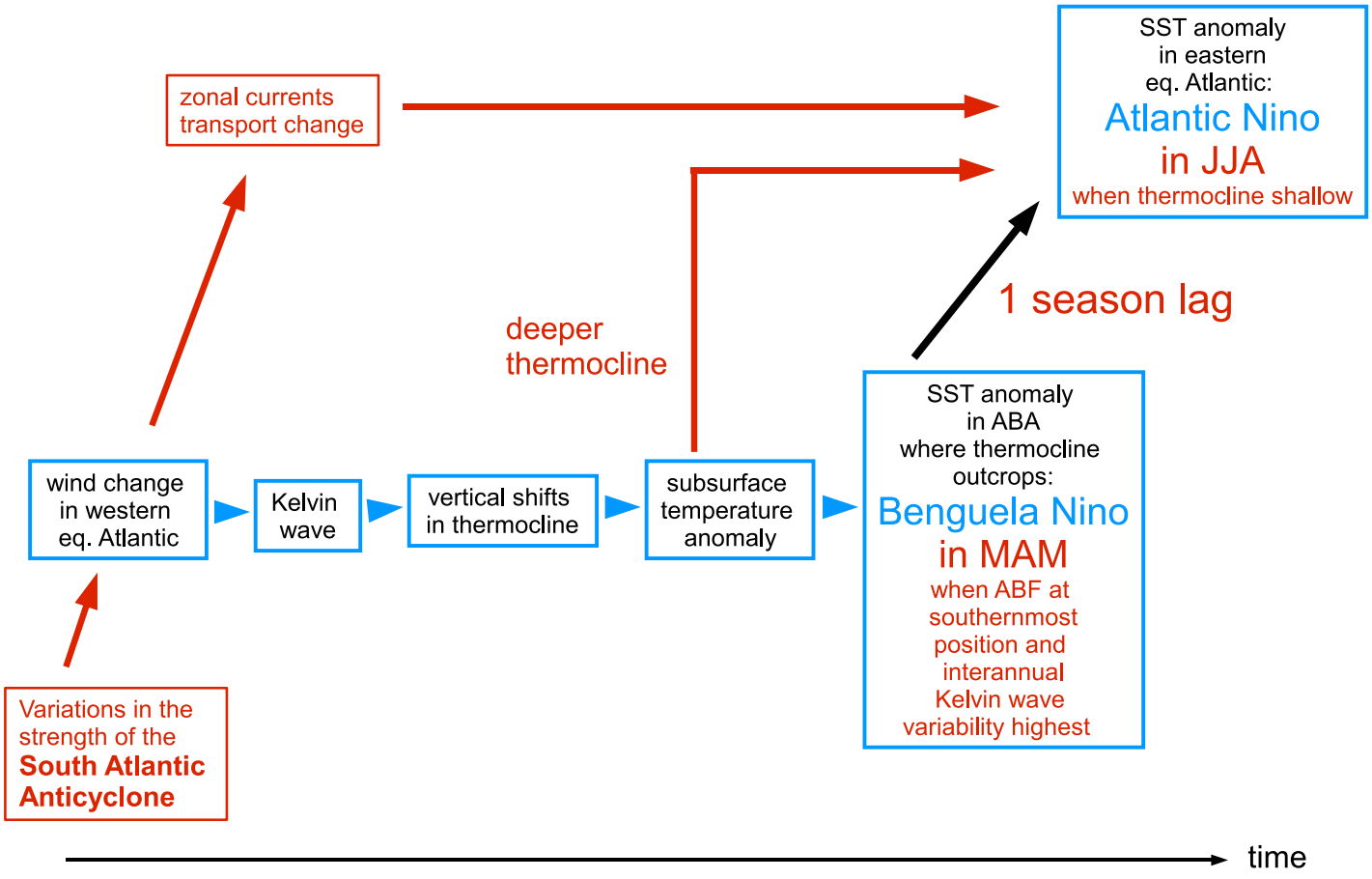

Figure 6.1: Schematic representation of the mechanism suggested for the generation of Atlantic and Benguela Niños as shown in the Introduction (Fig. 1.3) with findings from this study added in red

Atlantic warm events that will be discussed below. Even though local conditions might influence whether an event passes the threshold to be considered as a Benguela or Atlantic Niño on its own, warm events that occur concurrently in the two regions should be summarized under the term "Eastern Tropical Atlantic Niño". Such an eastern Tropical Atlantic warm event starts with a weakening of the southeasterly Trades that are part of the South Atlantic anticyclone. The relaxation of the Trade Winds excites equatorial Kelvin waves in the western equatorial Atlantic that propagate towards the east deflecting the thermocline. The associated subsurface temperature anomalies reach the Atl3 region on their way eastward but the thermocline is too deep for them to excite a temperature response at the surface. Thus they first outcrop as SST anomalies in the ABA in March/April. In June, as a result of the sea-

sonal shallowing of the thermocline, the subsurface-surface coupling in the cold tongue region intensifies, eventually giving rise to SST anomalies there. Additionally, the weakening of the zonal currents, in particular the Equatorial Undercurrent, in response to a trade wind relaxation may contribute to a warming in the cold tongue region. Fig. 6.1 provides a summarizing schematic.

Role of the South Atlantic Anticyclone

The study suggests that variations in the strength of the South Atlantic anticyclone play an important role for the developement of eastern Tropical Atlantic Niños. This is consistent with *Venegas et al.* (1997) and *Sterl and Hazeleger* (2003) who found the variability in the strength of the SAA accompanied by SST fluctuations to be the leading mode of observed coupled variability in the South Atlantic. The presence of a large-scale atmospheric precursor bears potential ramifications for the predictability of eastern equatorial Atlantic SST variability, which is of particular interest since so far no significant predictability has been demostrated. There are currently two ideas for the origin of potential predictability of eastern equatorial Atlantic SST. One is the recharge-oscillator mechanism in which mean equatorial ocean heat content provides a memory (*Zebiak*, 1993; *Jansen et al.*, 2009; *Ding et al.*, 2010). The other one is based on the delayed ocean response to wind stress forcing in the western part of the basin. *Marin et al.* (2009) as well as *Hormann and Brandt* (2009) compared observations from 2005, a year with extreme cold SST anomalies in the cold tongue with the warm years 2002 and 2006, respectively. They found the warm event to be associated with relaxed equatorial easterlies in the west while the cold event occured in conjunction with intensified winds in the western Atlantic. This suggests that wind variability in the western equatorial Atlantic in spring preconditions the subsurface conditions in the eastern part of the basin. As an oceanic response to wind variations equatorial Kelvin waves adjust the thermocline and thus set the stage for warm and cold events in the cold tongue region in austral winter. The present demonstration of a connection between the strength of the South Atlantic Anticyclone in austral summer and eastern Tropical Atlantic SST anomalies in the subsequent fall and winter bears the potential to improve the predictability of eastern Tropical Atlantic Niño events. It suggests that the large-scale SLP field could serve as a simple, and well observed diagnostic for detecting early stages of anomalies developing in the eastern Tropical Atlantic system.

Limitations of the model configuration and outlook

Although the NEMO-ORCA05 model provides a reasonable realistic simulation of the eastern Tropical Atlantic and is a valuable tool to gain insight in the mechanisms governing the SST variability, in particular due to the specific perturbation experiments, there are some caveats one should be aware of: One shortcoming of the configuration used here concerns the rather coarse resolution. A horizontal resolution of 0.5° is not fine enough to resolve the current structure of the equatorial Atlantic in detail. Thus, in this configuration, it is not possible to study the impact that the off-equatorial undercurrents might have on eastern tropical SST, nor can the role of eddy variability (i.e., tropical instability waves and vortices) be examined. The representation of coastal upwelling is also limited by resolution, which might explain the underestimation of the interannual SST variability off Angola in the current model setup. Models with higher horizontal resolution need to be analyzed to address these issues. Running these models is, however, computational expensive, which limits the number of perturbation experiments that can be performed. As an intermediate step, there are new approaches to nest certain regions with very high resolution ($O(\frac{1}{10}^\circ)$) into a coarser resolution global base model. First experiments show promising results and will be used for future analysis.

A specific question that might be addressed with a model better capable of simulating coastal upwelling is the representation of the 1995 Benguela Niño. Although this was a particularly strong event in the observations, models with different forcing fail to simulate its amplitude. In the NEMO-ORCA05 run analyzed in this study, the warming seems to be more surface-intensified compared to other Benguela Niño years. Consistent with that, *Richter et al.* (2010) found no Kelvin wave propagation from the equator to the ABA for this event in the AVISO SSH data. There is also no anomaly in the strength of the South Atlantic anticyclone observed in February 1995. The 1995 Benguela Niño might thus be more related to local upwelling or even heat flux anomalies resulting from local wind changes than other Benguela warm events. In addition to higher-resolution models, more local observations would be helpful to understand the different factors contributing to SST anomalies off Angola.

Another limitation of all ocean-only models is related to the need to prescribe the evolution of the atmospheric state in the formulation of a surface boundary condition for temperature. For the computation of the turbulent heat flux in terms of a bulk formula, surface air temperature and wind speed have to be prescribed. As already discussed in chapter 2.1.3 and 4.1, SST therefore effectively ceases to be a prognostic model variable and potentially important

air-sea feedbacks are eliminated. In order to account for these feedbacks and to allow SST to evolve more freely, coupled ocean-atmosphere models need to be analyzed. Unfortunately, standard CGCMs have major problems in the Tropical Atlantic. Most CGCMs display huge warm biases in the eastern Tropical Atlantic and, as a result, do not realistically simulate interannual variability of the region. Coupled models with reduced warm biases in the eastern Tropical Atlantic and the ability to simulate Eastern Tropical Atlantic Niño events would be necessary to address, e.g., the question of an atmospheric feedback from the Benguela region onto the equatorial Atlantic that was touched on in section 4.3.3.

Influence of the Subtropical Cells

In this study, a specific coupled model experiment with prescribed climatological wind forcing in a band around the equator has been used to examine the role of the subtropical-tropical cells (STCs) for SST variations in the cold tongue region. Variations in the strength of the STCs have been proposed to modulate SST in the eastern equatorial upwelling regions remotely from the subtropics (*Kleeman et al.*, 1999). Results from a KCM sensitivity experiment that allows to look specifically at the impact of off-equatorial wind variations on equatorial variability indicate that fluctuations in the strength of the southern STC has an impact on eastern Tropical Atlantic SST on decadal time scales with negative SST anomalies being preceded by anomalous strong transport of the southern cell. The SST anomalies are, however, only of magnitude O(0.2K) indicating that the effect of off-equatorial wind-induced variations on decadal time scales is rather weak, especially in comparison to the interannual variability.

Tropical Atlantic - Pacific Interaction

As discussed in the last part of this thesis, the Tropical Atlantic is not a closed system but interacts with the Tropical Pacific via atmospheric teleconnection processes on interannual time scales. Although numerous studies have addressed the Tropical Atlantic's response to remote ENSO forcing, there is still no consensus on the connection between El Niño in the Pacific and the Atlantic zonal mode. According to a study by *Chang et al.* (2006a) the inconsistent relationship between Pacific El Niños and Atlantic Niños might be due to destructive interference between the atmospheric and the oceanic response, i.e. the tropospheric-temperature-induced warming (*Chiang and Sobel*, 2002; *Chiang and Lintner*, 2005) and Bjerknes type ocean dynamics induced by the change in Trade Winds (*Latif and Barnett*, 1995). The analysis here fo-

cussed on the latter, i.e. the eastern equatorial Atlantic SST response to the Trade Winds changes associated with ENSO and its dependency on seasonality. Perturbation experiments performed with an intermediate complexity model support the idea that ENSO is an important factor in sustaining the Atlantic zonal mode and that Atlantic Trade Wind changes associated with ENSO can initiate a Bjerknes type response and thus modulate SST variations in the southeastern Tropical Atlantic. Pacific El Niño conditions enhance the Southeasterly Trades in the Atlantic which leads to a cooling in the cold tongue region while cold SST in the eastern Tropical Pacific reduces the easterly wind stress and thus favors an eastern equatorial Atlantic warming. Experiments in which the wind stress forcing peaks in different calendar months show that the strength of the SST anomalies as well as the time they lag the peak wind anomaly is dependent on the season. Consistent with the subsurface-surface coupling being strongest in boreal summer, highest SST anomalies are found in JJA. The lags range between one and three months with longest lags occuring for wind stress anomalies peaking in boreal spring when the eastern equatorial thermocline is deepest.

Recent studies indicate that the influence of Tropical Atlantic SST variability on the Tropical Pacific might be important as well. This aspect has only been touched on in the present study, but first results suggest a cooling signal in the Tropical Pacific in the winter following an equatorial Atlantic warm event. In future work, sensitivity experiments with the intermediate complexity model could contribute to the understanding of this issue.

References

Adcroft, A., C. Hill, and J. Marshall, Representation of topography by shaved cells in a height coordinate ocean model, *Mon. Wea. Rev.*, *125*, 2293–2315, 1997.

Alexander, M., and J. Scott, The influence of ENSO on air-sea interaction in the Atlantic, *Geophys. Res. Lett.*, *29(14)*, doi:10.1029/2001GL014,347, 2002.

Arakawa, A., and Y.-J. G. Hsu, Energy Conserving and Potential - Enstrophy Dissipating Schemes for the Shallow Water Equations, *Mon. Wea. Rev.*, *118*, 1960–1969, 1990.

Arakawa, A., and V. Lamb, Computational Design of the Basic Dynamical Processes of the UCLA General Circulation Model, *Methods in Computational Physics*, *17*, 174–267, 1977.

Barnier, B., G. Madec, T. Penduff, J.-M. Molines, A.-M. Treguier, A. Beckmann, A. Biastoch, C. Böning, J. Dengg, S. Gulev, J. L. Sommer, E. Remy, C. Talandier, S. Theetten, and M. Maltrud, Impact of partial steps and momentum advection schemes in a global ocean circulation model at eddy permitting resolution, *Ocean Dynamics*, *56(5)*, 543–567, 2006.

Bates, S. C., Coupled Ocean-Atmosphere Interaction and Variability in the Tropical Atlantic Ocean with and without an Annual Cycle, *J. Climate*, *21*, 5501–5523, 2008.

Biastoch, A., C. W. Böning, J. Getzlaff, J.-M. Molines, and G. Madec, Causes of Interannual - Decadal Variability in the Meridional Overturning Circulation of the Midlatitude North Atlantic ocean, *J. Climate*, *21*, 6599–6615, 2008.

Binet, D., B. Gobert, and L. Maloueki, El Niño-like warm events in the Eastern Atlantic (6°N and 20°S) and fish availability from Congo to Angola (1964 – 1999), *Aquat. Living Resour.*, *14*, 99–113, 2001.

Bjerknes, J., Atmospheric teleconnections from the equatorial Pacific, *Mon. Wea. Rev.*, *97*, 163–172, 1969.

Blanke, B., and P. Delecluse, Variability of the tropical Atlantic ocean simulated by a general circulation model with two different mixed layer physics, *J. Phys. Oceanogr.*, *23*, 1363–1388, 1993.

Brandt, P., F. A. Schott, C. Provost, A. Kartavtseff, V. Hormann, B. Bourlès, and J. Fischer, Circulation in the central equatorial Atlantic: Mean and intraseasonal to seasonal variability, *Geophys. Res. Lett.*, *33*, L07,609 and doi:10.1029/2005GL025,498, 2006.

Bryan, K., A numerical method for the study of circulation in the world ocean, *J. Computational Phys.*, *4:3*, 347–376, 1969.

Burgers, G., F.-F. Jin, and G. J. van Oldenburg, The simplest ENSO recharge oscillator, *Geophys. Res. Lett.*, *32*, L13,706, 2005.

Capotondi, A., M. A. Alexander, C. Deser, and M. J. M. Phaden, Anatomy and Decadal Evolution of the Pacific Subtropical-Tropical Cells (STCs), *J. Climate*, *18*, 3739–3758, 2005.

Carton, J. A., and B. Huang, Warm Events in the Tropical Atlantic, *J. Phys. Oceanogr.*, *24*, 888–903, 1994.

Carton, J. A., X. Cao, B. S. Giese, and A. M. da Silva, Decadal and Interannual SST Varibility in the Tropical Atlantic Ocean, *J. Phys. Oceanogr.*, *26*, 1165–1175, 1996.

Chang, P., L. Ji, and H. Li, A decadal climate variation in the tropical Atlantic Ocean from thermodynamic air-sea interaction, *Nature*, *385*, 516–518, 1997.

Chang, P., Y. Fang, R. Saravanan, L. Ji, and H. Seidel, The cause of the fragile relationship between the Pacific El Niño and the Atlantic Niño, *Nature*, *442*, doi:10.1038/nature05,053, 2006a.

Chang, P., T. Yamagata, P. Schopf, S. K. Behera, J. Carton, W. S. Kessler, G. Meyers, T. Qu, F. Schott, S. Shetye, and S.-P. Xie, Climate Fluctuations of Tropical Coupled Systems – The Role of Ocean Dynamics, *J. Climate*, *19*, 5122–5174, 2006b.

Chiang, J. H. C., and B. R. Lintner, Mechanisms of remote tropical surface warming during El Niño, *J. Climate*, *18*, 4130–4149, 2005.

Chiang, J. H. C., and A. H. Sobel, Tropical tropospheric temperature variations caused by ENSO and their influence on the remote tropical climate, *J. Climate*, *15*, 2616–2631, 2002.

Chiang, J. H. C., Y. Kushnir, and S. E. Zebiak, Interdecadal changes in eastern Pacific ITCZ variability and its influence on the Atlantic ITCZ, *Geophys. Res. Lett.*, *27*, 3687–3690, 2000.

Chiang, J. H. C., Y. Kushnir, and A. Giannini, Deconstructing Atlantic Intertropical Convergence Zone variability: Influence of the local cross-equatorial sea surface temperature gradient and remote forcing from the eastern equatorial Pacific, *J. Geophys. Res.*, *107 (D1, 4004)*, doi: 10.1029/2000JD000,307, 2002.

Colberg, F., C. J. C. Reason, and K. Rodgers, South Atlantic response to El Niño–Southern Oscillation induced climate variability in an ocean general circulation model, *J. Geophys. Res.*, *109,C12015*, doi:10.1029/2004JC002,301, 2004.

Davey, M. K., M. Huddleston, K. Sperber, P. Braconnot, F. Bryan, D. Chen, R. Colman, C. Cooper, U. Cubasch, P. Delecluse, D. DeWitt, L. Fairhead, G. Flato, C. Gordon, T. Hogan, M. Ji, M. Kimoto, A. Kitoh, T. Knutson, M. Latif, H. L. Treut, T. Li, S. Manabe, C. Mechoso, G. Meehl, S. Power, E. Roeckner, L. Terray, A. Vintzileos, R. Voss, B. Wang, W. Washington, I. Yoshikawa, J. Yu, S. Yukimoto, and S. Zebiak, STOIC: a study of coupled model climatology and variability in tropical ocean regions, *Clim. Dyn.*, *18*, 403–420, 2002.

Deser, C., A. Capotondi, R. Saravanan, and A. Philips, Tropical Pacific and Atlantic Climate Variability in CCSM3, *J. Climate*, *19*, 2451–2481, 2006.

Ding, H., N. S. Keenlyside, and M. Latif, Seasonal cycle in the upper Equatorial Atlantic Ocean, *J. Geophys. Res.*, *114 and C09016*, doi:10.1029/2009JC005,418, 2009.

Ding, H., N. S. Keenlyside, and M. Latif, Equatorial Atlantic interannual variability: the role of heat content, *J. Geophys. Res.*, *in press*, 2010.

Dommenget, D., and M. Latif, Interannual to Decadal Variability in the Tropical Atlantic, *J. Climate*, *13*, 777–792, 2000.

Dommenget, D., and M. Latif, Notes and Correspondence: A Cautionary Note on the Interpretation of EOFs, *J. Climate*, *15*, 216–225, 2002.

DRAKKAR Group, Eddy-permitting ocean circulation hindcasts of past decades, CLIVAR Exchanges and No. 42 (Vol. 12 and No. 3) and International CLIVAR Project Office and Southampton and UK and 8–10, 2007.

Enfield, D. B., and D. A. Mayer, Tropical Atlantic sea surface temperature variability and its relation to El Niño-Southern Oscillation, *J. Geophys. Res.*, *102*, 929–945, 1997.

ETOPO5, Data Announcement 88-MGG-02, Digital relief of the Surface of the Earth, NOAA, National Geophysical Data Center, Boulder, Colorado, 1988, 1988.

Fang, Y., A coupled model study of the remote influence of ENSO on tropical Atlantic SST variability, Ph.D. thesis, Texas A&M University, 2005.

Fichefet, T., and M. A. Morales-Marqueda, Sensitivity of a global sea ice model to the treatment of ice thermodynamics and dynamics, *J. Geophys. Res.*, *102*, 12,609–12,646, 1997.

Florenchie, P., J. R. E. Lutjeharms, C. J. C. Reason, S. Masson, and M. Rouault, The source of Benguela Ninos in the South Atlantic Ocean, *Geophys. Res. Lett.*, *30(10)*, doi:10.1029/2003GL017,172, 2003.

Florenchie, P., C. J. C. Reason, J. R. E. Lutjeharms, and M. Rouault, Evolution of Interannual Warm and Cold Events in the Southeast Atlantic Ocean, *J. Climate*, *17*, 2318–2334, 2004.

Fratantoni, D. M., W. E. Johns, T. L. Townsend, and H. E. Hurlburt, Low-Latitude Circulation and Mass Transport Pathways in a Model of the Tropical Atlantic Ocean, *J. Phys. Oceanogr.*, *30*, 1944–1966, 2000.

Góes, M., and I. Wainer, Equatorial currents transport changes for extreme warm and cold events in the Atlantic Ocean, *Geophys. Res. Lett.*, *30(5)*, doi:10.1029/2002GL015,707, 2003.

Gammelsrød, T., C. H. Bartholomae, D. C. Boyer, V. L. L. Filipe, and M. J. O'Toole, Intrusion of warm surface water along the Angolan–Namibian coast in February–March 1995: The 1995 Benguela Niño, *South Afr. J. Mar. Sci.*, *19*, 41–56, 1998.

Ganachaud, A., and C. Wunsch, Improved estimates of global ocean circulation, heat transport and mixing from hydrographic data, *Nature*, *408*, 453–457, 2001.

Gent, P. R., and J. McWilliams, Isopycnal mixing in ocean circulation models, *J. Phys. Oceanogr.*, *20*, 150–156, 1990.

Giannini, A., R. Saravanan, and P. Chang, Oceanic Forcing of Sahel Rainfall on Interannual to Interdecadal Time Scales, *Science*, *302*, 1027–1030, 2003.

Griffies, S. M., Biastoch, A., Böning, C., Bryan, F., Danabasoglu, G., Chassignet, E. P., England, M. H., Gerdes, R., Haak, H., Hallberg, R. W., Hazeleger, W., Jungclaus, J., Large, W. G., Madec, G., Pirani, A., Samuels,

B. L., Scheinert, M., S. Gupta, A., Severijns, C. A., Simmons, H. L., Treguier, A. M., Winton, M., Yeager, S., Yin, and J., Coordinated Ocean-ice Reference Experiments (COREs), *Ocean Modelling*, *26*, 1–46, 2009.

Gu, D., and S. G. H. Philander, Interdecadal Climate Fluctuations That Depend on Exchanges Between the Tropics end Extratropics, *Science*, *275*, 805–807, 1997.

Hastenrath, S., L. C. Castro, and P. Acietuno, The Southern Oscillation in the tropical Atlantic sector, *Atmos. Phys.*, *60*, 447–463, 1987.

Hazeleger, W., and P. de Vries, Fate of the Equatorial Undercurrent in the Atlantic, in *Interhemispheric Water Exchange in the Atlantic Ocean*, edited by G. J. Goni and P. Malanotte-Rizzoli, pp. 175–191, Elsevier Oceanographic Series, 2003.

Hazeleger, W., P. de Vries, and G. J. van Oldenbourgh, Do tropical cells ventilate the Indo-Pacific equatorial thermocline?, *Geophys. Res. Lett.*, *28(9)*, 1763–1766, 2001.

Hazeleger, W., P. de Vries, and Y. Friocourt, Sources of the Equatorial Undercurrent in the Atlantic in a High-Resolution Ocean Model, *J. Phys. Oceanogr.*, *33*, 677–693, 2003.

Hormann, V., and P. Brandt, Atlantic Equatorial Undercurrent and associated cold tongue variability, *J. Geophys. Res.*, *112 and C06017*, doi:10.1029/2006JC003,931, 2007.

Hormann, V., and P. Brandt, Upper equatorial Atlantic variability during 2002 and 2005 associated with equatorial Kelvin waves, *J. Geophys. Res.*, *114 and C03007*, doi:10.1029/2008JC005,101, 2009.

Hourdin, F., and A. Armengaud, The Use of Finite–Volume Methods for Atmospheric Advection of Trace Species: Part I: Test of Various Formulations in a General Circulation Model, *Mon. Wea. Rev.*, *127*, 822–837, 1999.

Hu, Z.-Z., and B. Huang, Physical Processes Associated with the Tropical Atlantic SST Gradient during the Anomalous Evolution in the Southeastern Ocean, *J. Climate*, *20*, 3366–3378, 2007.

Huang, B., Remotely forced variability in the tropical Atlantic Ocean, *Clim. Dyn.*, *23*, 133–152, 2004.

Huang, B., P. S. Schopf, and Z. Pan, The ENSO effect on the tropical Atlantic variability: A regionally coupled model study, *Geophys. Res. Lett.*, *29(21)*, 2039 and doi:10.1029/2002GL014,872, 2002.

Huang, B., P. S. Schopf, and J. Schukla, Intrinsic Ocean–Atmosphere Variability of the Tropical Atlantic Ocean, *J. Climate*, *17*, 2058–2077, 2004.

Hüttl, S., Mechanisms of near-surface current and upwelling variability in the tropical Atlantic, Ph.D. thesis, IfM-Geomar Kiel, 2006.

Hüttl, S., and C. Böning, Mechanisms of decadal variability in the shallow subtropical-tropical circulation of the Atlantic Ocean: a model study, *J. Geophys. Res.*, *111(C07011)*, doi:10.1029/2005JC003,414, 2006.

Inui, T., A. Lazar, P. Malonotte-Rizzoli, and A. Busalacchi, Wind Stress Effects on Subsurface Pathways from the Subtropical to Tropical Atlantic, *J. Phys. Oceanogr.*, *32*, 2257–2276, 2002.

Jansen, M. F., D. Dommenget, and N. S. Keenlyside, Tropical Atmosphere–Ocean Interactions in a Conceptual Framework, *J. Climate*, *22(3)*, 550–567, 2009.

Jochum, M., and P. Malanotte-Rizzoli, Influence of the Meridional Overturning Circulation on Tropical-Subtropical Pathways, *J. Phys. Oceanogr.*, *31*, 1313–1323, 2001.

Kalney, E., and Coauthors, The NCEP/NCAR 40-year reanalysis project, *Bull. Am. Met. Soc.*, *77*, 437–470, 1996.

Katz, E. J., J. A. Carton, and A. Chakraborty, Dynamics of the equatorial Atlantic from altimetry, *J. Geophys. Res.*, *100 (C12)*, 25,061–25,067, 1995.

Keenlyside, N. S., Improved modelling of zonal currents and SST in the tropical Pacific, Ph.D. thesis, Monash Univ. and Melbourne and Victoria and Australia, 2001.

Keenlyside, N. S., and R. Kleeman, Annual Cycle of Equatorial Zonal Currents in the Pacific, *J. Geophys. Res.*, *107(C8)*, 3093 and doi:10.1029/2000JC000,711, 2002.

Keenlyside, N. S., and M. Latif, Understanding Equatorial Atlantic Interannual Variability, *J. Climate*, *20*, 131–142, 2007.

Kleeman, R., J. P. McCreary, and B. A. Klinger, A mechanism for generating ENSO decadal variability, *Geophys. Res. Lett.*, *26(12)*, 1743–1746, 1999.

Klein, S. A., B. J. Soden, and N. C. Lau, Remote sea surface temperature variations during ENSO: Evidence for a tropical atmospheric brigde, *J. Climate*, *12*, 917–932, 1999.

Kröger, J., A. J. Busalacchi, J. Ballabrera-Poy, and P. Malanotte-Rizzoli, Decadal variability of shallow cells and equatorial sea surface temperature in a numerical model of the Atlantic, *J. Geophys. Res.*, *110 (C12003)*, doi:10.1029/2004JC002,703, 2005.

Kushnir, Y., W. A. Robinson, P. Chang, and A. W. Robertson, The Physical Basis for Predicting Atlantic Sector Seasonal-to-Interannual Climate Variability, *J. Climate*, *16*, 5949–5970, 2006.

Large, W., and S. Yeager, Diurnal to decadal global forcing for ocean and sea-ice models: the data sets and flux climatologies and NCAR Technical Note: NCAR/TN–460+STR, *CGD Division of the National Center for Atmospheric Research*, 2004.

Large, W. G., Core Forcing for Coupled Ocean and Sea - Ice Models, *WGSF/WCRP Flux News*, *3*, 2–3, 2007.

Latif, M., and T. P. Barnett, Interactions of the tropical oceans, *J. Climate*, *8*, 952–964, 1995.

Latif, M., and A. Grötzner, The equatorial Atlantic oscillation and its response to ENSO, *Clim. Dyn.*, *16*, doi:10.1007/s003820050,014, 2000.

Lazar, A., R. Murtugudde, and A. J. Busalacchi, A model study of temperature anomaly propagation from the subtropics to tropics within the South Atlantic thermocline, *GRL*, *28(7)*, 1271–1274, 2001.

Levitus, S., T. P. Boyer, M. E. Conkright, T. O'Brian, J. Antonov, C. Stephens, L. Stathopolos, D. Johnson, and R. Gelfeld, World Ocean Database 1998, NOAA Atlas NESDID18, 1998.

Liu, Z., S. G. H. Philander, and R. C. Pacanowski, A GCM Study of Tropical-Subtropical Upper-Ocean Water Exchange, *J. Phys. Oceanogr.*, *24*, 2606–2623, 1994.

Lohmann, K., and M. Latif, Tropical Pacific Decadal Variability and the Subtropical-Tropical Cells, *J. Climate*, *in press*, 2005.

Lohmann, K., and M. Latif, Influence of El Niño on the Upper-Ocean Circulation in the Tropical Atlantic Ocean, *J. Climate*, *20*, 5012–5018, 2007.

Lorbacher, K., J. Dengg, C. W. Böning, and A. Biastoch, Regional Patterns of Sea Level Change Related to Interannual Variability and Multi-decadal Trends in the Atlantic Meridional Overturning Circulation, *J. Climate*, *in press*, 2010.

Losada, T., B. Rodríguez-Fonseca, I. Polo, S. Janicot, S. Gervois, F. Chauvin, and P. Ruti, Tropical response to the Atlantic Equatorial mode: AGCM multimodel approach, *Clim. Dyn.*, pp. doi:10.1017/s00,382–009–0624–6, 2009.

Lübbecke, J. F., C. W. Böning, and A. Biastoch, Variability in the subtropical-tropical cells and its effect on near-surface temperature of the equatorial Pacific: a model study, *Ocean Sci.*, *4*, 73–88, 2008.

Madec, G., NEMO ocean engine, Technical Report and Note du Pôle de modélisation de l'Institut Pierre-Simon Laplace No 27 and ISSN No 1288-1619, 2008.

Madec, G., and M. Imbard, A global ocean mesh to overcome the North Pole singularity, *Clim. Dyn.*, *12*, 381–388, 1996.

Malanotte-Rizzoli, P., K. Hedstrom, H. Arango, and D. B. Haidvogel, Water mass pathways between the subtropical and tropical ocean in a climatological simulation of the North Atlantic ocean circulation, *Dyn. Atmos. Oceans*, *32*, 331–371, 2000.

Marin, F., B.Bourlès, G. Caniaux, H. Giordani, Y. Gouriou, and E. Key, Why Were Sea Surface Temperatures so Different in the Eastern Equatorial Atlantic in June 2005 and 2006?, *J. Phys. Oceanogr.*, *39*, 1416–1431, 2009.

McCreary, J., A linear stratified ocean model of the equatorial undercurrent, *Philos. Trans. Roy. Soc. London*, *298*, 306–345, 1981.

McCreary, J. P., and P. Lu, Interaction between the Subtropical and Equatorial Ocean Circulations: The Subtropical Cell, *J. Phys. Oceanogr.*, *24*, 466–496, 1994.

McPhaden, M. J., Continuously stratified models of the steady state equatorial ocean, *J. Phys. Oceanogr.*, *11*, 337–354, 1981.

McPhaden, M. J., and D. Zhang, Slowdown of the meridional overturning circulation in the upper Pacific Ocean, *Nature*, *415*, 603–608, 2002.

Meeuwis, J. M., and J. R. E. Lutjeharms, Surface Thermal Characteristics of the Angola-Benguela Front, *South Afr. J. Mar. Sci.*, *9*, 261–279, 1990.

Mehta, V. M., Variability of the tropical ocean surface temperatures at decadal-multidecadal time scales. Part I: The Atlantic Ocean, *J. Climate*, *11*, 2351–2375, 1998.

Merle, J., Annual and interannual variability of temperature in the eastern equatorial Atlantic - The hypothesis of an Atlantic El Nino, 1980.

Moura, A., and J. Shukla, On the dynamics of droughts in the northeast Brazil: Observations and theory and numerical experiments with a general circulation model, *J. Atmos. Sciences*, *38*, 2653–2675, 1981.

Münnich, M., and J. D. Neelin, Seasonal influence of ENSO on the Atlantic ITCZ and equatorial South America, *Geophys. Res. Lett.*, *32*, L21,709,doi:10.1029/2005GL023,900, 2005.

Nicholson, S. E., An analysis of the ENSO signal in the tropical Atlantic and western Indian oceans, *Int. J. Climatol.*, *17*, 345–375, 1997.

Nonaka, M., S.-P. Xie, and J. McCreary, Decadal variations in the Subtropical Cells and equatorial Pacific SST, *Geophys. Res. Lett.*, *29(7)*, 20–1–20–3, 2002.

Okumura, Y., and S.-P. Xie, Interaction of the Atlantic Equatorial Cold Tongue and the African Monsoon, *J. Climate*, *17*, 3589–3602, 2004.

Okumura, Y., and S.-P. Xie, Some Overlooked Features of Tropical Atlantic Climate Leading to a New Niño-Like Phenomenon, *J. Climate*, *19*, 5859–5874, 2006.

Park, W., N. Keenlyside, M. Latif, A. Stroeh, R. Redler, E. Roeckner, and G. Madec, Tropical Pacific climate and its response to global warming in the Kiel Climate Model, *J. Climate*, *22*, 71–92, 2009.

Peterson, R., and L. Stramma, Upper-level circulation in the South Atlantic Ocean, *Progr. Oceanogr.*, *26(1)*, 1–73, 1991.

Philander, S. G. H., and R. C. Pacanowski, The oceanic response to cross-equatorial winds (with application to coastal upwelling in low latitudes), *Tellus*, *33*, 201–210, 1981.

Philander, S. G. H., and R. C. Pacanowski, A Model of the Seasonal Cycle in the Tropical Atlantic Ocean, *J. Geophys. Res.*, *91(C12)*, 4,192–14,206, 1986.

Polo, I., A. Lazar, B. Rodriguez-Fonseca, and S. Arnault, Oceanic Kelvin Waves and Tropical Atlantic intraseasonal Variability. Part I: Kelvin wave characterization, *J. Geophys. Res.*, *113 and C07009*, doi:10.1029/2007JC004,495, 2008a.

Polo, I., B. Rodriguez-Fonseca, T. Losada, and J. Garcia-Serrano, Tropical Atlantic Variability Modes (1979-2002). Part I: Time-Evolving SST Modes Related to West African Rainfall, *J. Climate*, *21*, 6457–6475 and doi:10.1175/2008JCI2607.1, 2008b.

Rabe, B., F. A. Schott, and A. Köhl, Mean Circulation and Variability of the Tropical Atlantic during 1952–2001 in the GECCO Assimilation Fields, *J. Phys. Oceanogr.*, *38*, 177–192, 2008.

Reason, C. J. C., and M. Rouault, Sea surface temperature variability in the tropical South Atlantic Ocean and West African rainfall, *Geophys. Res. Lett.*, *33*, L21,705: doi:10.1029/2006/GL027,145, 2006.

Reynolds, R. W., N. A. Rayner, T. M. Smith, D. C. Stokes, and W. Wang, An Improved In Situ and Satellite SST Analysis for Climate, *J. Climate*, *15*, 1609–1625, 2002.

Richter, I., S. Behera, Y. Masumoto, B. Taguchi, N. Komori, and T. Yamagata, On the triggering of Benguela Niños - remote equatorial vs. local influences, *Geophys. Res. Lett.*, *submitted*, 2010.

Robertson, A. W., J. D. Farrara, and C. R. Mechoso, Simulations of the Atmospheric Response to South Atlantic Sea Surface Temperature Anomalies, *J. Climate*, *16*, 2540–2551, 2003.

Rodríguez-Fonseca, B., I. Polo, J. García-Serrano, T. Losada, E. Mohino, C. R. Mechoso, and F. Kucharski, Are Atlantic Niños enhancing Pacific ENSO events in recent decades?, *Geophys. Res. Lett.*, *36*, L20,705,doi:10.1029/2009GL040,048, 2009.

Roeckner, E., G. Bäuml, L. Bonaventura, R. Brokopf, M. Esch, M. Girogetta, S. Hagemann, I. Kirchner, L. Kornblueh, E. Manzini, A. Rhodin, U. Schlese, U. Schulzweida, and A. Tompkins, The atmospheric general circulation model ECHAM 5 and Part I, MPI Report 349 and Max-Planck-Institut für Meteorologie and Hamburg, 2003.

Rouault, M., P. Florenchie, N. Faucherau, and C. J. C. Reason, South East tropical Atlantic warm events and southern African rainfall, *Geophys. Res. Lett.*, *30,8009*, doi:10.1029/2003GL014,840, 2003.

Rouault, M., S. Illig, C. Bartholomae, C. J. C. Reason, and A. Bentamy, Propagation and origin of warm anomalies in the Angola Benguela upwelling system in 2001, *J. Mar. Systems*, *68*, 473–488, 2007.

Rouault, M., Servain, J., C. J. C. Reason, B. Bourlès, M. J. Rouault, and N. Fauchereau, Extension of PIRATA in the tropical South-East Atlantic: an initial one-year experiment, *Afr. J. Mar. Sci.*, *31*, 63–71, 2009.

Ruiz-Barradas, A., J. A. Carton, and S. Nigam, Structure of Interannual-to-Decadal Climate Variabilty in the Tropical Atlantic Sector, *J. Climate*, *13*, 3285–3297, 2000.

Schott, F., J. Fischer, and L. Stramma, Transports and Pathways of the Upper-Layer Circulation in the Western Tropical Atlantic, *J. Phys. Oceanogr.*, *28*, 1904–1928, 1998.

Schott, F., P. Brandt, M. Hamann, J. Fischer, and L. Stramma, On the boundary flow off Brazil at 5-10°S and its connection to the interior tropical Atlantic, *Geophys. Res. Lett.*, *29(17)*, doi:10.1029/2002GL014,786, 2002.

Schott, F., M. Dengler, P. Brandt, K. Affler, J. Fischer, B. Bourlès, Y. Gouriou, R. L. Molinari, and M. Rhein, The zonal currents and transports at 35°W in the tropical Atlantic, *Geophys. Res. Lett.*, *30(7)*, 1349 and doi:10.1029/2002GL016,849, 2003.

Schott, F., M. Dengler, R. Zantopp, L. Stramma, J. Fischer, and P. Brandt, The Shallow and Deep Western Boundary Circulation of the South Atlantic at 5-11°S, *J. Phys. Oceanogr.*, *35*, 2031–2053, 2005.

Schott, F. A., J. P. M. Creary, and G. Johnson, Shallow overturning circulation of the tropical-subtropical oceans, in *Earth Climate: The Ocean-Atmoshere Interaction*, edited by Wang, C, S.-P. Xie, and J. A. Carton, pp. 261–304, AGU Geophysical Monograph Series 147, 2004.

Schouten, M. W., R. P. Matano, and T. P. Strub, A description of the seasonal cycle of the equatorial Atlantic from altimeter data, *Deep-Sea Res. I*, *52*, 477–493, 2005.

Servain, J., Simple Climatic Indices for the Tropical Atlantic Ocean and Some Applications, *J. Geophys. Res.*, *96(C8)*, 15,137–15,146, 1991.

Shannon, L. V., and G. Nelson, The Benguela: large scale features and processes and system variability, in *The South Atlantic – Present and Past Circulation*, edited by Wefer, G., W. H. Berger, G. Siedler, and D. J. Webb, pp. 163–210, Springer and Berlin, 1996.

Shannon, L. V., A. J. Boyd, G. B. Bundrit, and J. Taunton-Clark, On the existence of an El Niño–type phenomenon in the Benguela system, *J. Mar. Sci.*, *44*, 495–520, 1986.

Shannon, L. V., J. J. Agenbag, and M. E. L. Buys, Large and mesoscale features of the Angola-Benguela front, *South Afr. J. Mar. Sci.*, *5*, 11–34, 1987.

Snowden, D. P., and R. L. Molinari, Subtropical Cells in the Atlantic Ocean: An Observational Summary, in *Interhemispheric Water Exchange in the Atlantic Ocean*, edited by G. J. Goni and P. Malanotte-Rizzoli, pp. 287–312, Elsevier Oceanographic Series, 2003.

Steele, M., Morley, R., Ermold, and W., PHC: A Global Ocean Hydrography with a High-Quality Arctic Ocean, *J. Climate*, *14(9)*, 2079–2087, 2001.

Sterl, A., and W. Hazeleger, Coupled variability and air-sea interaction in the South Atlantic Ocean, *Clim. Dyn.*, *21*, 559–571 and doi: 10.1007/s00,382–003–0348–y, 2003.

Stramma, L., and F. Schott, The mean flow field of the tropical Atlantic Ocean, *Deep-Sea Res. II*, *46*, 279–303, 1999.

Sutton, R. T., Jewson, S. P., Rowell, and D. P., The Elements of Climate Variability in the Tropical Atlantic Region, *J. Climate*, *13*, 3261–3284, 2000.

Valcke, S., E. Guilyardi, and C. Larsson, PRISM and ENES: a European approach to earth system modelling, Concurrency Comput. Pract. Expert 18:231–245, 2006.

Venegas, S. A., L. A. Mysak, and D. N. Straub, Atmosphere-Ocean Coupled Variability in the South Atlantic, *J. Climate*, *10*, 2904–2920, 1997.

Wahl, S., The Tropical Atlantic SST Bias in the Kiel Climate Model, Ph.D. thesis, IfM-Geomar Kiel, 2009.

Wahl, S., M. Latif, W. Park, and N. Keenlyside, On the Tropical Atlantic SST warm bias in the Kiel Climate Model, *Clim. Dyn.*, pp. doi:10.1007/s00,382–009–0690–9, 2009.

Wang, C., An overlooked feature of tropical climate: Inter-Pacific-Atlantic variability, *Geophys. Res. Lett.*, *33*, L12,702, doi:10.1029/2006GL026,324, 2006.

Wedepohl, P. M., J. R. E. Lutjeharms, and M. Meeuwis, Surface drift in the South-East Atlantic Ocean, *South Afr. J. Mar. Sci.*, *22(1)*, 71–79, 2000.

Xie, S.-P., Interaction between the Annual und Interannual Variations in the Equatorial Pacific, *J. Phys. Oceanogr.*, *25*, 1930–1941, 1995.

Xie, S.-P., Ocean-Atmosphere Interaction in the Making of the Walker Circulation and Equatorial Cold Tongue, *J. Climate*, *11*, 189–201, 1998.

Xie, S.-P., and J. A. Carton, Tropical Atlantic Variability: Patterns and Mechanisms and and Impacts, in *Earth Climate: The Ocean-Atmoshere Interaction*, edited by Wang, C, S.-P. Xie, and J. A. Carton, AGU Geophysical Monograph Series 147, 2004.

Xie, S.-P., and S. G. H. Philander, A coupled ocean-atmosphere model of relevance to the ITCZ in the eastern Pacific, *Tellus*, *46A*, 340–350, 1994.

Zebiak, S. E., Air-sea interaction in the equatorial Atlantic region, *J. Climate*, *6*, 1567–1686, 1993.

Zelle, H., G. Appeldoorn, G. Burgers, and G. van Oldenborgh., The Relationship between Sea Surface Temperature and Thermocline Depth in the Eastern Equatorial Pacific, *J. Phys. Oceanogr.*, *34*, 643–655, 2004.

Zhang, D., McPhaden, M. J., and W. E. Johns, Observational Evidence for Flow between the Subtropical and Tropical Atlantic: The Atlantic Subtropical Cells, *J. Phys. Oceanogr.*, *33*, 1783–1797, 2003.

Zhang, R.-H., R. Kleeman, S. E. Zebiak, N. Keenlyside, and S. Raynaud, An Empirical Parameterization of Subsurface Entrainment Temperature for Improved SST Anomaly Simulations in an Intermediate Ocean Model, *J. Climate*, *18*, 350–371, 2005.

Acknowledgements

"But I don't want to go among mad people," said Alice. "Oh, you can't help that," said the cat. "We're all mad here."

(Lewis Carroll, Alice in Wonderland)

It is a pleasure to thank those people who spent their time and shared their knowledge for helping me to complete my thesis:

First and foremost, I would like to thank my supervisor Prof. Claus Böning for giving me the opportunity to work in my area of interest, for his guidance and for his continuous support in spite of some rather unorthodox decisions I made and despite the fact that we spent most of the time on different continents. His lectures as well as my time as a diploma and Ph.D. student in his group certainly shaped the way I think about and work on oceanographic questions.

I am extremely grateful to Noel Keenlyside for his help and advice and especially for improving my knowledge on statistics, which – in combination with many critical discussions – considerably strengthened this study. Meetings of his group were also always fun and I am glad I could be a part of it.

Working separated from the "Theory and Modelling" group for a long time would have been a lot harder without the fast-email-connection to Arne Biastoch who patiently replied to the endless stream of questions. I am very thankful for everything I learned about NEMO, ORCA, CRUSH & Co., many helpful discussions and words of encouragement.

I appreciate the contributions by Prof. Shang-Ping Xie who happened to be in the right place at the right time to give valuable input to this work. I am grateful for the constructive discussions we had in Princeton and for his ongoing interest in my work.

I would also like to thank all the people at GFDL who supported me in various ways and made the time in Princeton enjoyable.

Special thanks goes to many of my colleagues, in particular to Sabine Hüttl and Verena Hormann for sharing their knowledge on the Tropical Atlantic, and to Markus Scheinert, Franziska Schwarzkopf and Mirjam Glessmer for proofreading, answering ferret and matlab questions and, maybe most important, numerous coffee breaks.

The effort of the DRAKKAR group in developing the NEMO ocean model is greatly acknowledged. Thanks to Arne Biastoch for providing most of the NEMO-ORCA05 runs, to Wonsun Park and Sebastian Wahl for providing the KCM simulations as well as to Stéphane Raynaud for a well commented version of the IOM code.

Funding through the EU project AMMA, through Bundesministerium für Bildung und Forschung (BMBF) as part of Verbundvorhaben Nordatlantik, through Deutsche Forschungsgemeinschaft (DFG) as part of project SFB754 and through Bundesministerium für Familie, Senioren, Frauen und Jugend (BMFSFJ) via parental allowence is greatly acknowledged.

Lastly, I would like to express my gratitude to my friends and family, especially my parents, Torge, and Jarik, for their constant moral support and encouragement during the completion of the thesis.

Erklärung

Hiermit erkläre ich, dass ich die vorliegende Dissertation, abgesehen durch die Beratung meiner akademischen Lehrer, selbstständig verfasst habe und keine weiteren Quellen und Hilfsmittel als die hier angegebenen verwendet habe.
Diese Arbeit hat weder ganz, noch in Teilen, bereits an anderer Stelle einer Prüfungskommission zur Erlangung des Doktorgrades vorgelegen.
Ich erkläre, dass die vorliegende Arbeit gemäß der Grundsätze zur Sicherung guter wissenschaftlicher Praxis der Deutschen Forschungsgemeinschaft erstellt wurde.

Kiel, den 02.06.2010

(Joke Lübbecke)

Teile dieser Arbeit sind bei "Journal of Geophysical Research - Oceans" zur Veröffentlichung akzeptiert unter:
Lübbecke, J. F., C. W. Böning, N. S. Keenlyside and S.-P.Xie: On the connection between Benguela and Equatorial Atlantic Niños and the role of the South Atlantic Anticyclone, J. Geophys. Res., doi:10.1029/2009JC005964, in press, 2010